Flood Hazard Delineation at Tuktoyaktuk

R. F. Henry

Institute of Ocean Sciences
Department of Fisheries and Oceans
Sidney, B.C. V8L 4B2

1984

Canadian Contractor Report of Hydrography and Ocean Sciences No. 19

Canada

85-2511/

Canadian Contractor Report of Hydrography and Ocean Sciences

These reports are unedited final reports from scientific and technical projects contracted by the Ocean Science and Surveys (OSS) sector of the Department of Fisheries and Oceans.

The contents of the reports are the responsibility of the contractor and do not necessarily reflect the official policies of the Department of Fisheries and Oceans.

If warranted, Contractor Reports may be rewritten for other publications series of the Department, or for publication outside the government.

Contractor Reports are produced regionally but are numbered and indexed nationally. Requests for individual reports will be fulfilled by the issuing establishment listed on the front cover and title page. Out of stock reports will be supplied for a fee by commercial agents.

Regional and headquarters establishments of Ocean Science and Surveys ceased publication of their various report series as of December 1981. A complete listing of these publications and the last number issued under each title are published in the *Canadian Journal of Fisheries and Aquatic Sciences*, Volume 38: Index to Publications 1981. The current series began with Report Number 1 in January 1982.

Rapport canadien des entrepreneurs sur l'hydrographie et les sciences océaniques

Cette série se compose des rapports non publiés réalisés dans le cadre des projets scientifiques et techniques par des entrepreneurs travaillant pour le service des Sciences et Levés océaniques (SLO) du ministère des Pêches et des Océans.

Le contenu des rapports traduit les opinions de l'entrepreneur et ne reflète pas nécessairement la politique officielle du ministère des Pêches et des Océans.

Le cas échéant, certains rapports peuvent être rédigés à nouveau de façon à être publiés dans une autre série du Ministère, ou à l'extérieur du Gouvernement.

Les rapports des entrepreneurs sont produits à l'échelon régional mais sont numérotés et placés dans l'index à l'échelon national. Les demandes de rapports seront satisfaites par l'établissement auteur dont le nom figure sur la couverture et la page de titre. Les rapports épuisés seront fournis contre rétribution par des agents commerciaux.

Les établissements des Sciences et Levés océaniques dans les régions et à l'administration centrale ont cessé de publier leurs diverses séries de rapports depuis décembre 1981. Vous trouverez dans l'index des publications du volume 38 du *Journal canadien des sciences halieutiques et aquatiques*, la liste de ces publications ainsi que le dernier numéro paru dans chaque catégorie. La nouvelle série a commencé avec la publication du Rapport n° 1 en janvier 1982.

Canadian Contractor Report of
Hydrography and Ocean Sciences 19
1984

FLOOD HAZARD DELINEATION AT TUKTOYAKTUK

by
R. F. Henry
Institute of Ocean Sciences
Sidney, B.C. V8L 4B2

Report on Contract for Inland Waters Branch,
Department of Environment carried out by
Department of Fisheries and Oceans

Copyright Minister of Supply and Services Canada - 1984

Cat. No. FS 97-17 /19 ISSN 0711-6748

Correct citation for this publication:
Henry, R.F. 1984. Flood Hazard Delineation at Tuktoyaktuk
Can. Contract. Rep. Hydrogr. Ocean Sci.:19 : 117p.

DISCLAIMER

In view of the paucity of synoptic water level records of past surge episodes in the Beaufort Sea, the conclusions reported here must be considered only as the informed estimates of the Contractor and should not be used for design purposes.

ABSTRACT

Henry, R.F. 1984. Flood Hazard Delineation at Tuktoyaktuk, Can. Contract. Rep. Hydrogr. Ocean Sci. 19 : 117p.

The extent of inundation at Tuktoyaktuk and its environs in the event of a "100-year" storm surge is investigated. The extreme water level is estimated by using numerical models to compute the surge and wind wave response of the coastal shelf waters to a design storm obtained by statistical extrapolation from observed storm winds. The results of the investigation are summarised in a flood risk map.

key words: inundation, Tuktoyaktuk, storm surge, extreme water level, flood risk map.

RÉSUMÉ

Henry, R.F. 1984. Flood Hazard Delineation at Tuktoyaktuk, Can. Contract. Rep. Hydrogr. Ocean Sci. 19 : 117p.

On a étudié l'importance de l'inondation de Tuktoyaktuk et de ses environs suite au passage d'une onde de tempête comme il en survient une fois par siécle. Le niveau maximal de l'eau a été estimé a l'aide de modèles numériques du calcul de l'onde de tempête et de la houle due au vent qui seraient produites dans les eaux du plateau côtier par une tempête "type" établis par extrapolation statistique de vents de tempête observés. Les résultats de l'étude sont présentés sous forme d'une carte des risques d'inondation.

Mots clés: inondation, Tuktoyaktuk, onde de tempête, niveau d'eau extrême, carte des risques d'inondation.

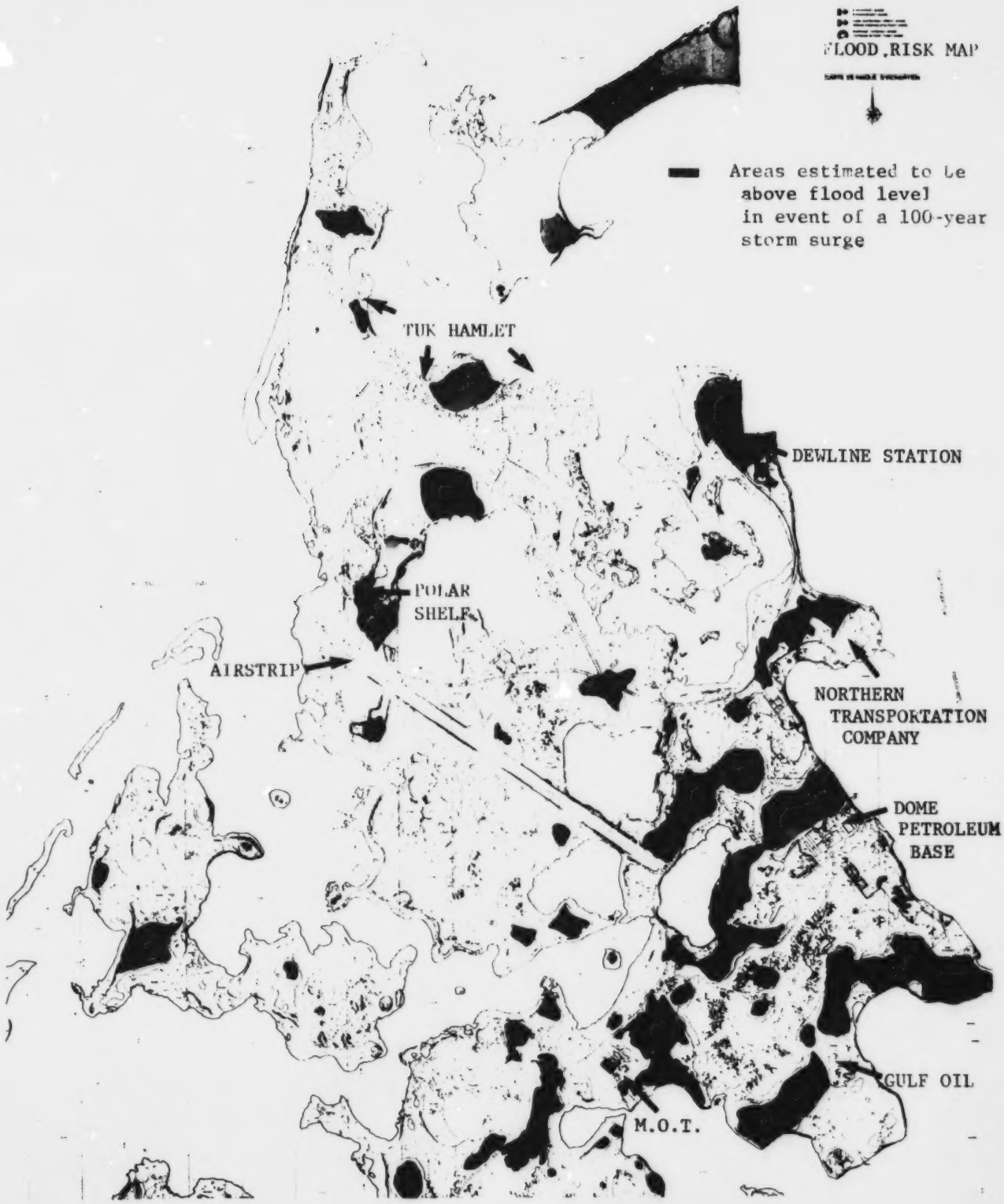
FLOOD RISK MAP
Areas estimated to be above flood level in event of a 100-year storm surge
TUK HAMLET
DEWLINE STATION
POLAR SHELF
AIRSTRIP
NORTHERN TRANSPORTATION COMPANY
DOME PETROLEUM BASE
GULF OIL
M.O.T.

TABLE OF CONTENTS

	Page
Abstract/Résumé	iv
Flood Risk Map	v
1. Introduction	1
2. Existing Data and Present Knowledge	
2.1 Tide gauge records	5
2.2 Wind wave measurements	7
2.3 Meteorological data	9
2.4 Ice data	11
2.5 Driftwood lines	12
3. Storm Surge Simulation	
3.1 Numerical Models	13
3.2 Calibration against past surges	16
3.3 Relation of shelf winds to observed winds at Tuktoyaktuk	20
4. Construction of Flood Delineation Maps	21
5. Conclusions	24
References	27
Figures	29
Appendix 1. Meteorological Conditions for Maximum Storm Surges in the Beaufort Sea. (Atmospheric Dynamics Corporation)	
Appendix 2. Extreme Wave Conditions at Tuktoyaktuk. (Seaconsult Marine Research Ltd.)	
Appendix 3. Extreme Wind Stresses over Beaufort Sea as determined from Tuktoyaktuk Winds. (Atmospheric Dynamics Corporation)	

1. Introduction

The Beaufort Sea coast is subject to storm surges whenever strong onshore winds occur during ice-free periods. A surge 1m above mean sea level at the open coast may increase to 2m at Tuktoyaktuk due to amplification by bathymetric features of Kugmallit Bay. During particularly severe storms in 1944 and 1970, even larger surges inundated parts of the township. With the recent increase in population and construction, the potential for loss of life and property in the event of an exceptionally large surge has increased considerably. The principal aim of this study is to determine, so far as is possible, how much of Tuktoyaktuk and its immediate environs would be inundated by a "100-year surge", i.e. one with a probability of only 0.01 of occurring in any given year. This is a customary recurrence interval to choose for engineering design purposes when dealing with randomly occurring natural disasters.

There are several contributions to the abnormal water level during a surge episode. These are : the true surge component, consisting of a rise in water level on about the same time scale as the tide and caused by tangential surface wind stress and to a lesser extent by the atmospheric pressure gradient; wind-generated waves; and thirdly, the tidal elevation. Fortunately, the tidal range is small in the Beaufort Sea and the tidal contribution to high water level at Tuktoyaktuk is less

than 0.25m. As there is no appreciable swell on the Beaufort Sea coast, the principal contributions to abnormal levels at Tuktoyaktuk are thus the surge and short-period wind waves. Sometimes the term "storm surge" is used loosely to mean the combined effect of surge, tide and wind-waves.

There are accepted extrapolation methods for predicting values corresponding to recurrence intervals greater than the total period covered by existing records (see e.g. Gumbel, 1958) but the 20 years of tide gauge readings collected at Tuktoyaktuk contain too few major surges to permit reasonably reliable extrapolation to the 100-year mark. Unfortunately, the gauge was not working in September 1970 when the largest surge during this period occurred. Further, the fact that ice cover largely eliminates the chance of surges occurring in "bad" ice years (Henry and Heaps, 1976) may invalidate the theoretical basis for the extrapolation.

The alternative approach adopted in this study, and also previously by Hodgins, LeBlond and Brink-Kjaer (1981), is to construct a suitably severe storm, by extrapolating from existing meteorological records, and then to calculate the resulting 100-year flood level by driving a numerical model of the Beaufort Sea with this design storm. The meteorological records constitute a better basis for extreme value extrapolation because there are fewer gaps, and, since there are several storms each

summer, whether the sea is ice-covered or not, there is a definable maximum annual storm in each year, as required for the extreme value extrapolation. The work of defining the design storm was subcontracted to Atmospheric Dynamics Corporation, whose report (Danard, 1983) is included here as Appendix 1. The relation between the recurrence intervals of the design storm and the resulting surge is discussed in Section 2.4 .

The numerical modelling techniques used to compute the surge caused by a given storm are quite standardised. Accurate account can be taken of the actual bathymetry and coastline configuration in the region studied, but certain other important physical effects are difficult to model correctly, in particular, frictional resistance to water motion and the actual surface stress field produced by a given storm. Usually, in numerical models friction is taken to be proportional to the square of water speed, the constant of proportionality or friction coefficient being found by "calibrating" the model, that is, by simulating past surge episodes and repeating the simulation with various values of the unknown coefficient until a satisfactory fit is found. If enough past surges have been recorded, the calibrated model is "verified" by simulating surges not already used in the calibration process. Too few water records from the Beaufort Sea are available to permit proper model calibration, far less verification, but, fortunately, tests made with the model showed that uncertainty about the friction coefficient was

not a serious problem, as the computed surge at Tuktoyaktuk heights were not particularly sensitive to the value of this parameter.

Deducing the surface wind stress field during a storm does, however, remain a serious difficulty, for reasons which are discussed in Section 2.3 of this report. Briefly, the sparseness of observing stations leads to underestimation of pressure gradient and surface winds over the Beaufort Sea shelf. Given enough records of past surges, this problem could probably also be tackled by setting the value of the drag coefficient in the wind stress calculation experimentally, as in the case of the friction coefficient already mentioned. Here, particularly, the absence of enough records of past surges constitutes a practically insurmountable barrier at the present time. One clear conclusion from the present study is that more permanent tide gauges are needed on the Beaufort Sea coast.

Calculation of extreme wind-wave height occurring during the 100-year design storm also depends on fairly accurate knowledge of the temporal and spatial distribution of surface wind speed, and consequently is less reliable than in other better-observed coastal seas. Due to the exceptionally long reach of very shallow water between Tuktoyaktuk and the shelf edge, some influences which are negligible in other places, such as frictional losses and local generation, cannot be ignored in this

case. Considerable research is still required into the quantitative effects of these factors on wind-waves. In order to obtain acceptable estimates of extreme wave height, this portion of the work was sub-contracted to Seaconsult Marine Research Ltd., who have access to proprietary software based on recent research into this problem (Hodgins, LeBlond and Huntley, 1983).

The estimated extent of inundation which would be caused at Tuktoyaktuk by a 100-year surge with accompanying wind waves and tidal elevation is shown on the maps included with this report. From the comments above, it should be obvious that the flood limits shown must be regarded as quite tentative. In the writer's opinion, good synoptic meteorological and water level records for at least four or five major surges are required to resolve the present difficulties. In other words, it will be necessary to augment the number of tide gauges and quality of meteorological data and operate the resulting improved observing network for upwards of ten years before extreme flood limits at Tuktoyaktuk can be predicted with much confidence.

2. Existing Data and Present Knowledge

2.1 Tide gauge records

The periods when tide gauges have been in operation in the Beaufort Sea are summarised in Figures 1(a) to (d). By far the longest record is at Tuktoyaktuk, but there have been some

breaks, the most significant being in 1970, when the largest surge in the last 40 years occurred (Anon, 1971). Accurate records of such an exceptional surge would have been most valuable for extreme value calculations, since less extrapolation is involved. Another major shortcoming is the poor spatial coverage. To be sure that the adjustable friction and drag coefficients are set correctly, it is necessary to have simultaneous water level records well spaced through the study area. The only period for which this condition held was in the summer of 1975, during the Beaufort Sea Project. Unfortunately, that was a bad ice year and only very minor surges occurred. It can be seen from Figure 2 that partial coverage was achieved for periods of about a month in 1972, 1974, 1975 and 1976. No major surges were recorded, except on September 1-2, 1972, when a surge of about 1m registered on four coastal gauges. The Tuktoyaktuk gauge was again out of operation at the time, but the other records are still of some use for calibration purposes. Judging from model results, this surge must have reached about 1.7m at Tuyktoyaktuk. Since neither this surge nor two of about 2m which occurred in September 1962 were considered remarkable, it seems reasonable to conclude that the 1944 and 1970 surges, both of which caused damage and flooding, must have been noticeably higher, in the neighbourhood of 3m. This gives a rough lower limit for the 100-year surge height at Tuktoyaktuk, including tide and excluding wind-waves.

Since the data basis is so sparse, it is essential to make the very best use of what is available, including periods where only the Tuktoyaktuk gauge was operating. Model tests showed that surge height at Tuktoyaktuk is fairly insensitive to the value of friction coefficient: it seemed justifiable therefore to make the friction coefficient uniform throughout the model and give it a value (k=0.0025) known to have proved satisfactory in several similar problems (e.g. Flather and Heaps, 1975; Davies and Flather, 1977). With this parameter now fixed, it becomes more feasible to attempt calibration of the other unknown, the drag coefficient, using mainly the records from Tuktoyaktuk.

2.2 Wind wave measurements and prediction

The state of current knowledge on wind-waves in the Beaufort Sea has been reviewed recently in detail by Hodgins (1983). Figure 2, reproduced from Hodgins, shows sites and periods where Waverider buoys have been in operation, starting from 1970. Direct estimation of extreme wave heights at Tuktoyaktuk on a purely statistical basis is not possible, since no nearby wave data is available. In fact, even if all the existing records are taken together, irrespective of site, there are too few observations to permit very reliable estimation of "100-year" extreme wave height, particularly since data are missing for some of the most severe storms.

It is possible, however, to use the existing records for

verification of wave hindcast models over the part of the shelf beyond the 10m depth contour. With certain assumptions, this in turn permits wave hindcasting in the neighbourhood of Tuktoyaktuk under extreme storm conditions. The technique used by Hodgins for estimating maximum wave height at Tuktoyaktuk during the 100-year design storm is outlined in Niwinski and Hodgins (1984), included here as Appendix 2. Essentially, hourly surface winds were used to calculate the directional wave spectrum to be expected at the outer edge (roughly the 30m contour) of that part of the shelf where bottom effects become significant. From there to the coast at Tuktoyaktuk, a linear spectral refraction model was used to take into account the effects of shoaling, refraction and bottom friction on the incoming waves. In view of the exceptionally large fetch of very shallow water in this location, allowance was made for wave growth due to local wind stress. Finally, a maximum wave height was calculated from the wave spectrum computed at the coast, after adjustment for wave breaking.

In the course of the present work it was not feasible to deal objectively with the question of wave attenuation over inundated areas. In the event of any surge over about 2.5m, some of the land in and around Tuktoyaktuk becomes inundated. The wind waves will decay as they propagate over the flooded area, but it is very difficult to estimate how maximum wave height might decrease with distance from the coastline. The question of wave

refraction over the flooded area could possibly be handled by developing a model with resolution fine enough to describe the rapidly-varying topography, but frictional losses depend on the nature of the ground surface, particularly the vegetation, and the only observations made so far have been over uniform terrain Anon, 1977. The flood delineation maps accompanying this report have had to be drawn up using fairly arbitrary methods of estimating how extreme wind-wave height decreases across the flooded areas (see Section 4.2).

2.3 Meteorological data

It is clear from surface pressure charts that surges on the Beaufort Sea coast are caused by north-westerly to westerly winds in the southwest sector of low pressure systems crossing the Beaufort Sea. Only relatively infrequent minor surges can occur when the sea is ice-covered (Henry, 1975), so that major surges are confined to the summer months of so-called "good" ice-years, when the pack ice retreats 100 km or more from the shore. The centres of the lows travel roughly eastward and are generally well north of the coast (Burns, 1973). Unfortunately, the network of meteorological observing stations is quite sparse, with the result that the intensities of the lows are far less precisely known than for similar systems over land. Part of the difficulty is that the observing stations lie on an irregular arc at or near the coast and this coverage is insufficient for

reconstruction of the two-dimensional pressure field. In other words, analysis of cyclones over the Beaufort Sea involves extrapolation, which is inherently less accurate than interpolation. The numerical weather prediction models run by the Canadian Meteorological Centre CMC cannot help much with this problem, as the present coarse spatial resolution used results in considerable smoothing of the pressure field.

Since 1976, pressure and wind observations have been transmitted from an automatic station deployed by Canmar on the ice about 200 km from shore. This information, together with pressures reported from stations positioned much further north as part of the Arctic Ocean Buoy Program, has improved the coverage, but judging from the results discussed later, pressure gradients and winds are still underestimated.

As part of the present study, Atmospheric Dynamics Corporation (ADC) estimated extreme wind speeds, tangential sea surface stresses and pressure gradients over the Beaufort Sea, based on the most severe storms occurring in the 11 years 1970, 1972 and 1974-82 (see Appendix 1). Assuming a Gumbel distribution for maximum winds, extreme winds for various return periods were calculated. A maximum probable storm (App. 1, Fig. 1) was then constructed from an actual severe storm, by modifying the intensity and path of the latter. The recurrence interval for this storm is approximately 70 years, but for reasons given in

19

the following section, it was adopted as the required "100-year" design storm.

After the above work had been completed by ADC, the writer obtained access to a report by Meteorology and Environmental Planning Co. (Anon, 1981) which was carried out in support of a study of extreme water levels by Seaconsult (Hodgins, LeBlond and Brink-Kjaer, 1981). MEP constructed a 100-year storm by methods very similar to those used by ADC and with a data base of similar length (1969-1978), yet there is a significant difference between the MEP 100-year wind, 31 m/s, and the 26.1 m/s estimated by ADC. The ADC figure of 26.1 m/s actually refers to a 70-year storm, as already noted, but the corresponding 100-year wind is 27.8 m/s, still 10% below the MEP figure of 31 m/s. The fact that the MEP estimate is higher is surprising in view of the fact that MEP used CMC-analyzed data, while ADC used more detailed surface pressure charts from Arctic Weather Centre and the Beaufort Weather and Ice Office, which incorporated the offshore observations noted above. This discrepancy is illustrative of the uncertainty which prevails in quantitative meteorology over the Beaufort Sea.

2.4 Ice data

It is clear from the available water level records that severe storms cannot cause major surges in the Beaufort Sea in bad ice years, that is, when the edge of the pack ice retreats only tens

of kilometres from the coast. It is not known whether partial, unconsolidated ice cover suppresses or enhances surge response, but wind-waves are certainly suppressed. Consequently, in estimating extreme water levels due to the combined effects of surge and wind-waves, it is appropriate to assume that ice cover is completely absent.

The uncertainty about the effect in surge generation of partial ice cover causes some problem in relating the recurrence intervals of surges and storms. On the basis of the information available concerning ice cover on the Beaufort Sea shelf (e.g. Burns, 1973; Markham, 1975), it was assumed here that in roughly 3 summers out of 10, the ice cover is sufficient to prevent formation of large surges. It follows that the storm with recurrence interval of 70 years discussed in Section 2.3 corresponds to a surge with a recurrence interval of 100 years, and for this reason will be treated here as the required 100-year design storm.

2.5 Driftwood lines

Many observers have reasoned that the upper limit of driftwood on the Beaufort Sea beaches should mark the maximum water levels reached during large surges. Reimnitz and Maurer (1979) have established that useful information can be obtained in this way from certain beaches on the north shore of Alaska, but it is doubtful if similar conclusions can be drawn with confidence in

the neighbourhood of Tuktoyaktuk, unless surveys can be carried out soon after a major surge occurs. According to Kolberg and Shah (1976), the coastline adjacent to Tuktoyaktuk receded between 60 and 850ft. in the period 1950 t0 1972. In the same period, the shoreline of the settlement peninsula and of Tuktoyaktuk Island receded about 130 ft. In these circumstances, the driftwood line probably marks the most recent exceptional high water mark, but can hardly represent a reliable record of surges many years earlier.

3. Storm Surge Simulation

3.1 Numerical models

The numerical model used here for calculating surge heights is a slightly modified version of an explicit finite-difference model developed for the Beaufort Sea Project. The numerical details have been described in Henry (1975) and Henry and Heaps (1976). The fact that this model simulated the semi-diurnal tides in the Beaufort Sea very accurately (Henry and Foreman, 1977) gives good grounds for confidence in its representation of shallow-water phenomena, including surges, provided, of course, that appropriate forcing can be specified.

In order to reduce computing costs, numerical tests were carried out at an early stage of this project to discover whether any parts of the extensive model described in Henry and Heaps could

be omitted when computing surge levels at Tuktoyaktuk. It was found that the model grid could be reduced to the area shown in Figure 3, since winds and pressure gradients elsewhere had practically no effect on maximum water level reached at Tuktoyaktuk.

Another modification introduced was the use of a higher resolution nested model of Kugmallit Bay based on the grid shown in Figure 4. The boundary velocities required to drive this model (Model 2) are obtained by interpolation between the values computed in the coarser shelf model (Model 1). In practice, the elevations calculated for Tuktoyaktuk from the two models did not differ significantly.

Model 2 was useful however in checking whether allowing for coastal inundation reduced maximum surge height reached at Tuktoyaktuk. The shaded grid rectangles in Figure 4 represent a coastal strip, one grid interval (approximately 2.6 km) wide, where flooding could be simulated by assigning each shaded rectangle a negative mean water depth of 2m (representing approximate mean land height in the coastal strip) and computing water level and velocities in each such rectangle only when water level in the adjoining seaward rectangle rose more than 2m above mean level. In fact, this degree of coastal flooding had a fairly minor effect on peak surge heights: maximum levels reached at Tuktoyaktuk were reduced by approximately 3%. This effect,

being substantially less than other suspected uncertainties in the surge calculations, was ignored subsequently, and most of the remaining tests discussed in this report were carried out using Model 1.

Before the model was used to simulate real surge episodes, some investigative runs were carried out with hypothetical storms to check relationships between meteorological forces and maximum surge height at Tuktoyaktuk. The total surge effect at Tuktoyaktuk can be expected to contain increases of elevation required to:

(i) produce a pressure gradient to balance the shoreward component of surface wind stress;

(ii) balance the shoreward component of atmospheric pressure gradient;

(iii) bring about geostrophic balance in longshore currents set up by longshore components of wind stress and atmospheric pressure gradient.

In shallow water, (ii) is normally considerably less than (i). Tests with Model 1 driven by realistic storms showed that the pressure gradient contribution (ii) was about 12% of the surface stress effect (i) for a surge reaching 2m at Tuktoyaktuk, and 0.76% for a more severe surge of 3.5m. Since wind speed is proportional to pressure gradient and wind stress is roughly

proportional to the square of wind speed, this decrease in the importance of (ii), relative to (i), with increasing storm severity, is to be expected. Contribution (iii) requires time for a longshore current to be set up and come close to geostrophic balance. The resulting elevation at the coast should be proportional to current speed, which is inversely proportional to the magnitude of frictional effects limiting the current. To check the importance of (iii) at Tuktoyaktuk, two simulations of the same surge were run, first using the customary value of 0.0025 for the coefficient of quadratic bottom friction and again using half this figure. As there was no apparent difference in the surge heights computed at Tuktoyaktuk in the two cases, it was concluded that effect (iii) is insignificant.

In summary, the shoreward component of surface wind stress is clearly the dominant meteorological influence on maximum surge height reached at Tuktoyaktuk. Scaling up the magnitude of the wind stress throughout a given surge simulation confirmed that the maximum surge height reached at Tuktoyaktuk did in fact vary almost linearly with the peak wind stress level applied.

3.2 Calibration against past surge episodes

The occasions when surges were recorded or are suspected to have occurred at Tuktoyaktuk are indicated in Figure 1(a). For model calibration purposes, the best cases are those in which

(a) water level records are available at Tuktoyaktuk and, preferably, at several additional sites;

(b) maximum surge height at Tuktoyaktuk is greater than 1.5m;

(c) the surface pressure charts available permit reasonably accurate estimation of wind speed.

None of the surges noted in Figure 1(a) meet all these conditions. The three large surges in 1962 and 1963 were recorded only at Tuktoyaktuk and only coarse resolution surface pressure charts are available. No gauges were in operation during the severe surge on September 14, 1970 and only rough guesses of surge height ("6 to 10 feet") could be made.

The Tuktoyaktuk gauge was again out of action during the surge on September 3, 1972. However, the fact that four other gauges recorded this surge on the coasts east and west of Kugmallit Bay makes this episode of some interest for overall calibration purposes. None of the surges recorded since 1972 have much exceeeded 1m and it is clear that the information available concerning large surges provides a very inadequate data basis for calibrating both the frictional and driving forces for the storm surge model, even with the simplifying assumptions discussed in the preceding section. In the circumstances, it seems best to assume a uniform value for the bottom friction coefficient based on values found satisfactory in other similar storm surge models,

say k=0.0025 (e.g. Flather and Heaps, 1975; Davies and Flather, 1977), and concentrate on checking the validity of the wind stress calculations.

The first case simulated was the surge of September 3, 1972, which was recorded on gauges at Baillie Island, Cape Dalhousie, Atkinson Point and Pelly Island. Using the wind stress and pressure gradient time histories computed by ADC for this storm (Appendix 1,Table 4), Model 1 gave maximum elevations which were, on average, 38% of the observed maximum values. In view of the proportionality established earlier between wind stress and maximum surge height, this indicates that the wind stress values need to be multiplied by a factor 2.6 . When this was done, and the model rerun, surge levels at the four sites were scaled up as required. The model results also showed that the maximum surge height reached at Tuktoyaktuk was then 1.7m .

It is an important question why the computed stresses have to be multiplied by such a large factor to produce realistic results. Some scaling up of the stresses can be justified on the grounds that inadvertent smoothing of the pressure field takes place in the analysis represented on the AWC surface pressure charts. No offshore meteorological observations were available in 1972, so that the low pressure system may have been more intense than could be deduced from land station data. Some smoothing is also included in the computation of wind stress from the surface

pressure chart information. Nevertheless, a scaling factor of 2.6 is surprisingly large. In this connection, two further model runs were carried out, using the 100-year design storm discussed in Section 2.3 . Model 1 was first run using the wind stresses and pressure gradients as computed by ADC (App.1, Table 4) and again with this input scaled up by the above-mentioned factor of 2.6 . The first case resulted in a maximum surge level at Tuktoyaktuk of 2.6m, while the scaled-up stresses gave a maximum of 6.7m. The former figure seems low for the 100-year surge in view of levels already recorded at Tuktoyaktuk, while the latter is implausibly high, being at least 2m above any eyewitness estimate. It was concluded that some scaling factor greater than 1 is necessary but that a figure of 2.6 is too high.

Hodgins, LeBlond and Brink-Kjaer (1981) were also obliged to scale up wind speeds to well above geostrophic values in order to obtain agreement between computed and observed surge heights in this storm. Other cases with which these authors attempted to calibrate their surge model occurred on August 11, 1975 and August 27, 1975. The true surge component in both cases was barely 1m and there is evidence that these small surges were caused by short-duration high-intensity local winds associated with fronts imbedded in moderate lows, whereas major surges are caused by larger-scale wind fields associated with severe lows. It is for this reason that condition (b) above seems necessary when selecting surge episodes to use for calibration purposes.

The few surges recorded between 1975 and 1982 have also been relatively small, around 1m .

It must be concluded that the surge records available are inadequate to resolve the question of what scaling factor to use to compensate for the underestimation of wind stresses and pressure gradients. Hodgins, LeBlond and Brink-Kjaer were forced to conclude that "wind fields based on measured wind data should be used to test the [surge] model instead of the modelled [computed] wind fields." As 1982 provided no notable surges and the 1983 records are not yet available, the position is basically the same as when these authors completed their study in 1981. It was decided therefore at this stage to follow their above suggestion, as discussed in the following section, in order to obtain an independent estimate of extreme wind speed and stress.

3.3 Relation of shelf winds to observed winds at Tuktoyaktuk

Hall, Baird and Wright (1983) showed that winds over the shelf waters north-west of Tuktoyaktuk could be calculated from winds observed at Tuktoyaktuk by correlating observed wind speeds and directions at two drilling sites with the same variables observed at Tuktoyaktuk, for 16 months of data. A transfer function was obtained which should permit calculation of overwater winds for any period for which wind observations are available from Tuktoyaktuk.

Wind data collected at 10 drilling sites during the summer of 1982 provided a more extensive data base for estimating the transfer functions. Appendix 3 of this report contains the results of a study based of this approach conducted by Atmospheric Dynamics Corporation. In order to improve reliability in later applications to storm surges, attention was paid only to episodes involving winds blowing towards shore with speeds of 20km/h or above. Under these conditions, the overwater wind speed is, on average, 1.18 times the observed speed at Tuktoyaktuk and there is negligible average difference in direction between overwater and Tuktoyaktuk winds (App. 3, Table 4).

ADC also analysed 12 years of Tuktoyaktuk wind data to find annual peak wind speeds. Fitting a Gumbel distribution to this data led to a predicted 70-year wind of 24.1 m/s at Tuktoyaktuk. To compensate for gaps in the data, which could have caused underestimation of the peak wind speed in some years, it was considered to be advisable to raise this figure by 5% to 25.3 m/s. Then applying the overwater/Tuktoyaktuk wind factor of 1.18 referred to above, the estimated 70-year maximum wind speed over the shelf is 29.9 m/s. This is compatible with the average 100-year wind speed of 31 m/s suggested by MEP (Anon, 1981).

4. Construction of Flood Delineation Charts

The new estimate of 70-year extreme wind speed over the shelf,

described above, offered a more definite scaling factor for the design storm wind stresses. The surface stress corresponding to the 70-year wind speed of 29.9 m/s was evaluated using the drag coefficient versus wind speed relationship given in Gray and Danard (1982), and the whole wind stress record corresponding to the design storm was then scaled up so that its peak value equalled the computed 70-year wind stress. The storm surge model was then rerun using this revised wind-stress record as input. The resulting maximum surge height at Tuktoyaktuk, which should represent the 100-year surge level (see Section 2.4), was found to be 3.5m above hydrographic chart datum. The topographic Flood Risk Maps prepared for this project use a datum which is 1.2m above the hydrographic chart datum (according to F. Stephenson, I.O.S.). Consequently, the estimated 100-year surge level is 2.3m above the topographic map datum. To this must be added a tidal contribution, because in the worst case, the peak surge could coincide with high tide. Tests with the numerical model showed, however, that in that case, the surge had a moderating influence on the tidal amplitude, and instead of adding half the tidal range to the maximum surge level, it was judged appropriate to add only 0.2m to the surge level to allow for tidal effect. The combined effect of the design surge plus tide is thus to raise the water level to 2.5m above topographic map datum.

Both surge and tide have fairly similar time scales, so that it is clear that the 2.5m rise in level should be experienced all

31

along the shores at Tuktoyaktuk, both outside and inside the harbour. The 2.5m contour on the flood risk maps therefore delineates the probable extent of flooding due to surge plus tide, ignoring wind-waves.

The additional contribution from wind-waves depends on exposure and so must vary considerably with distance from the coast. The estimated extreme wave height outside Tuktoyaktuk harbour is 4.9m (Appendix 2). Following Shore Protection Manual procedures (Anon, 1977), the maximum crest height above mean water depth is then 4.2m. It was assumed that the west shore of the settlement peninsula and the north shore of Tuktoyaktuk Island would suffer the full effect of these wind waves and would be flooded or awash up to the 6.7m contour, that is, 4.2m higher than the 2.5m level reached by the surge and tide contributions.

In order to estimate wave heights in areas not exposed to the open sea, temporary mean water depths were worked out for those areas flooded by the surge and tide, i.e. those below the 2.5m contour on the Flood Risk Maps. Lanes 200m wide and parallel to the predicted wave direction were drawn on the maps and wave heights were then calculated in each lane, starting from the open coast, assuming that wave height would be reduced to 78% of the least mean water depth encountered, unless greater wave heights prevailed in either of the immediately neighbouring lanes. In that case, empirical allowance for local refraction was made by

increasing wave height to the level in the neighbouring lane.

The harbour shoreline was treated seperately. It was estimated that extreme crest height would be reduced from 4.2m to an average of 1.7m by the constricted entrances, and that crest height would be further attenuated with distance into the harbour, to a minimum of 0.5m at the southern end.

The crest heights calculated through the study area by the methods detailed above were added to the 2.5m increase in level due to surge and tide, to find the total flood level. Where predicted flood level was higher on the seaward side of a relatively narrow patch of high ground, it was assumed that flood level on the harbour side was determined by waves spilling around from the seaward side rather than by waves approaching from the direction of the harbour. For larger areas of high ground, flood levels on the seaward and sides were calculated using the crest heights expected from these respective directions. Land calculated to be awash under the design flood is shown as flooded on the Flood Risk Maps.

5. Conclusions

It is clear from this report and the contractors' reports apppended that calculation of the 100-year flood level requires many assumptions to cover gaps in present scientific knowledge of surge and wave phenomena in the Beaufort Sea. Consequently, the

flood limits shown on the Flood Risk Maps (labelled Preliminary Version I) must be regarded as tentative, empirical estimates. They are intended to be on the conservative side, that is, the areas not inundated by a 100-year surge will probably be somewhat larger than those now shown on the maps.

In order to provide an adequate basis for satisfactory scientific treatment of the extreme flood problem at Tuktoyaktuk, a program on the following lines is required :

- additional permanent tide gauges along the coast east and west of Kugmallit Bay

- directional wave measurement arrays at the entrance to Kugmallit Bay and off Tuktoyaktuk; a waverider buoy in Tuktoyaktuk harbour; aerial observation of wave breaking behaviour in Kugmallit Bay under severe storm conditions

- improved surface wind forecasting over the Beaufort Sea shelf. Steps required include deployment of at least two additional automatic buoys each summer; numerical model studies of pressure and wind fields over the shelf; correlation studies of winds observed at drilling sites and on land; small scale objective meteorological analysis for surge episodes

- surveys of driftwood levels at sites where erosion is relatively slow

- numerical modelling hindcast studies of storm surges and wind waves to coordinate the results of the above studies and existing data

The eventual benefits from such a program would be more accurate prediction of flood levels during all surges and more accurate delineation of those areas safe from inundation under most severe conditions, e.g. a 100-year surge. Since large surges below the 100-year level can endanger life and property, a strong case can be made for including surge prediction in routine weather forecasting for the Beaufort Sea and also for organisation of a public flood warning system.

35

REFERENCES

Anon, 1971. "Investigation of Storm, September 13-16, 1970, Mackenzie Delta Region, Beaufort Sea." Engineering Programs Branch, Dept. of Public Works, Ottawa.

Anon, 1981. "Beaufort Sea Water Level Hindcast Study; Meteorology Section." Meteorological and Environmental Planning Ltd., Downsview, Ont.

Anon, 1977. Shore Protection Manual, 3rd. Edn., 3 Vols., U.S. Army Coastal Engineering Research Center, Fort Belvoir, Virginia.

Burns, B.M., 1973. "The Climate of the Mackenzie Valley-Beaufort Sea." 2 Vols., Climatological Studies No. 24, Atmospheric Environment Service, Toronto.

Danard, M., 1983. "Meteorological Conditions for Maximum Storm Surges in the Beaufort Sea." Atmospheric Dynamics Corp., Victoria, B.C.

Danard, M. and M. Gray, 1984. "Extreme Wind Stresses over Beaufort Sea as Determined from Tuktoyaktuk Winds." Atmospheric Dynamics Corp., Victoria, B.C.

Davies, A.M. and R.A. Flather, 1977. "Computation of the Storm Surge of 1 to 6 April 1973 Using Numerical Models of the North West European Continental Shelf and the North Sea." Dt. Hydrogr. Z., 30, pp. 139-162.

Flather, R.A. and N.S. Heaps, 1975. "Tidal Computations in Morecambe Bay." J. Roy. Astr. Soc., 42, pp. 489-517.

Gray, M. and M. Danard, 1982. "A Review of Methods of Computing Storm Surges in Canadian Waters." Atmospheric Dynamics Corp., Victoria, B.C.

Gumbel, E.J., 1958. Statistics of Extremes, Columbia University Press, New York.

Hall, K., W. Baird and B. Wright, 1983. "Results of a Ten Year Hindcast Study for the Beaufort Sea." Proc. Can. Coastal Conf., Vancouver, May 11-14, 1983, pp. 107-122.

Henry, R.F. 1975. "Storm Surges." Beaufort Sea Tech. Rep. No. 19, Institute of Ocean Sciences, Sidney, B.C.

36

Henry, R.F. and M.G.G. Foreman, 1977. "Numerical Model Studies of Semi-diurnal Tides in the Southern Beaufort Sea." Pac. Mar. Sci. Rep. 77-11, Institute of Ocean Sciences, Sidney, B.C.

Henry, R.F. and N.S. Heaps, 1976. "Storm Surges in the Southern Beaufort Sea." J. Fish. Res. Bd., 33, pp. 2362-2376.

Hodgins, D.O. 1983. "A Review of Extreme Wave Conditions in the Beaufort Sea." Seaconsult Marine Research Ltd., Vancouver.

Hodgins, D.O., P.H. LeBlond and O. Brink-Kjaer, 1981. "A Hindcast Study of Extreme Water Levels in the Beaufort Sea." Seaconsult Marine Research Ltd., Vancouver, and Danish Hydraulic Institute, Horsholm, Denmark.

Hodgins, D.O., P.H. LeBlond and D.A. Huntley, 1983. "Shallow-Water Wave Calculations." Seaconsult Marine Research Ltd., Vancouver.

Kolberg, T.O. and V.K. Shah, 1976. "Shore Erosion and Protection Study - Stage 2. Tuktoyaktuk, N.W.T." Report No. 41, Dept. of Public Works.

Markham, W.E., 1975. "Ice Climatology of the Beaufort Sea." Beaufort Sea Tech. Rep. No. 26, Institute of Ocean Sciences, Sidney, B.C.

Niwinski, C.T. and D.O. Hodgins, 1984. "Extreme Wave Conditions at Tuktoyaktuk." Seaconsult Marine Research Ltd., Vancouver.

Reimnitz, E. and D.K. Maurer, 1979. "Effects of Beaufort Sea Surges on the Beaufort Sea Coast, Northern Alaska." Arctic, 32, pp. 329-344.

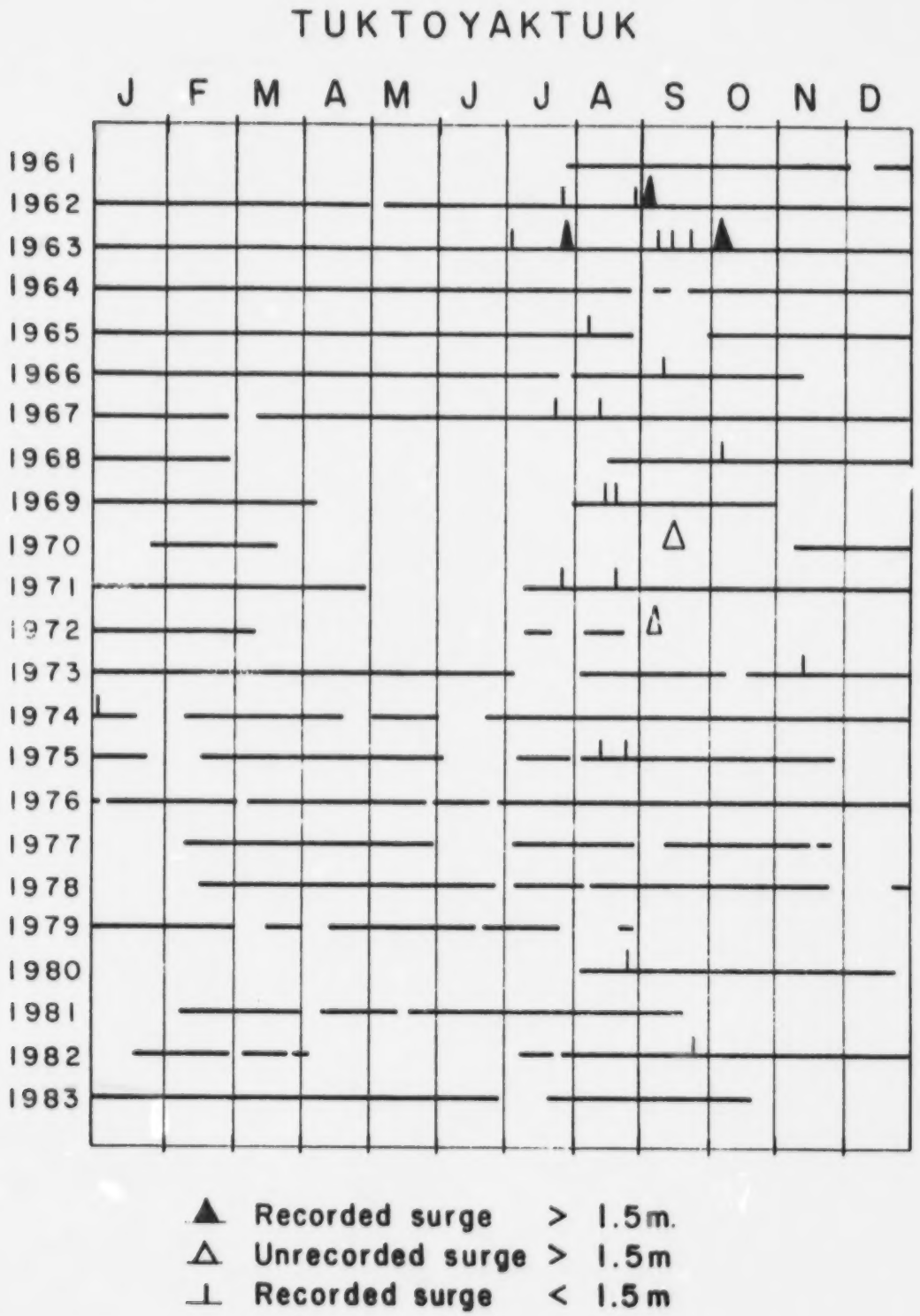

Fig. 1(a) Periods of Tide Gauge Operation

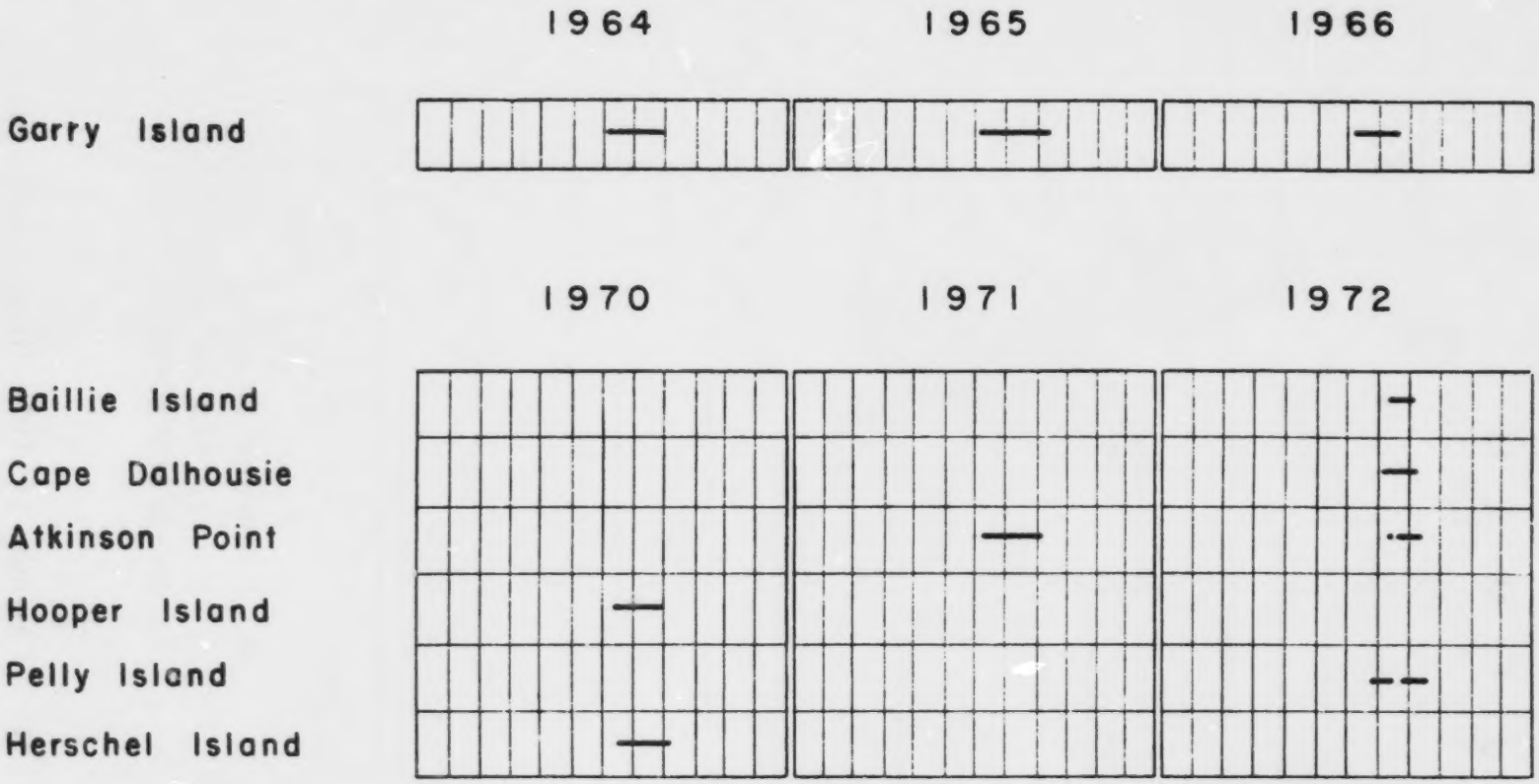

Fig. 1(b) Periods of Tide Gauge Operation

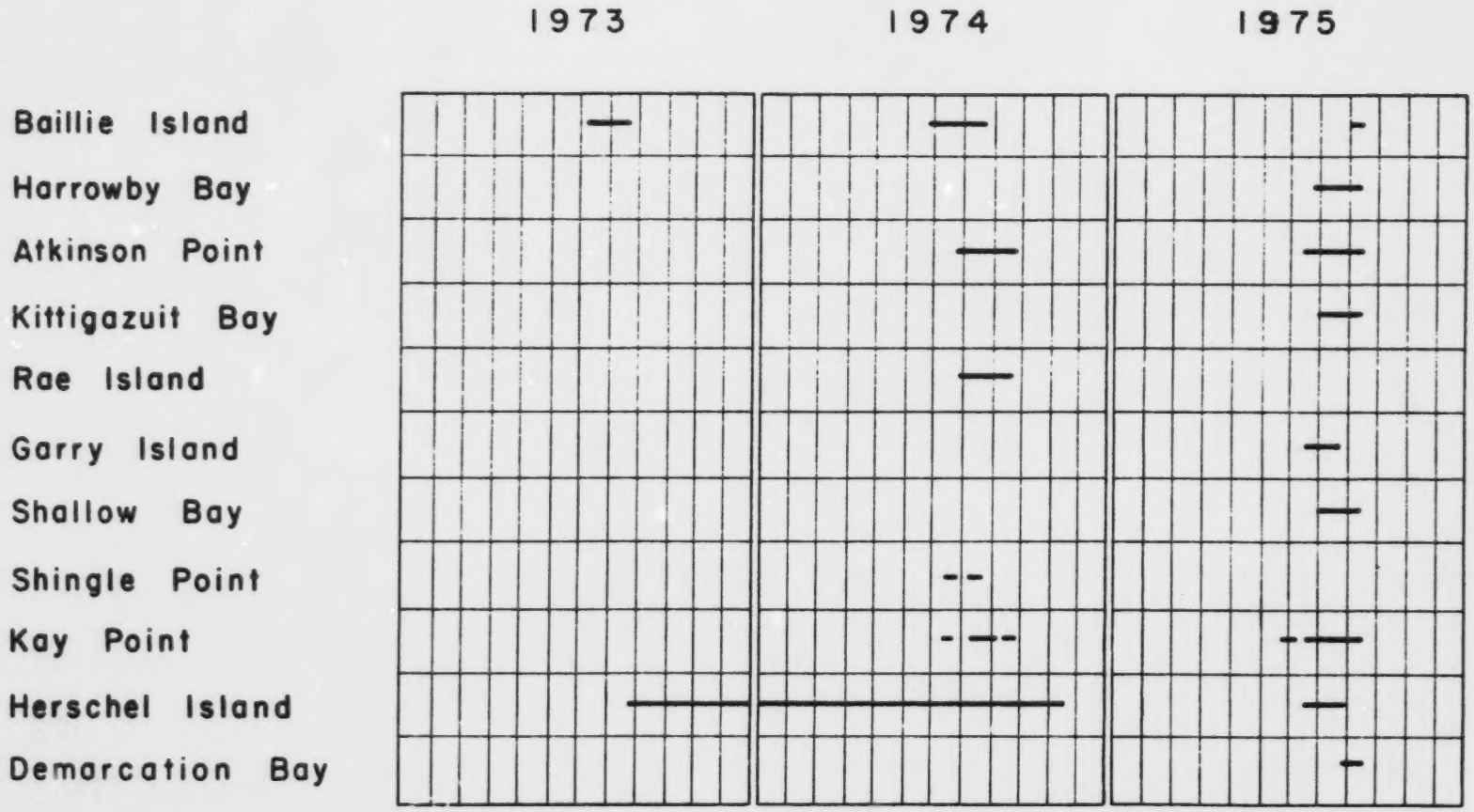

Fig. 1(c) Periods of Tide Gauge Operation

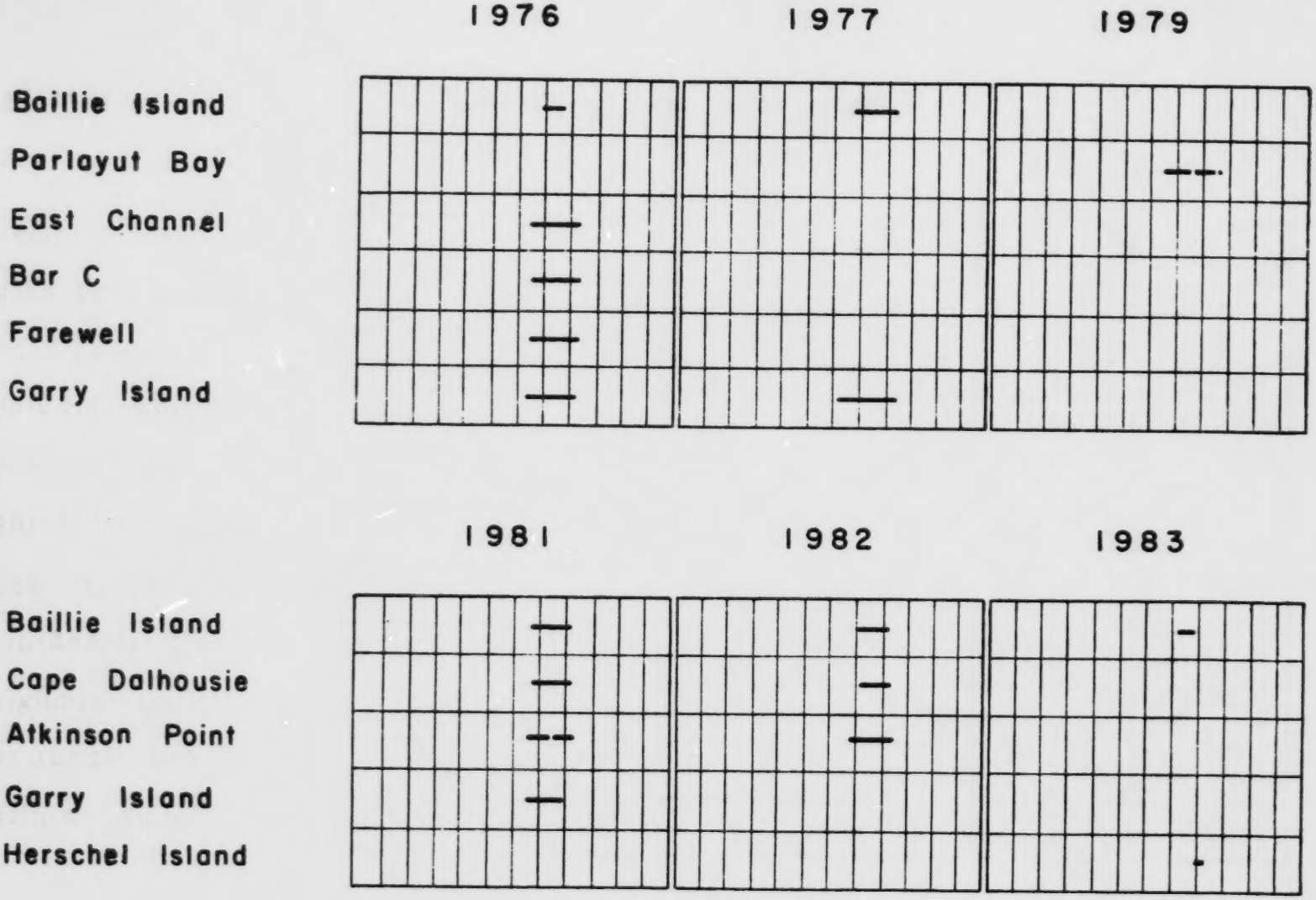

Fig. 1(d) Periods of Tide Gauge Operation

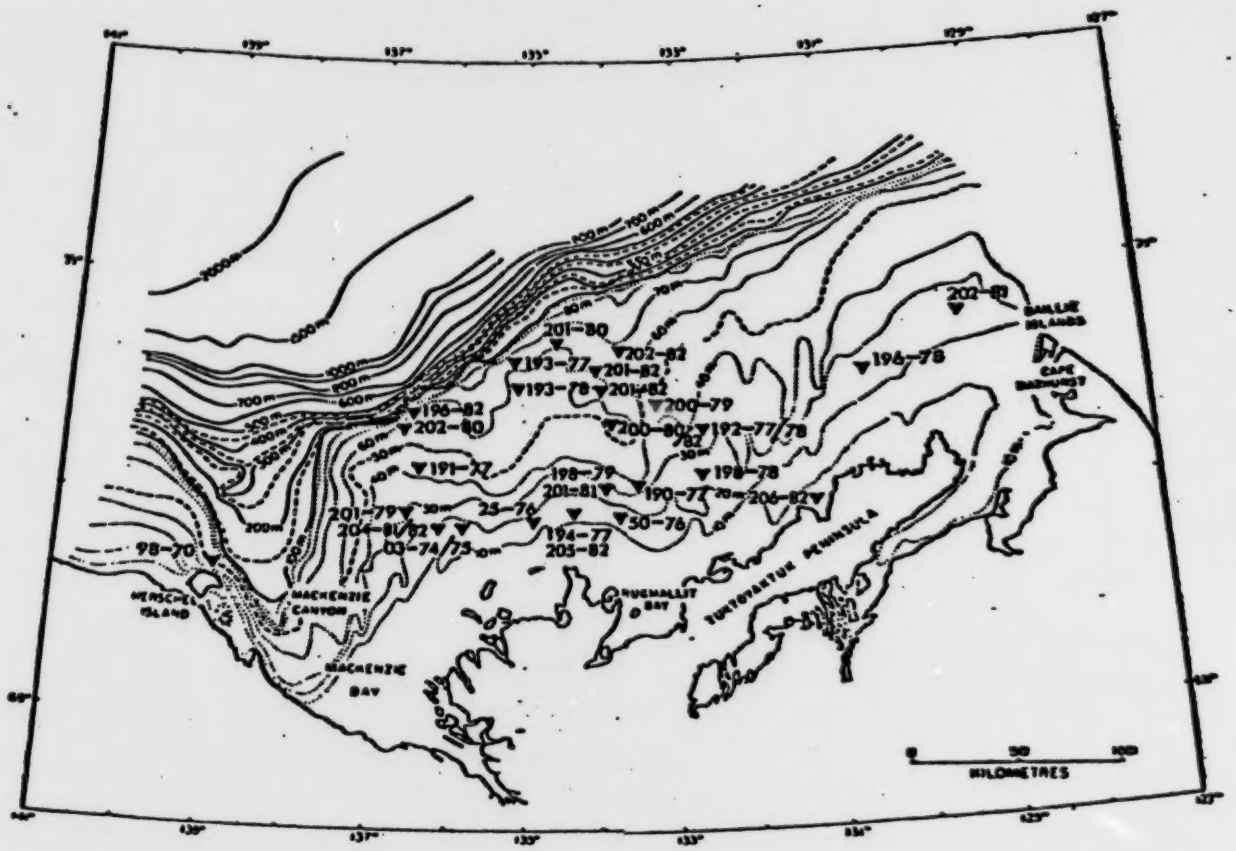

Stn. No.	Name	Location N Lat W Long	From D/M	To D/M	Year	Depth (m)
98	Nerochol Is	69-39 139-00	01/08	30/08	78	50.0
03	Tuktoyaktuk	69-53 135-57	26/08	30/08	74	21.0
03	Tuktoyaktuk	69-53 135-57	08/08	06/09	75	21.0
25	Pullen NW	69-39 134-59	08/08	09/10	76	15.0
30	Pullen WE	69-37 133-50	08/08	08/10	76	15.0
190	Calf-1	70-04 133-38	15/08	13/10	77	33.2
191	Calf-3	70-08 136-25	16/08	11/10	77	42.7
192	Canmar-1	70-11 132-45	07/08	02/10	77	34.1
193	Canmar-2	70-24 135-04	07/08	01/10	77	44.0
194	Isserk	69-58 134-26	11/08	16/09	77	14.0
192	(Khalerk)	70-10 132-44	23/07	04/10	78	31.0
193	(Kopanoar)	70-23 135-06	02/09	04/10	78	57.0
196	Tarsuit	70-34 130-51	31/08	01/09	78	27.0
198	Issungnak	70-04 132-27	04/08	13/08	78	24.0
198	Issungnak	70-04 132-27	19/08	15/10	79	24.0
200	Nerlerk	70-32 133-21	03/08	10/09	79	46.0
201	Tarsuit	69-58 136-36	13/08	18/09	79	30.0
200	Nerlerk	70-24 133-54	11/08	22/09	80	50.0
201	Tarsuit	70-34 134-35	16/08	13/09	80	60.0
202	Explorer IV	70-18 136-36	15/08	07/09	80	60.0
201	Issungnak	70-05 134-26	28/07	31/08	81	27.0
202	Kilannak	70-46 129-21	05/08	14/08	81	25.0
204	Tarsuit	69-53 136-11	13/08	15/08	81	20.0
196	Nerlerk	70-25 133-27	22/07	25/08	82	52.0
196	Orvilruk	70-22 136-32	01/09	29/09	82	58.0
201	Irkaluk	70-35 134-14	22/07	21/08	82	58.0
201	Alvark	70-26 133-59	01/09	29/09	82	62.0
202	Kannalonak	70-44 133-58	22/07	26/07	82	71.0
202	Kannalonak	70-41 133-58	NO DATA		82	70.0
204	Tarsuit	69-53 136-00	30/07	30/08	82	20.0
204	Tarsuit	69-51 136-00	01/09	29/09	82	20.0
205	Ikiyak	69-57 134-30	03/08	25/09	82	14.0
206	McKinley Bay	- - - -	07/08	04/10	82	-

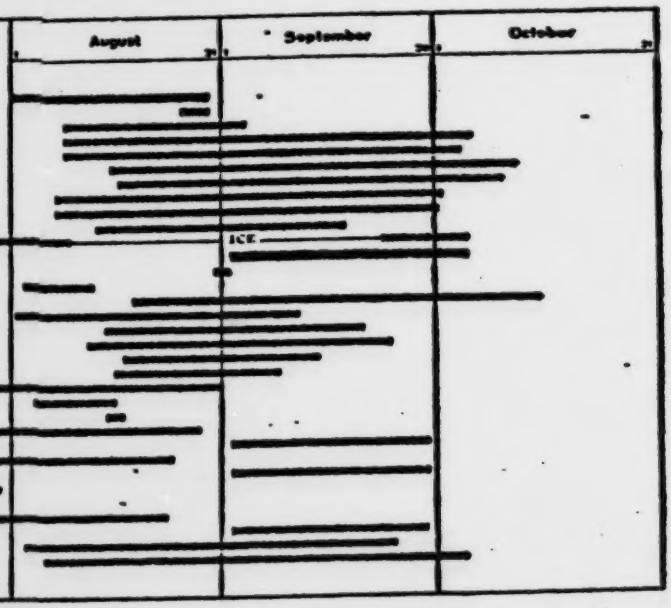

Figure 2 Spatial and temporal distribution of Waverider data in the Beaufort Sea. 1970 to 1982.
. (from Hodgins, 1983)

Seacomsult

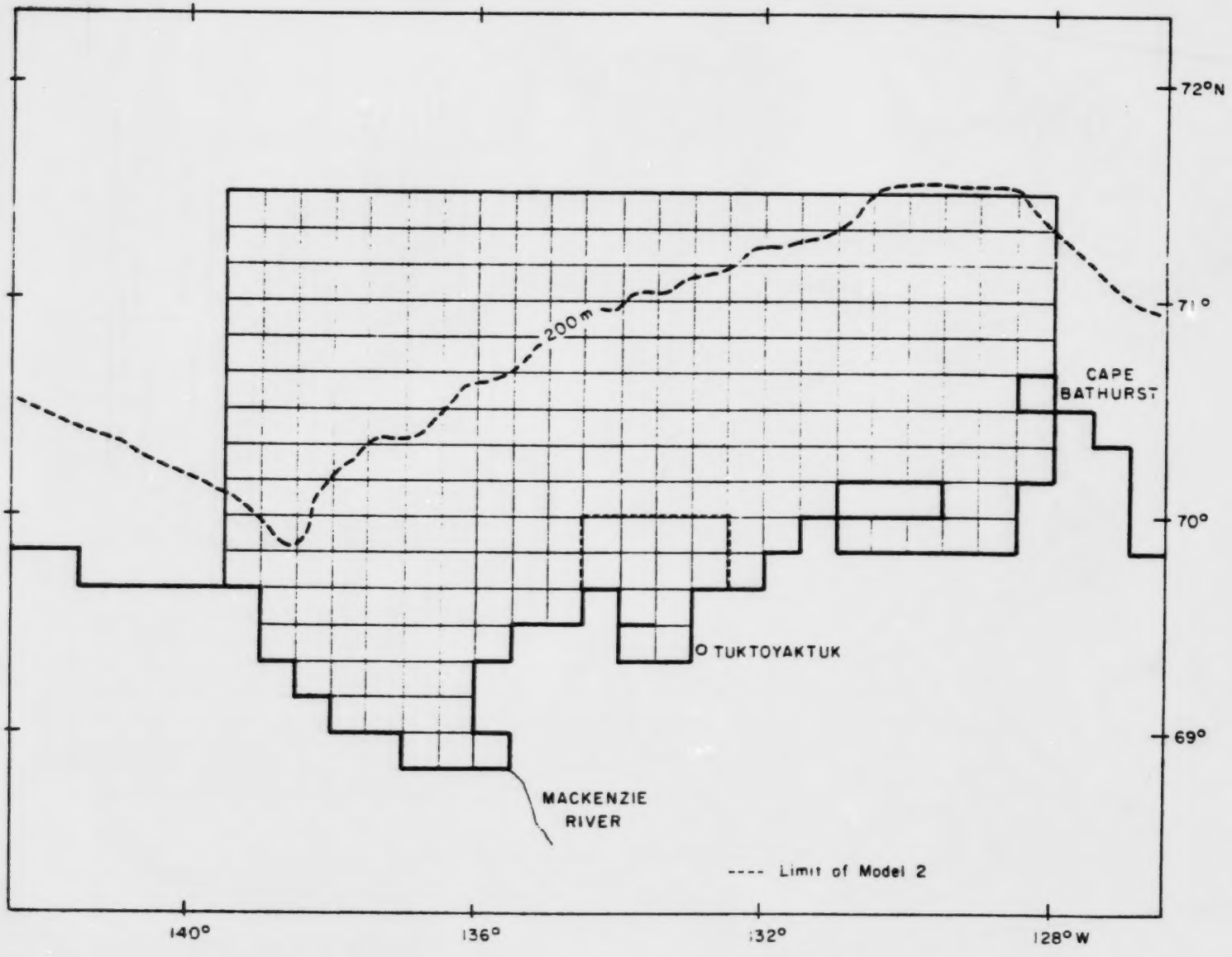

Fig. 3 Grid for Model 1

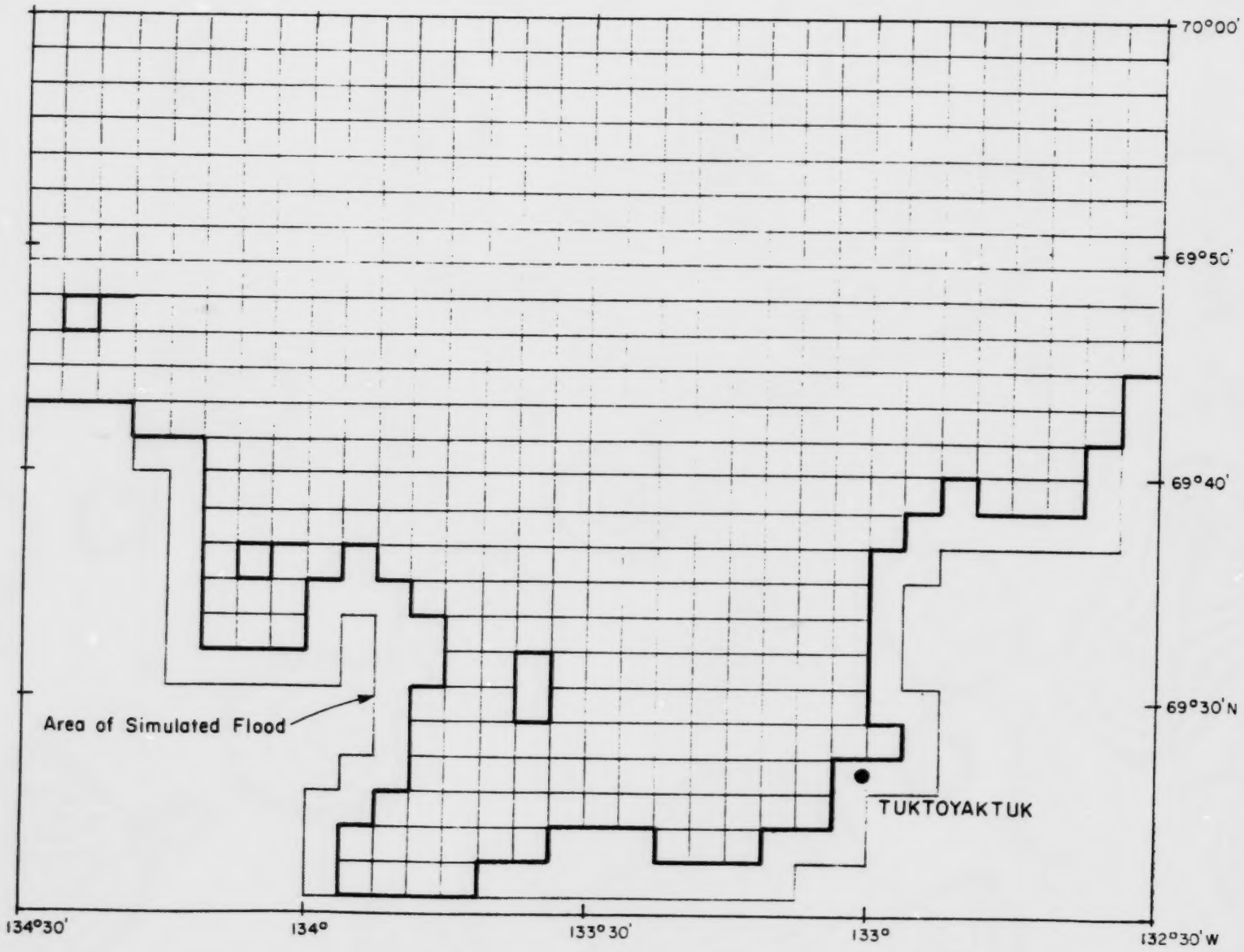

Fig. 4 Grid for Model 2

45

METEOROLOGICAL CONDITIONS FOR

MAXIMUM STORM SURGES

IN THE BEAUFORT SEA

Prepared for

Institute of Ocean Sciences
9860 West Saanich Road
Sidney, B.C. V8L 4B2

Contract Ser. No. OSB83-00117

Prepared by

Maurice Danard
Atmospheric Dynamics Corporation
Woodridge Place, R.R. 7
Victoria, B.C.
V8X 3X3

July 1983

CONTENTS

	Page
Abstract	*ii*
1. Selection of Case Studies	1
2. Computation of Wind Stresses	5
3. Results	7
3.1 Extreme Winds	7
3.2 Time Sequences of Winds, Stresses and Pressure Gradients	7
4. Concluding Remarks	8
Acknowledgments	8
References	9
Figure 1	10
Tables 1 - 4	11 - 13

ABSTRACT

The purpose of this report is to determine extreme wind stresses and pressure gradients producing storm surges at the Tuktoyaktuk peninsula. Sea level pressure maps were examined for the months of June to October during the years of 1970 to 1982, omitting 1971 and 1973 due to unavailability of data. Cases with strong onshore winds were selected during each of the 11 years. The maximum geostrophic wind for each year was then fit to the Gumbel distribution to give extreme values for various return periods. In addition, the "maximum probable storm" was designed by selecting the most intense cyclone which occurred in the vicinity of the Beaufort Sea during the 11 years and assuming its track had been such as to maximize winds over the domain of interest. This hypothetical storm was estimated to have a return period of 90 y.

Stresses were calculated using Monin-Obukhov similarity theory. Time sequences of winds, stresses and pressure gradients are presented for the extreme actual storms of 1972 and 1981 (return periods of 3 and 10 y, respectively), a hypothetical 25-y storm and the "maximum probable storm".

1. SELECTION OF CASE STUDIES

Sea-level pressure maps analysed by Arctic Weather Central in Edmonton were examined for the months of June to October, inclusive. Maps were available for 11 years from 1970 to 1982, inclusive, with the omission of 1971 and 1973. Cases were selected with an onshore component of the geostrophic wind to the Tuktoyaktuk Peninsula. That is, directions ranged from 253° (17° south of west) through north to 073° (17° north of east). All periods with significant geostrophic winds from the appropriate direction were initially included. Each year had at least one time period and some years (e.g., 1981 and 1982) had several.

For each map time the pressures were first abstracted at the four points 1, 2, 5 and 6 in Fig. 1. This approximates the area covered by IOS's storm surge model. The coordinates of the points are given in Table 1. There were a total of 27 storm periods and 170 individual maps so treated in the 11-year period. The following equation was fit by least squares to the pressures at the 4 corner points:

$$p = a_0 + a_1 x + a_2 y \tag{1}$$

where

$$x = -(\lambda - \bar{\lambda}) a \overline{\cos \phi} \tag{2}$$

$$y = a(\phi - \bar{\phi}) \tag{3}$$

ϕ and λ are latitude and longitude in radians, a is the earth's radius, and the bar indicates an average over the four corner points. Obviously from (1)

$$\frac{\partial p}{\partial x} = a_1 \tag{4}$$

49

$$\frac{\partial p}{\partial y} = a_2 \tag{5}$$

The geostrophic wind components are

$$u_g = -\frac{1}{\rho f}\frac{\partial p}{\partial y} = -\frac{a_2}{\rho f} \tag{6}$$

$$v_g = \frac{1}{\rho f}\frac{\partial p}{\partial x} = \frac{a_1}{\rho f} \tag{7}$$

As the lows passed t[illegible]gh, there was typically an interval of about 24 h from the time of a significant offshore wind to the establishment of a moderate onshore wind. Therefore, resurgence (rapid change from a negative to a positive surge) should not be an important factor.

For the purpose of computing return periods, in each year the storm was selected which had the highest geostrophic wind speed. This was considered to be the storm which would produce the highest storm surge for that year, without regard to ice conditions. This gave a sample of 11 peak storm periods, one for each year. These were not necessarily the 11 most intense storms in the entire 11 years. In fact the top 2 storms both occurred in 1981 but only the most severe was retained.

In addition, the "maximum probable storm" was constructed by choosing the most intense low pressure area of the 11 years which passed near the Beaufort Sea and assuming its history had been such as to produce the maximum pressure gradient over the model domain. This was a 966 mb low actually located at (70°N, 107°E) at 1800 GMT 15 Sept. 1970. The record low sea-level pressure in this area for the period 1953-1977 is also given by Burrows *et al.* (1979) as 966 mb. However, probably only long-term stations with continuous records were used in their study so that the record

50

extreme would likely be even lower. To maximize conditions over the Beaufort Sea we simply moved the low westward 600 km. This same low actually produced the maximum real storm period of 1970 as it passed through the model domain from 13 - 15 Sept., deepening as it moved eastward. In effect we essentially assumed the deepening took place when the low was 600 km to the west. The hypothetical map at the time of maximum winds is given in Fig. 1.

However, the geostrophic wind computed as described above is probably an underestimate since it is essentially a vector average over the area, extreme pressure gradients in strong winds tend to be underestimated since data is sparse, the analysis procedure smooths out small-scale features, and Eq. (1) does not exactly fit all 4 points. Therefore, to obtain a more realistic geostrophic wind for the annual extreme and "maximum probable" storm periods, we abstracted the pressures at the additional points 3 and 4 in Fig. 1. Eq. (1) was then fit exactly to the pressures at the vertices of the triangles 123, 234, 345 and 456. The root-mean-square geostrophic wind over the four triangles was then calculated and pressure gradients computed from this.

The root-mean-square geostrophic wind may still produce unrealistically low surface winds due to neglect of mesoscale accelerations as the air moves from cold ice to warmer water (an "ice-breeze" effect) with a further acceleration near shore if the land is warmer than the water. Another factor contributing to underestimating winds is anticyclonic curvature of the air trajectories although this is evident in only some of the cases. To account for these and other influences discussed earlier, the surface (10 m) wind will be assumed equal to the root-mean-square geostrophic wind for the purpose of computing stresses. This is consistent with the experience

51

of Beaufort Weather and Ice Office (Ed Hudgson, personal communication) that surface winds are approximately equal to the geostrophic value if conditions are unstable.

52.

2. COMPUTATION OF WIND STRESSES

These were calculated from the 10 m wind V using Monin-Obukhov similarity theory and Deardorff's (1972) equations (integrated forms of the flux profiles originally derived by Paulson (1970) with Businger *et al's.* (1971) values of the numerical constants). The following equations were solved iteratively:

$$u_* = CV \tag{8}$$

$$z_0 = 0.032\, u_*^2/g \tag{9}$$

$$L = -\frac{u_*^2 \theta}{k\, g\, C_h\, \Delta\theta} \tag{10}$$

$$C = \frac{k}{\ell n\left(\frac{z}{z_0}\right) + f_1\left(\frac{z}{L}\right)} \tag{11}$$

$$C_h = \frac{k}{0.74\left[\ell n\left(\frac{z}{z_0}\right) + f_2\left(\frac{z}{L}\right)\right]} \tag{12}$$

Here u_* is the friction velocity, z_0 is the roughness length (see Charnock (1955) and Delsol *et al.* (1971)), L is the Monin-Obukhov length, $\Delta\theta$ is the surface potential temperature minus the potential temperature at z = 10 m (sea temperature minus the air temperature), and $f_1(z/L)$ and $f_2(z/L)$ are stability corrections to the logarithmic profile. Hsu (1973) interpreted the constant (0.032) in Eq. (9) as the ratio of wave height to length. If this ratio is greater in the shallow water near the shore than in deep water, then a larger value of the constant should be used.

53

The surface stress is

$$\tau = \rho u_*^2 = \rho C^2 V^2 \qquad (13)$$

and is in the direction of the 10 m wind. We used $\Delta\theta = 5°C$ since the air was colder than the water in the cases investigated. The above procedure gave drag coefficients C^2 varying from 1.8×10^{-3} for $V = 10$ m/s to 4.2×10^{-3} for $V = 40$ m/s (see Fig. 17 of Gray and Danard (1982)).

3. RESULTS

3.1 Extreme Winds

Extreme on-shore surface winds, computed as described in Section 1 (see last paragraph), are given in Table 2. Since these are averages over the entire model domain, some observed winds will be higher. Speeds in Table 2 range from 9.4 m/s in 1979 (evidently a non-stormy year) to 19.5 m/s in 1981. In fact, 1981 had a second stormy period (06/30/01/81) with stronger winds than the maximum in any of the other 10 years.

Extremes for various return periods are presented in Table 3. These were calculated using the Gumbel extreme value distribution (Gumbel (1958)). The values must be interpreted cautiously since only 11 years of data are available. Normally, the sample size should be at least 15.

The peak area-average wind for the "maximum probable storm" (see Section 1) was 26.1 m/s, which has an estimated return period of about 70 yr.

3.2 Time Sequences of Winds, Stresses and Pressure Gradients

Table 4 gives conditions for the extreme storms of 1972 and 1981, which have return periods of about 3 and 10 yrs, respectively.

Table 5 gives similar values for two hypothetical storms. For the 25 yr storm, the maximum speed is given by Table 3. The time variation of direction and speed was found by averaging the four top storms of the 11 years (3-4 Oct. 1981, 29-30 Oct. 1981, 27 Aug. 1975 and 14-15 Sept. 1970) and scaling the speeds to the 25 yr storm. The method of determining the "maximum probable storm" was described in Section 1.

4. CONCLUDING REMARKS

One striking feature of this study was that observed winds were stronger than would be expected from the analysed pressure gradient. Although steps were taken to offset this (see Section 1), the winds given in Tables 2 and 3 and the stresses in Table 4 may still be underestimated. If the true winds are only 10% higher than those in Tables 2 and 3, the true stresses will be more than 21% higher than those in Table 4 (z_0 increases with wind speed so that the stress varies more rapidly than the square of the wind). Therefore it is recommended that an engineering "factor of safety" be applied to the stresses of Table 4. This factor is probably best determined by storm surge model simulations verified with actual water level data.

ACKNOWLEDGMENTS

The assistance of Coralie Wallace and Cindy Powell in preparing the data and Georgina Smith in typing the report is gratefully acknowledged.

REFERENCES

Burrows, W.R., R.A. Treidl and R.G. Lawford, 1979: The southern Ontario blizzard of January 26 and 27, 1978. Atmos.-Ocean. 17, 306-320.

Businger, J.A., J.C. Wyngaard, Y. Izumi and E.F. Bradley, 1971: Flux profile relationships in the atmospheric surface layer. J. Atmos. Sci., 28, 181-189.

Charnock, H., 1955: Wind stress on a water surface. Quart. J. Roy. Meteor. Soc., 81, 639-640.

Deardorff, J.W., 1972: Parameterization of the planetary boundary layer for use in general circulation models. Mon. Wea. Rev., 100, 93-106.

Delsol, F., K. Miyakoda and R.F. Clarke, 1971: Parameterized processes in the surface boundary layer of an atmospheric circulation model. Quart. J. Roy. Meteor. Soc., 97, 181-208.

Gray, M. and M.B. Danard, 1982: A review of methods of computing storm surges in Canadian Waters. Prepared for Meteorological Services Research Branch, Atmospheric Environment Service, Downsview, Ont., by Atmospheric Dynamics Corporation, Victoria, B.C., March 1982, 116 pp.

Gumbel, E.J., 1958: Statistics of Extremes. Columbia University Press, New York.

Hsu, S.A., 1973: A dynamic roughness equation and its application to wind stress determination at the air-sea interface. J. Phys. Ocean., 4, 116-120.

57

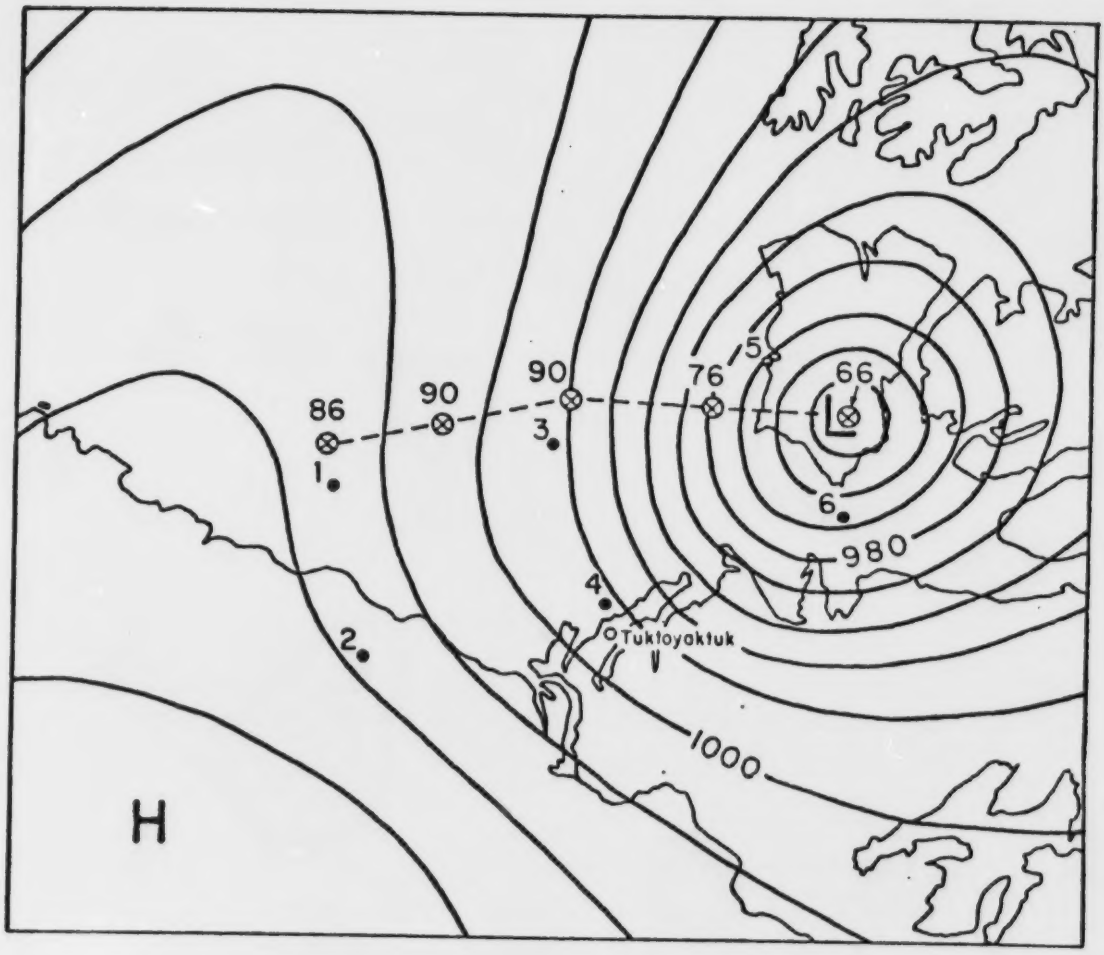

FIG. 1. Hypothetical sea level pressure field (mb) for the "maximum probable storm". Circles indicate successive 6 h positions of the low centre. The six dots labelled 1,•••,6 are points at which pressures were abstracted. Map scale is $1:10^7$.

TABLE 1. Coordinates of points 1 - 6 in Fig. 1.

Point	Latitude	Longitude
1	71.0°N	144.3°W
2	68.8	142.2
3	71.9	134.9
4	69.7	132.9
5	72.9	125.5
6	70.7	123.5

TABLE 2. Computed extreme onshore surface winds from June to October, inclusive, of each year averaged over entire storm surge model domain.

Date (GMT/day/mo./yr.)	Speed (m/s)	Direction (°)
00/28/07/82	16.0	341
06/04/10/81	19.5	357
12/30/08/80	15.1	282
18/14/06/79	9.4	336
00/26/08/78	12.1	298
18/21/09/77	11.5	312
18/18/10/76	12.8	306
12/27/08/75	18.2	264
12/11/08/74	15.2	286
12/02/09/72	15.8	339
18/14/09/70	15.9	308

TABLE 3. Extreme surface wind speeds for various return periods, computed from data of Table 2.

Return period (yr)	Speed (m/s)
2	14.3
5	17.8
10	20.1
25	23.0
50	25.2
70	26.18

Sample size (11)

TABLE 4. Time sequences of winds, stresses and pressure gradients for the storms of 1-2 Sept. 1972 (return period of about 3 yrs), 3-4 Oct. 1981 (return period of about 10 yrs), a hypothetical 25-yr storm, and the "maximum probable storm". t is the time of maximum winds. The x-axis points east and the y-axis north.

Storm	Time	Speed (m/s)	Direction (°)	τ_x (n m^{-2})	τ_y (n m^{-2})	$\partial p/\partial x$ (n m^{-3})	$\partial p/\partial y$ (n m^{-3})
1972	t-18 h	9.5	326	0.12	-0.18	$-1.4\ 10^{-3}$	$-0.9\ 10^{-3}$
	t-12	12.9	326	0.24	-0.36	-1.9	-1.3
	t-6	15.1	332	0.30	-0.56	-2.4	-1.3
	t	15.8	339	0.25	-0.66	-2.6	-1.0
	t+6	11.6	021	-0.12	-0.32	-1.9	0.7
1981	t-18	8.4	044	-0.12	-0.12	-1.1	1.0
	t-12	15.4	044	-0.46	-0.48	-2.0	1.9
	t-6	18.2	019	-0.33	-0.97	-3.0	1.0
	t	19.5	357	0.06	-1.22	-3.4	-0.2
	t+6	18.6	352	0.15	-1.08	-3.3	-0.5
	t+12	17.1	343	0.26	-0.84	-2.9	-0.9
25 yr	t-12	16.2	340	0.25	-0.70	-2.7	-1.0
	t-6	19.2	341	0.38	-1.12	-3.2	-1.1
	t	22.3	334	0.76	-1.55	-3.5	-1.7
	t+6	20.2	339	0.48	-1.25	-3.3	-1.3
max. prob.	t-18	12.5	293	0.38	-0.16	-0.9	-2.0
	t-12	18.7	284	1.07	-0.27	-0.8	-3.2
	t-6	21.4	309	1.21	-0.98	-2.4	-2.9
	t	26.1	342	0.80	-2.47	-4.4	-1.4

61

EXTREME WAVE CONDITIONS AT TUKTOYAKTUK

Prepared For

Fisheries and Oceans, Canada
Institute of Ocean Sciences
9860 West Saanich Road
Sidney, British Columbia

D.S.S. Contract No. 06SB.FP941-3-2961

By

Seaconsult Marine Research Ltd.
405 - 1200 W. 73rd Avenue,
Vancouver, British Columbia

February 29, 1984

Seaconsult

62

SUMMARY

The purpose of this study was to determine extreme wave heights at Tuktoyaktuk. An extreme wind history provided by the Institute of Ocean Sciences was input to a parametric hindcast model in order to predict the maximum deep-water significant wave height (H_s) and period (T_s). A spectral refraction model was used to modify the deep water wave condition in to shore, where Glukhovskii's (1966) depth dependent wave height distribution was applied to predict the maximum wave heights at the entrance to Tuktoyaktuk harbour. Inshore breaking wave height limits were also established using empirical results from the Shore Protection Manual. The extreme deep water wave condition was found to be given by H_s = 7.6 m and T_s = 11 s. Based on the results of the spectral refraction analysis and Glukhovskii's short-term distribution, a maximum wave height H_m = 4.9 m was predicted for the inshore site near the harbour. This was between the breaking wave height limits (4.6 m and 5.3 m) as given by Shore Protection Manual procedures. The corresponding maximum wave period was 13 to 14 s. The spectral refraction analysis also revealed that the mean direction of the inshore wave energy was incident from 342°T (±1°T) and was not sensitive to changes in the offshore mean wave energy direction. The inshore wave energy spectrum was saturated for frequencies above f = 0.08 Hz; storms less severe than the one used in this study could thus produce maximum waves nearly equal in magnitude to those predicted by this study, assuming that a nearly equal surge response would also be generated.

C.T. Niwinski, P.Eng.
D.O. Hodgins, P.Eng.

Seaconsult

63

TABLE OF CONTENTS

	PAGE
Summary	i
List of Tables	iii
List of Figures	iv
Terms of Reference	v
1. Introduction	1
1.1 Study Purpose	1
1.2 Approach	3
1.2.1 Deep Water Wave Conditions	4
1.2.2 Spectral Refraction Modelling	10
1.2.3 Derivation of Shallow Water Wave Heights	13
2. Discussion of Results	16
2.1 Deep Water Wave Conditions	16
2.2 Storm Water Depth	19
2.3 Spectral Refraction Results	21
2.4 Individual and Breaking Wave Heights	32
2.5 Periods Associated with Maximum Waves	33
3. Extreme Wave Conditions	35
References	39

LIST OF TABLES

64

Table	Title	Page
1	Extreme Wind Time-Series	6
2	Input Parameters for the Spectral Refraction Analysis	19
3	Directional Wave Energy Spectrum at Site A for $\bar{\theta}_o$=340°T	25
4	Directional Wave Energy Spectrum at Site A for $\bar{\theta}_o$=8°T	26
5	Directional Wave Energy Spectrum at Site B for $\bar{\theta}_o$=340°T	27
6	Directional Wave Energy Spectrum at Site B for $\bar{\theta}_o$=8°T	28
7	Results of Spectral Refraction Analysis	32
8	Maximum Wave Heights	32
9	Extreme Wave Parameters	36

Seaconsult

LIST OF FIGURES

Figure	Title	Page
1	Map of Kugmallit Bay showing Tuktoyaktuk and the sites (A,B) at which wave spectra have been calculated.	2
2	Fetch lengths for parametric hindcast.	7
3	Modified SMB hindcast for extreme storm.	8
4	Reverse ray diagrams for T=11.9s.	12
5	Breaking wave height limits.	15
6	Forward ray refraction diagrams for Kugmallit Bay.	17-18
7	Deep water directional wave energy spectra.	20
8	Water elevation in metres above mwl at peak wind (hour no. 18) during simulated extreme surge, from nested model of Kugmallit Bay.	22
9	Refraction model grid (5 km spacing).	23
10	Water depths in meters and shoreline as resolved by 5 km grid spacing.	24
11	Deep and shallow-water wave energy spectra for $\bar{\theta}_o$=340°T.	29
12	Deep and shallow-water wave energy spectra for $\bar{\theta}_o$=8°T.	30
13	Energy spectrum at site A for $\bar{\theta}$=8°.	34
14	Different breaking wave profiles.	37
15	Ranges of deep water wave steepness H_0/L_0 and beach slope m over which different kinds of breakers form.	37

Seaconsult

TERMS OF REFERENCE

Estimates of shallow-water maximum wave heights and their corresponding periods in Kugmallit Bay and the entrance to Tuktoyaktuk Harbour were requested for a single design storm. The wind history for this storm would be supplied to Seaconsult, together with the maximum storm surge levels in and around Kugmallit Bay, for estimating these wave conditions. The return period of this storm would not be specified and the inshore wave heights would not be assigned a probability of occurrence. It was agreed that the extreme wave properties would be interpreted as expected maximum conditions for the specified storm, and that data presented in Seaconsult's report would not be used for design purposes.

The work was executed under the terms of reference of Contract No. 06SB.FP941-3-2961, Supply and Services, Canada for the Department of Fisheries and Oceans, Institute of Ocean Sciences. Dr. Falconer Henry was the Scientific Authority.

67

1. INTRODUCTION

The town of Tuktoyaktuk, and the entrance to its harbour, are located on the Eastern shore of Kugmallit Bay (Figure 1). They are exposed to storm-generated waves arriving onshore from the North and Northwest directions. Because of the low elevation of the townsite and the coincidence of large storm surges with westerly-northwesterly winds, inundation and accelerated damage to harbour facilities by wind waves is a major concern. The situation is complicated by the shallowness of Kugmallit Bay, averaging only 3 to 4 m below Chart Datum over most of its area (Figure 1). As a result large storm waves will be breaking, and in fact may break at several points between deep water and the shoreline area.

The Department of Fisheries and Oceans has been studying maximum storm surge conditions in Kugmallit Bay using a design storm approach, in which one particular storm expected to give the worst surge and wind wave conditions is analyzed in detail for its wind history. These winds have then been used to hindcast surge, and in this study, offshore wave data.

1.1 Study Purpose

The purpose of the present study was to estimate maximum wave heights near the entrance to Tuktoyaktuk harbour, and to present some information on the breaking properties of these waves for the extreme storm. In particular, the shallow-water directional wave spectrum would be estimated, incorporating the depth-dependent saturation spectrum as derived by Kitaigorodskii et al. (1975). From this, the significant and maximum wave heights at the inshore point would be calculated and compared with empirical models of depth-limited breaking waves. A recommended maximum wave height and its associated period would then be given.

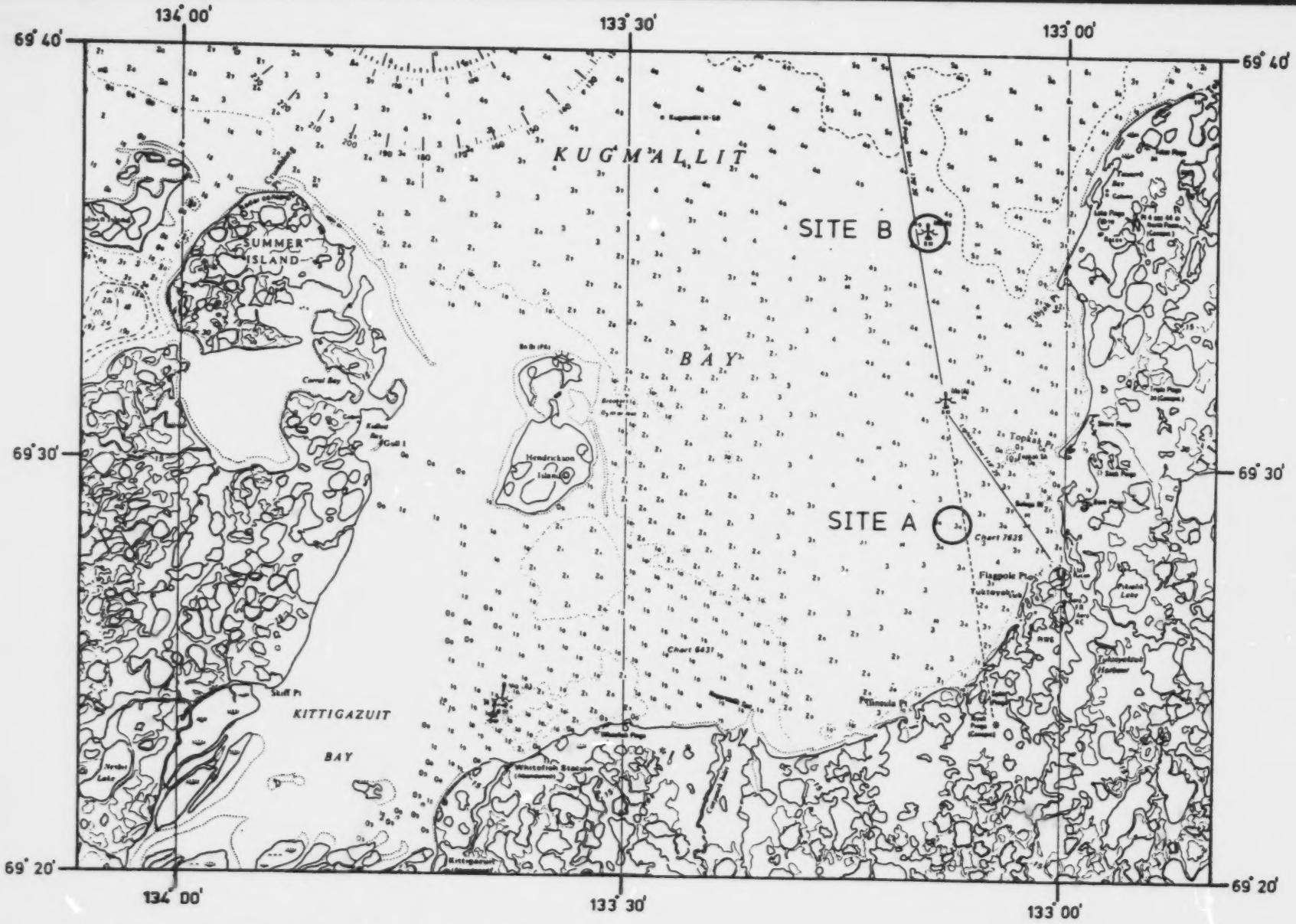

Figure 1 Map of Kugmallit Bay showing Tuktoyaktuk and the sites (A,B) at which wave spectra have been calculated.

69

1.2 Approach

Estimates of the shallow-water wave heights were made as follows:

(1) deep-water wave heights and periods were calculated using the extreme storm wind history as input to a parametric hindcast model;

(2) these were translated into shore using a spectral refraction model accounting for depth-induced refraction, shoaling, and wave breaking; and

(3) the resulting inshore spectra were used to estimate significant and maximum wave heights (Glukhovskii's (1966) distribution); these were compared with empirical depth-limited wave heights.

Extreme wave conditions inshore are strongly dependent on the direction from which the deep-water waves come. This is due to refraction by the bathymetry just outside and in Kugmallit Bay. For this reason two incident wave directions in deep water have been examined, specifically these are 340°T, the storm wind direction, and 8°T, found to give the greatest convergence of wave energy near Tuktoyaktuk. In using 8°T we visualize the storm tracking from west to east (see Hodgins, 1983) for a discussion of severe storms in the Beaufort Sea), and in doing so producing extreme onshore waves from just east of north a few hours later than waves from 340°T.

Wave properties have also been evaluated at two locations: the first, site A (Figure 1), is a representative inshore point on the refraction grid and can be interpreted for the entrance to the harbour area; the second, site B, is located near the end of the shipping channel at the mouth of Kugmallit Bay and is convenient for comparing with conditions at A.

Two numerical models have been used to compute the inshore wave

70

spectra; these are discussed in more detail in the following two sections. The method of computing maximum wave heights from the shallow-water spectra are discussed in the final section of this chapter.

1.2.1 Deep Water Wave Conditions

The deep water wave conditions offshore of Kugmallit Bay were obtained using a parametric wave model based on the Sverdrup-Munk-Bretschneider (SMB) equations modified for variable wind speeds and directions. The SMB equations predict the significant wave height H_s and period T_s given the wind speed and duration over a specified fetch. A method similar to that described by Baird (1978) is used to account for varying wind speed and direction. Directional sectors are defined about the hindcast site, and each wind speed value is assigned, based upon its direction, to a unique sector. The fetch for each sector is provided as input to the model. It is assumed that the winds in each sector act independently of all other sectors.

To account for changes in wind speed within each sector as a function of time, average wind speeds and durations are calculated at each time step in the wind data record. These mean wind speeds are calculated as an average of the values prior to and including the current time step, n, back to the first time step, m, in the active generation-decay sequence. The values for H_s and T_s are taken to be the maximum value for wave height found from each of the (n-m+1) mean wind and duration pairs, and the wave period corresponding to this maximum height value respectively.

Wave decay is assumed to occur when the wind speed falls below the phase speed of the waves, or if the wind changes direction, leaving a wind speed of zero in the sector from which the wind shifted. The wave height decay is taken to be proportional to

71

$(1-t/T_d)$ where t is the time after the decay started and T_d is a constant (for the duration of the decay) equal to the fetch length divided by the deep water wave group velocity, which is in turn calculated from the initial value of the wave period. The fetch length used is the minimum value of the coded fetch length and the duration-limited fetch. The attenuation of wave period is similarly assumed to be proportional to $(1-t/T_d)$.

The significant wave heights and periods are calculated either as actively generated or decaying parameters for each time step in each directional sector. The total significant wave height at each time step is calculated as the square root of the sum of the squares of the actively generated wave heights and of the decaying wave heights. The wave period is assumed to be that of the largest wave height in any sector at that time step.

For the present application, the fetch lengths were determined using the median ice position for the week of September 3 as given by Markham (1981). The fetch lengths were measured from the 20 m depth contour at 70° 00'N Lat. 134° 30'W Long. to the 5/10 ice coverage contour (Figure 2). The wind directions for the design storm used in this study were all within sectors 1, 7 or 8 and the fetch lengths for these sectors are noted in Figure 2. The hourly wind time-series used to hindcast the deep-water wave conditions is given in Table 1, as provided by the Institute of Ocean Sciences, and plotted in Figure 3 as input to the parametric model. The growing limb of the curve was extrapolated linearly back in time to zero wind speed.

The time-series of significant wave heights H_s and period T_s as obtained from the modified SMB hindcast model are also shown in Figure 3 concurrent with the wind input. The deep-water condition analyzed for inshore extreme wave heights was defined by the peak wave height (H_s) in the storm and its corresponding

72

Table 1

Extreme Wind Time-Series

Hour Number	Wind Speed U(m/s)	u	v
0	14.58040	13.43781	-5.65803
1	16.10015	15.14713	-5.45705
2	17.42530	16.58466	-5.34697
3	18.60480	17.83701	-5.28960
4	19.67119	18.95355	-5.26487
5	20.64703	19.96541	-5.26139
6	21.54856	20.89364	-5.27223
7	21.96599	20.69911	-7.35197
8	22.43439	20.42977	-9.26963
9	22.93842	20.11389	-11.02735
10	23.46548	19.77355	-12.63468
11	24.00564	19.42484	-14.10483
12	24.55142	19.07879	-15.45225
13	25.24081	17.18380	-18.48826
14	26.04898	15.31561	-21.07086
15	26.92331	13.55530	-23.26312
16	27.82621	11.93210	-25.13808
17	28.73303	10.45970	-26.76157
18	29.62862	9.12941	-28.18704
19	29.22109	9.14106	-27.75452
20	28.80241	9.15609	-27.30833
21	28.37186	9.17492	-26.84741
22	27.92863	9.19804	-26.37052
23	27.41784	9.22603	-25.87629
24	27.00050	9.25955	-25.36312

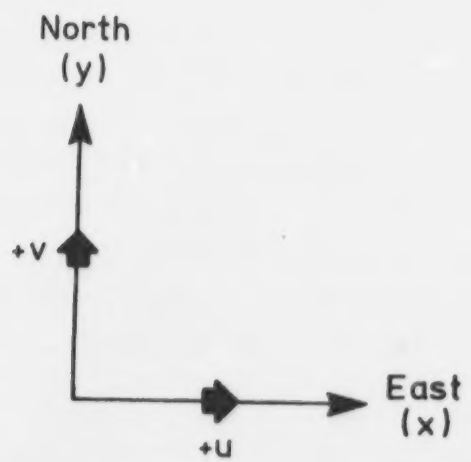

Seaconsult

73

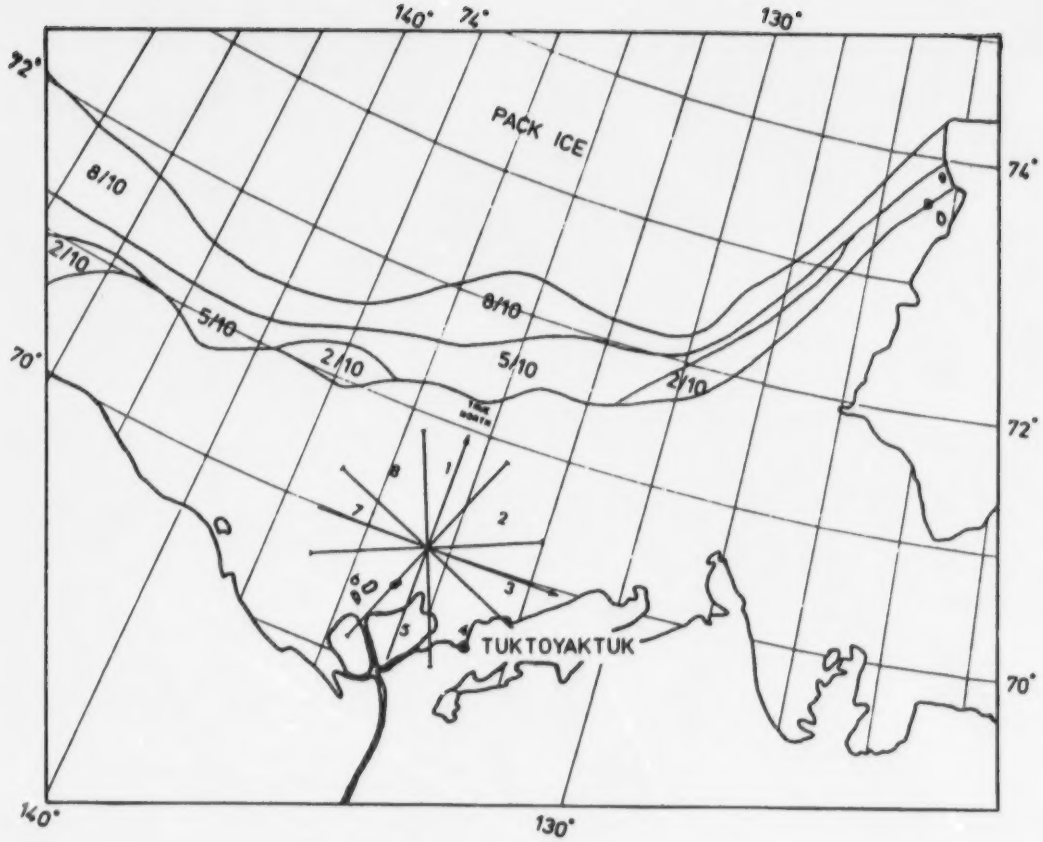

Sector	Fetch (km)
1	195
7	311
8	208

Figure 2 Fetch lengths for parametric hindcast.

Seaconsult

74

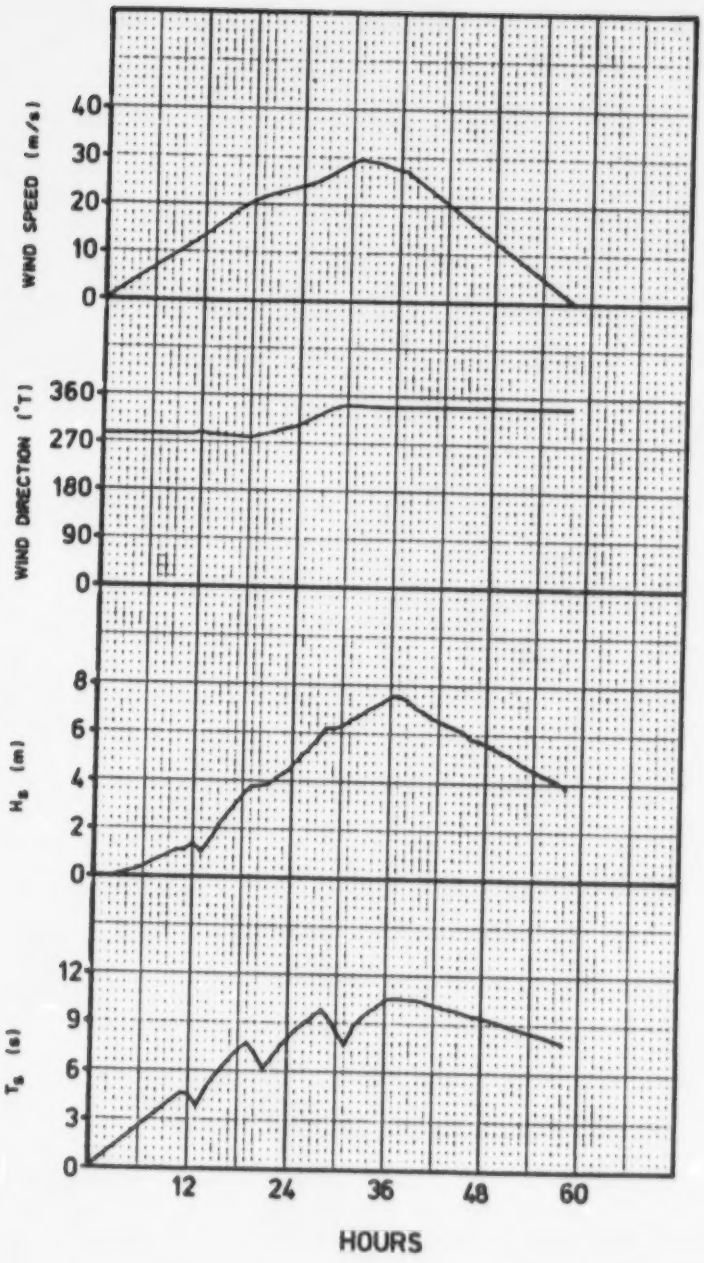

Figure 3 Modified SMB hindcast for extreme storm.

75

period (T_s), which were

$$H_s = 7.56 \text{ m}$$
$$T_s = 10.65 \text{ s} \qquad (1.1)$$

To convert H_s and T_s into a deep-water directional wave energy spectrum, the JONSWAP spectrum with a $\cos^4$ spreading function applied to it was used:

$$S(f,\theta) = S_J(f) \cdot G(\theta) \qquad (1.2)$$

where

$$S_J(f) = \frac{A}{f^5} \exp\ (-B/f^4)\gamma^a \qquad (1.3)$$

$$A \simeq 5H_s^2 f_o^4 / 16\gamma^{1/3} \qquad (1.4)$$

$$B = \frac{5}{4} f_o^4 \qquad (1.5)$$

$$a = \exp\ \left[-(f-f_o)^2/2\sigma^2 f_o^2\right] \qquad (1.6)$$

$$\sigma = 0.07 \quad f \leq f_o$$
$$= 0.09 \quad f > f_o \qquad (1.7)$$

and

$$G(\theta) = \frac{1}{2\sqrt{\pi}} \frac{\Gamma(3)}{\Gamma(2.5)} \cos^4 \left(\frac{\theta-\bar{\theta}}{2}\right) \qquad (1.8)$$

In (1.2) through (1.7), f is frequency, f_o is the peak frequency and γ is the peak enhancement factor. In (1.8) θ is the angle of energy propagation relative to a reference direction (true north was used in this study, with angles measured as positive clockwise in °T), $\bar{\theta}$ is the direction at which the energy spectrum is centred, and Γ is the Gamma function.

For the Beaufort Sea, LeBlond et al. (1982) have shown that $\gamma=2.2$ is an appropriate value, and f_o was obtained using the results of Wilson and Baird (1972):

$$T_p = 1.19\ T_{1/3} - 0.81 \qquad (1.9)$$

where

$$T_p = \frac{1}{f_o} \qquad (1.10)$$

Taking T_s = 10.65 s as in (1.1) for the peak of the hindcast storm, and assuming $T_s \approx T_{1/3}$, the following values were obtained for further analysis of the inshore wave conditions

$$\begin{aligned} T_p &= 11.9 \text{ s} \\ f_o &= 0.084 \text{ Hz.} \end{aligned} \qquad (1.11)$$

1.2.2 Spectral Refraction Modelling

The spectral refraction model used in this study is based on the reverse ray tracing technique employed by Abernethy and Gilbert (1975). A regular Cartesian grid with water depths specified at the nodes is used to define the bathymetry; the model calculates intermediate depths using a four point linear interpolation. A deep-water directional spectrum is provided as input to the model in a parametric form: the JONSWAP spectrum with $\cos^4$ spreading function was used for this study. The increments Δf and $\Delta\theta$ by which the deep and shallow-water directional spectra are discretized, as well as the lowest and highest frequencies (f_{min} and f_{max}) containing non-negligible amounts of wave energy, are also specified. The spectra are thus discretized into I frequencies and J directions with $S(f_i,\theta_j)$ evaluated for i=1,2,...I and j=1,2,...J.

To compute the spectrum at a shallow-water site, a ray is reverse

77

traced from the site for each (f_i, θ_j) combination. For those rays reaching deep water, the input deep-water spectral energy at the ray's deep water frequency and direction is modified along the ray back into the site, where it is assigned to the shallow-water frequency and direction. Discrete frequency-direction combinations for which the reverse traced rays do not reach deep water are assigned a value of 0 for the shallow-water spectral energy. The directional wave energy spectrum is thus computed by the model for a shallow water site. To illustrate the reverse ray tracing scheme, Figure 4 shows reverse ray diagrams that have been traced from sites A and B for f_o=0.084 Hz (T_p=11.9s) and $\Delta\theta$=4°.

The principle advantages of the spectral refraction model over forward ray tracing diagrams are that

(1) a spectral representation of the wave field is obtained in shallow water, from which statistical information about the wave heights may be extracted; and

(2) the uncertainty associated with interpretation of wave conditions inshore of a caustic (a point where forward traced rays cross) is eliminated.

In the present study, the shallow-water wave energy was limited in shallow water by the depth dependent saturation spectrum described by Kitaigorodskii et al. (1975). The maximum energy content for a frequency f has been given as:

$$S_m(f) = \frac{\alpha g^2 f^{-5} \phi(\omega_h)}{8\pi^4} \qquad (1.13)$$

where

$$\omega_h = 2\pi f \left(\frac{d}{g}\right)^{\frac{1}{2}} \qquad (1.14)$$

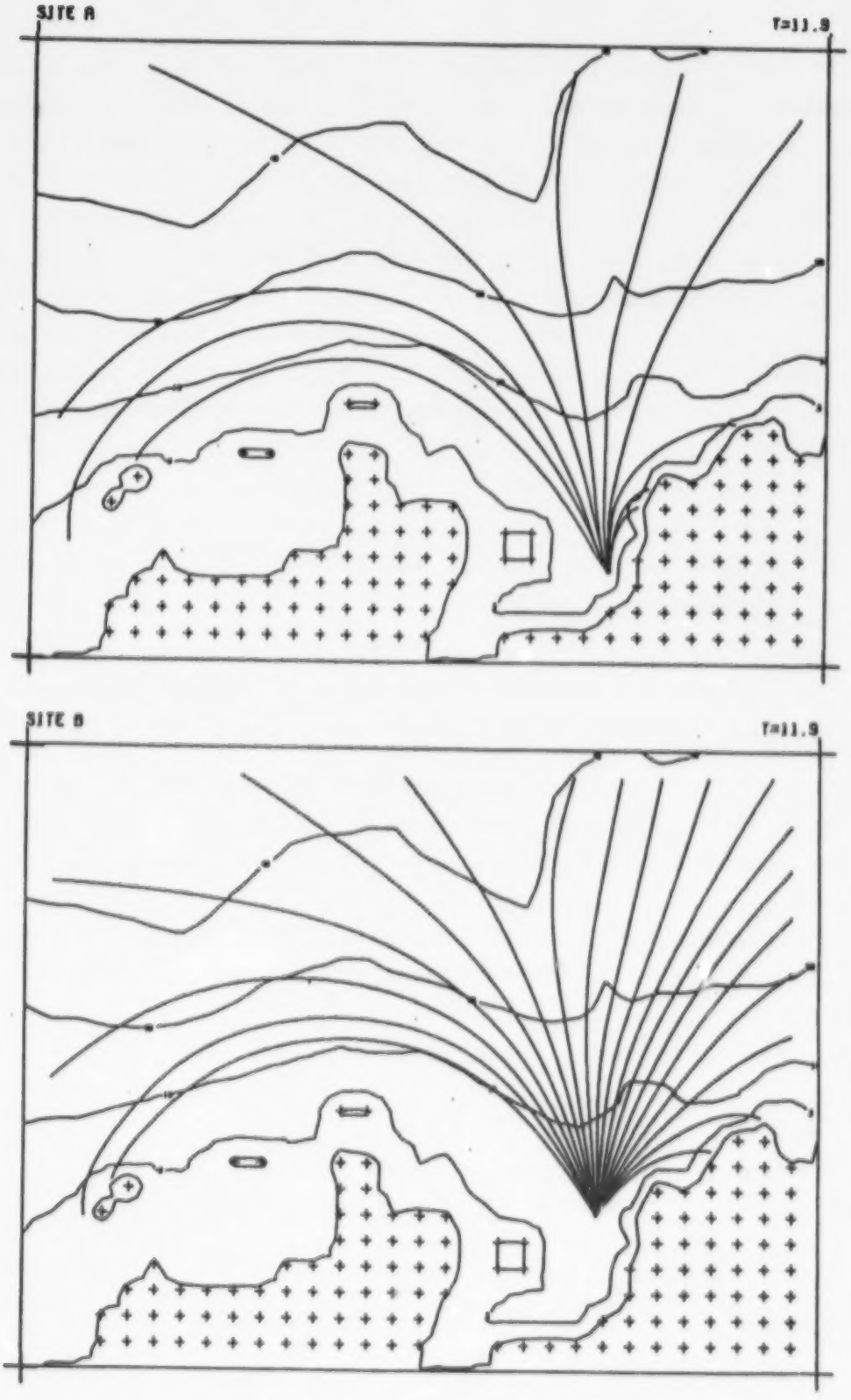

Figure 4 Reverse ray diagrams for T=11.9s.

79

and $\phi(\omega_h)$ is a dimensionless function which varies monotonically from 0 to 1. In (1.13) and (1.14), α is the Phillips parameter set equal to 0.0081, g is the acceleration due to gravity, and d is the water depth. When the shallow-water wave energy $S(f_i)$ for the ith frequency exceeded that defined by (1.13), then the dicrete values of $S(f_i,\theta_j)$ were scaled down linearly by the factor $S(f_i)/S_m(f_i)$ for θ_j, j=1,2,...J.

1.2.3 Derivation of Shallow Water Wave Heights

The shallow-water directional wave energy spectra obtained using the spectral refraction model described in the previous section were integrated numerically to provide the significant wave height (H_s) and mean wave height ($\bar{H}$). The Rayleigh distribution gives

$$H_s = 4\sqrt{m_o} \tag{1.15}$$

$$\bar{H} = \frac{\sqrt{2\pi}}{4} H_s \tag{1.16}$$

where

$$m_o = \sum_{i=1}^{I} \sum_{j=1}^{J} S(f_i,\theta_j)\Delta f \Delta\theta \tag{1.17}$$

The peak frequency (f_o) for the shallow-water spectrum was obtained directly as the discrete frequency containing the most wave energy, and the direction from which the highest waves are incident ($\bar{\theta}$) was taken as the mean direction of wave energy reaching the site.

The maximum wave height (H_m) was calculated using the shallow-water wave height distribution proposed by Glukhovskii (1966), which is similar in form to the Rayleigh distribution but modified to account for water depth. Assuming that the short-term probability distribution P(H) of individual wave heights is known for a given sea state characterized by H_s, the maximum

so

wave height (H_m) can be specified as that value equalled or exceeded once in N waves, where N is the total number of waves expected to occur during that sea state. For a sea state of duration D with peak period T_p, the probability is

$$P(H_m) = 1 - \frac{1}{N} \tag{1.18}$$

where $N=D/\bar{T}_z$ and $\bar{T}_z=0.71T_p$ (Sarpkaya and Isaacson, 1981). The Glukhovskii depth dependent modification to the Rayleigh distribution is:

$$P_G(H)=1-\exp\left[-A(d^*)\ (H/\bar{H})^{B(d^*)}\right] \tag{1.19}$$

where

$$A(d^*)= \frac{\pi}{4(1+d^*/\sqrt{2\pi})} \tag{1.20}$$

$$B(d^*)= \frac{2}{1-d^*} \tag{1.21}$$

and

$$d^*= \frac{\bar{H}}{\bar{d}} \tag{1.22}$$

Note that for deep water where $\bar{H}/d \to 0$, (1.19) reduces to the Rayleigh distribution.

It is expected that the highest waves at Tuktoyaktuk harbour are depth-limited breakers. Thus, the breaking wave condition given in the Shore Protection Manual (U.S. Army, 1977) was used to determine whether the highest waves are governed by depth-limited breaking. Figure 5, reproduced from the Short Protection Manual, defines an upper and lower bound for the breaking wave height H_b as a function of depth at breaking d_b and wave period T. Values of α and β, defining a range for H_b, can be found iteratively given T and d_b. These criteria have been used to calculate a range of breaking wave heights at both sites.

81

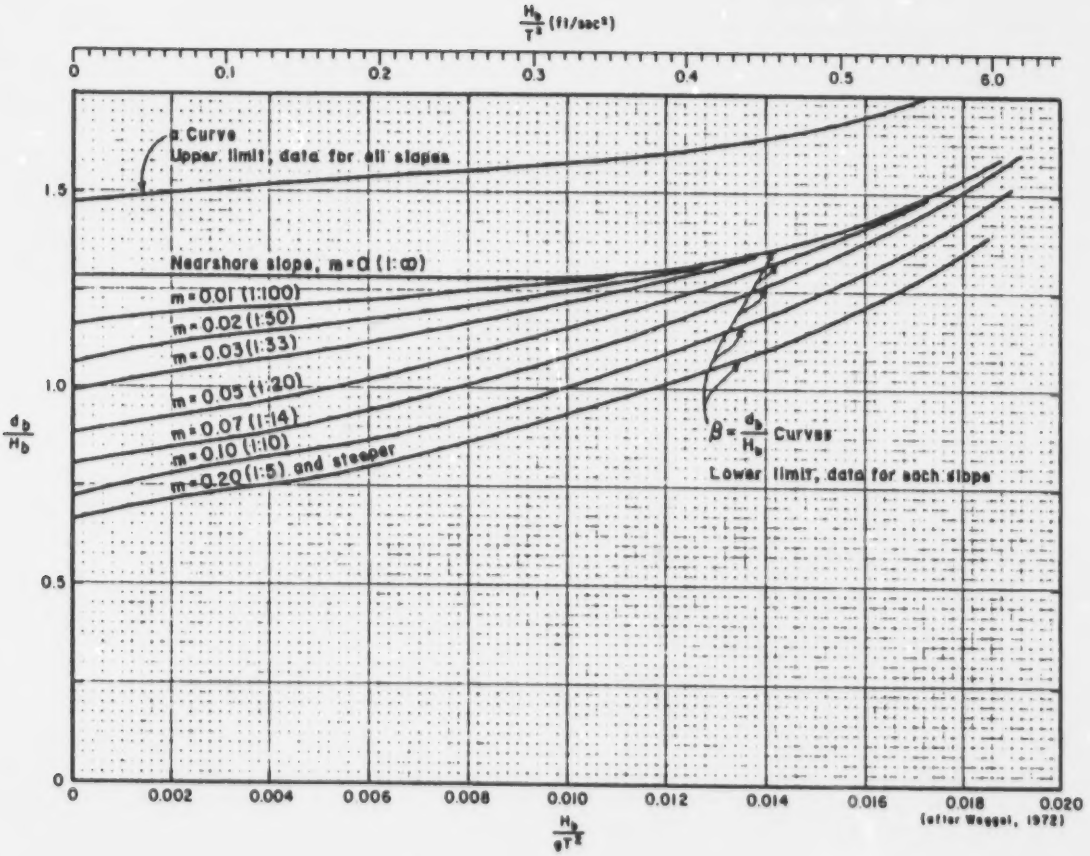

Figure 5 Breaking wave height limits.

Seaconsult

82

2. DISCUSSION OF RESULTS

2.1 Deep Water Wave Conditions

Using a modified SMB hindcast technique, a time-series of significant wave height (H_s) and period (T_s) has been generated from the time-series of wind speed and direction during the extreme storm (Figure 3). The peak wave height and corresponding period used as the extreme deep-water wave condition were given as

$$H_s = 7.56 \text{ m}$$
$$T_s = 10.65 \text{ s} \qquad (1.1)$$

for which

$$T_p = 11.9 \text{ s}$$
$$f_o = 0.084 \text{ Hz} \qquad (1.11)$$

The significant wave height (H_s) and peak frequency (f_o) were applied to a JONSWAP spectrum with a $\cos^4$ spreading function, as given by (1.2) through (1.8), to obtain the deep-water directional spectrum offshore of Kugmallit Bay; γ=2.2 was used for the Beaufort Sea (LeBlond et al., 1982).

The remaining parameter required to define the deep-water wave condition was the mean deep-water incident wave direction, $\bar{\theta}_o$, where the subscript o refers to deep water. During the peak of the storm used for the modified SMB hindcast, the winds were blowing from θ=340°T. However, maximum wave conditions along the east side of Kugmallit Bay would result from $\bar{\theta}_o \cong 10°T$, as revealed by the forward ray refraction diagrams shown in Figure 6 for T=11.9 s and $330°T \leq \theta \leq 10°T$. The diagrams show

83

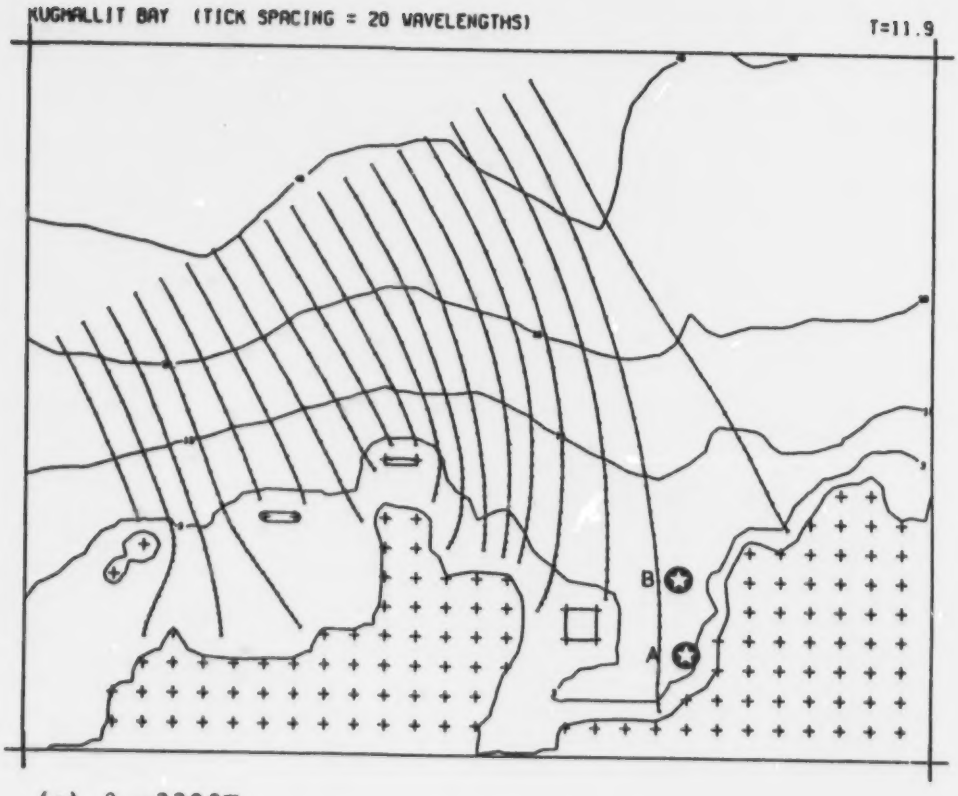

(a) θ_o=330°T

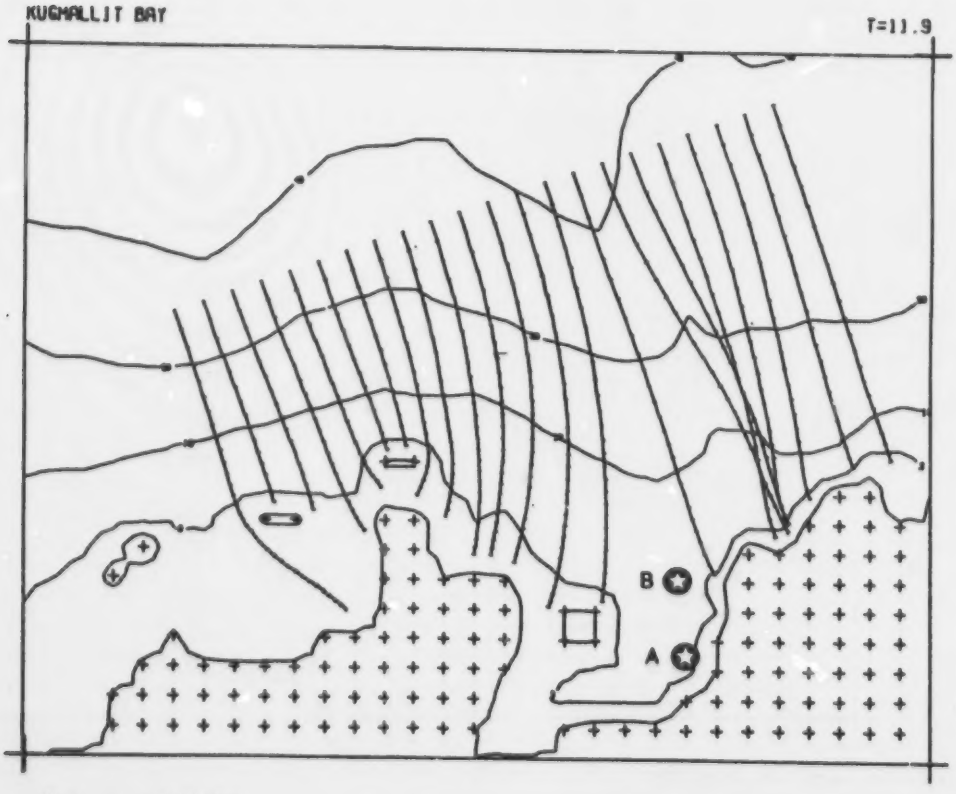

(b) θ_o=340°T

Figure 6 Forward ray refraction diagrams for Kugmallit Bay.

Seaconsult

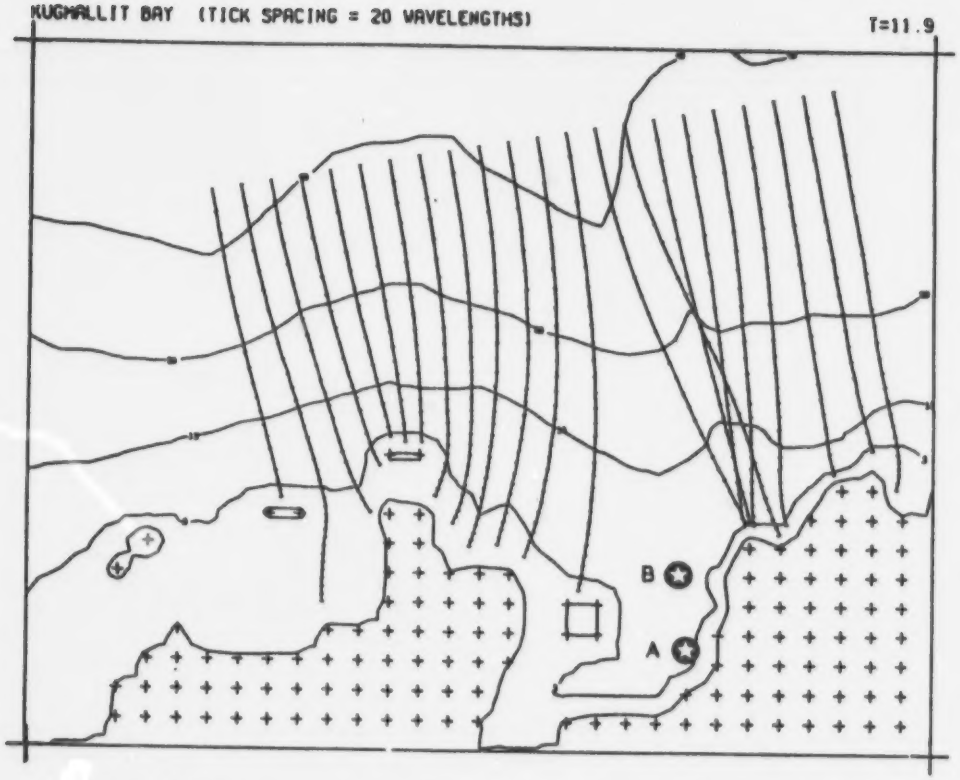

(c) θ_o=350°T

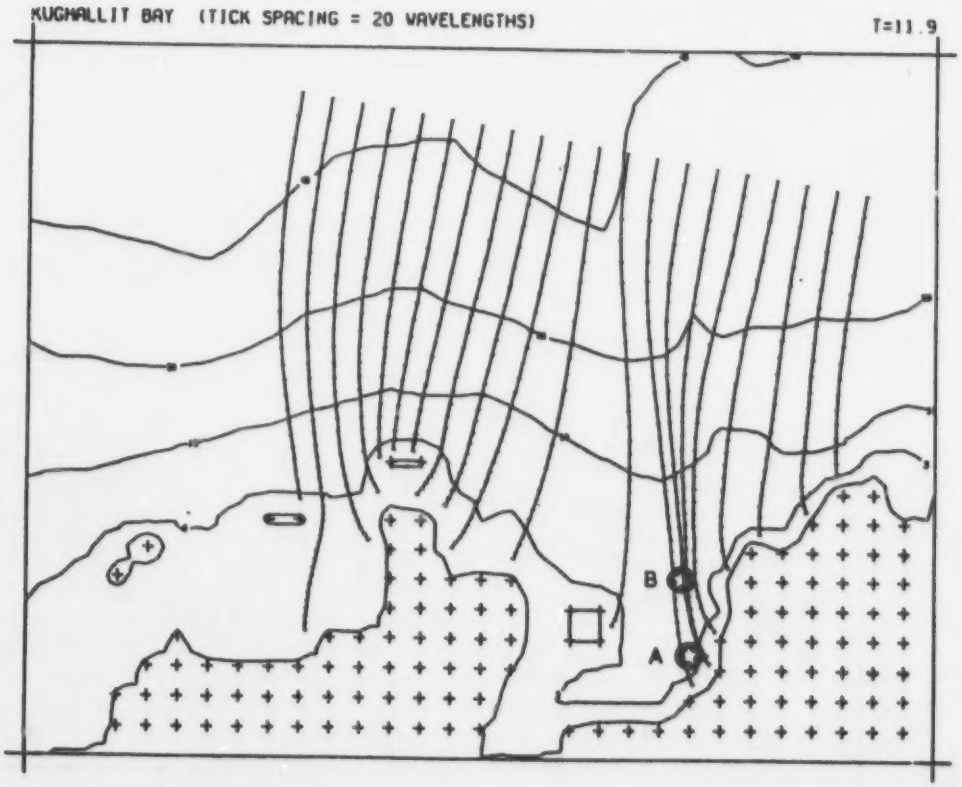

(d) θ_o=10°T

Figure 6 Continued

85

clearly that the promontories on both sides of Kugmallit Bay focus wave energy inshore while the submarine canyon north of the bay (prominent at the 40 m contour) diverges wave energy as it moves inshore. In particular, waves approaching Kugmallit Bay from $\bar{\theta}_o$=10°T (Figure 6(d)) are converged by the offshore extension of the east headland of the bay, producing a concentration of wave energy along the approach to Tuktoyaktuk passing over sites A and B. Consequently, the maximum wave conditions at site B may be expected for $\bar{\theta}_o$ near 10°T. Since the fetch along this direction is of the same order of magnitude (~200 km) as those used for the deep-water hindcast (Figure 2), maximum deep-water waves can, in principle, be generated by winds from just east of north. In view of this situation, the four cases listed in Table 2 were examined using the spectral refraction model.

Table 2

Input Parameters for the Spectral Refraction Analysis

Case	Site	H_s (m)	f_o (Hz)	α	$\bar{\theta}_o$ (°T)	f_{min} (Hz)	f_{max} (Hz)	Δf (Hz)	$\Delta\theta$ (deg)
1	A	7.56	.084	2.2	340	.065	.175	.010	4
2	A	7.56	.084	2.2	8	.065	.175	.010	4
3	B	7.56	.084	2.2	340	.065	.175	.010	4
4	B	7.56	.084	2.2	8	.065	.175	.010	4

The deep-water directional wave energy spectra for $\bar{\theta}_o$=340°T and 8°T are shown in Figure 7 as plotted from the discretized values of $S(f,\theta)$ calculated by the model.

2.2 Storm Water Depth

Extreme inshore wave conditions in Kugmallit Bay are governed by the total water depth at the time of maximum wave conditions. The

Seaconsult

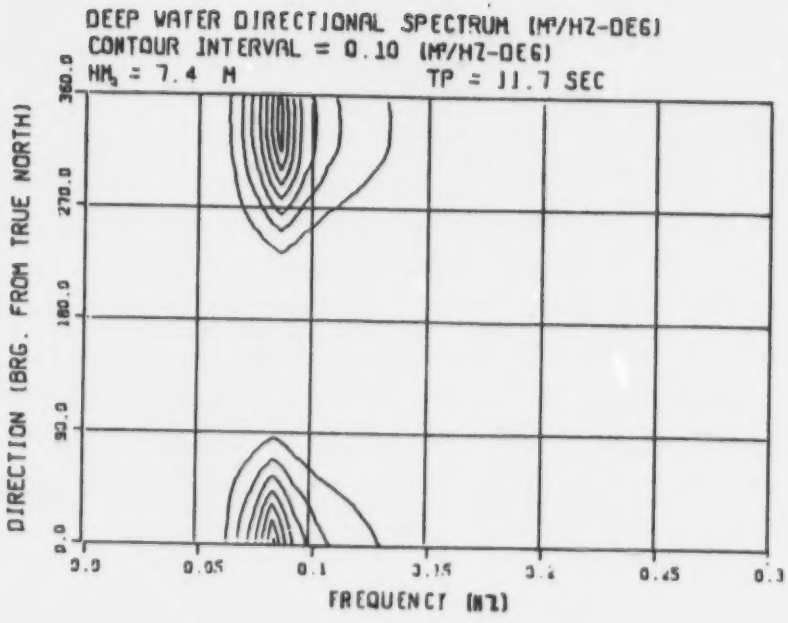

(a) $\bar{\theta}_o = 340°$

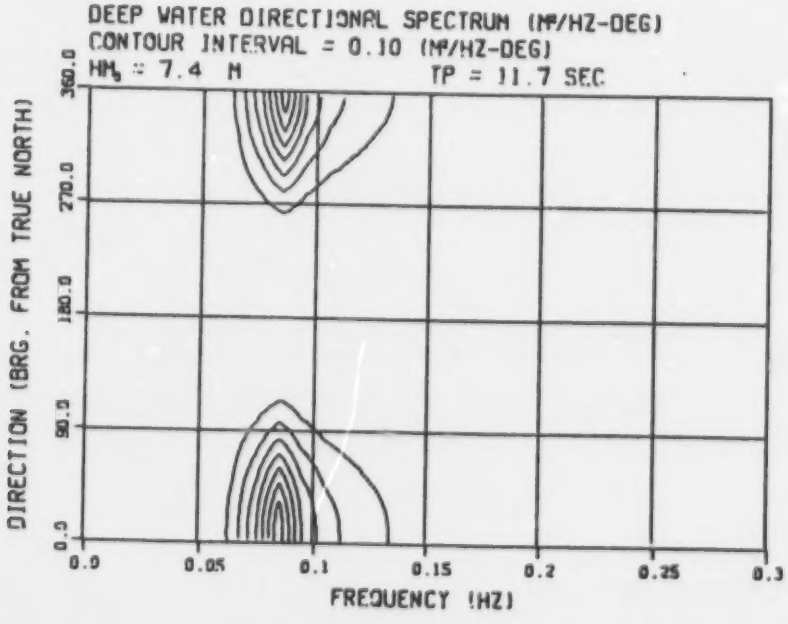

(b) $\bar{\theta} = 8°$

Figure 7 Deep water directional wave energy spectra.

Seaconsult

water depth is defined as the sum of the sounding depth below Chart Datum (CHS chart 23092-A) and the surge above Chart Datum. The storm surge levels were hindcast by the Institute of Ocean Sciences using winds given in Table 1; the predicted surge levels are shown in Figure 8.

A regular Cartesian bathymetry grid was input to the spectral refraction model, with water depths specified at the nodes. Since the bathymetry throughout the study area is gently sloping, generally less than 1:1000, a grid spacing equal to 5 km was small enough to resolve all major features of the bathymetry and shoreline. As shown in Figure 9, the bathymetry grid was extended from Kugmallit Bay out to the 50 m depth contour. It has been assumed that refraction and shoaling effects to the 50 m contour are negligible compared with those which take place from that depth into shore.

The bathymetry and shoreline are shown in Figure 10 as resolved by the 5 km spacing used for this study. Figure 10(a) shows the water depth below Chart Datum while (b) shows the effective bathymetry resulting from the superposition of (a) and the maximum storm surge (Figure 8). The water depths shown in Figure 10(b) were used for all refraction analyses. The total depths, that is depth below Chart Datum plus storm surge level, at sites A and B are 6.85 m and 7.98 m respectively.

2.3 Spectral Refraction Results

The calculated shallow-water spectra for cases 1 through 4 (Table 2) are presented in Tables 3 through 6; the same results are shown graphically in Figures 11 and 12. The results at both sites show that the saturated energy spectrum $S_m(f)$ determines the energy content for between 0.08 and 0.14 Hz, whereas outside this frequency range the calculated values of S(f) lie below $S_m(f)$. Hence, the major modification of wave energy in Kugmallit

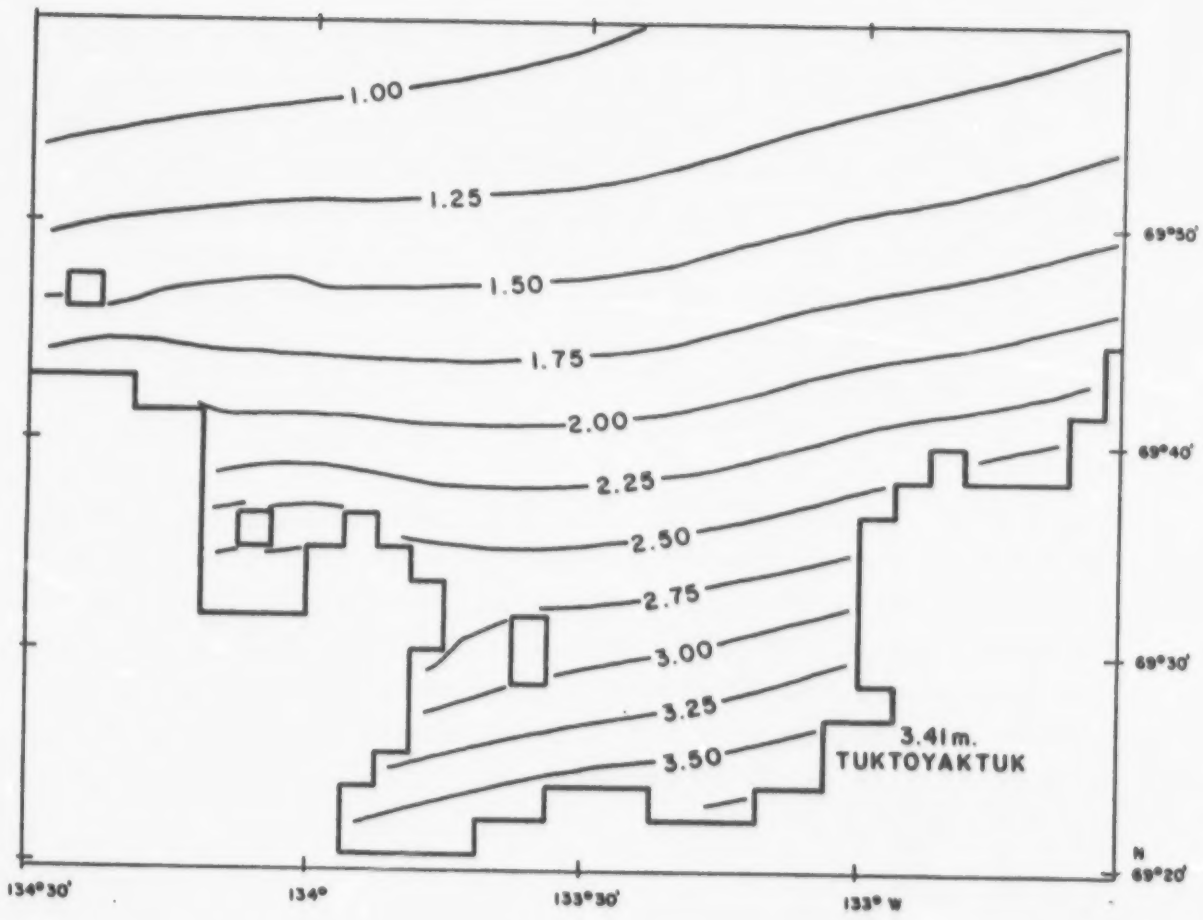

Figure 8 Water elevation in metres above MWL at peak wind (hour no. 18) during simulated extreme surge, from the IOS model of Kugmallit Bay.

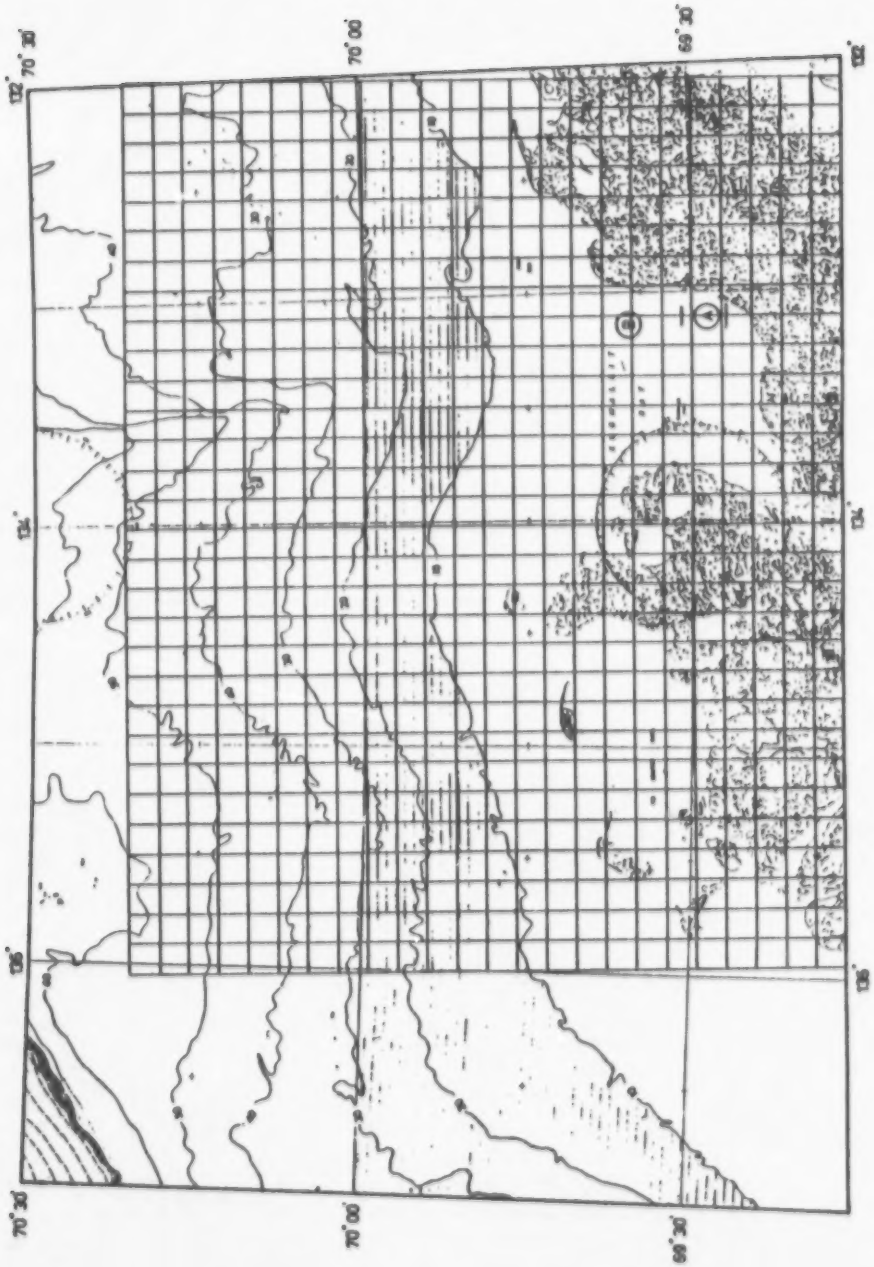

Figure 9 Refraction model grid (5 km spacing).

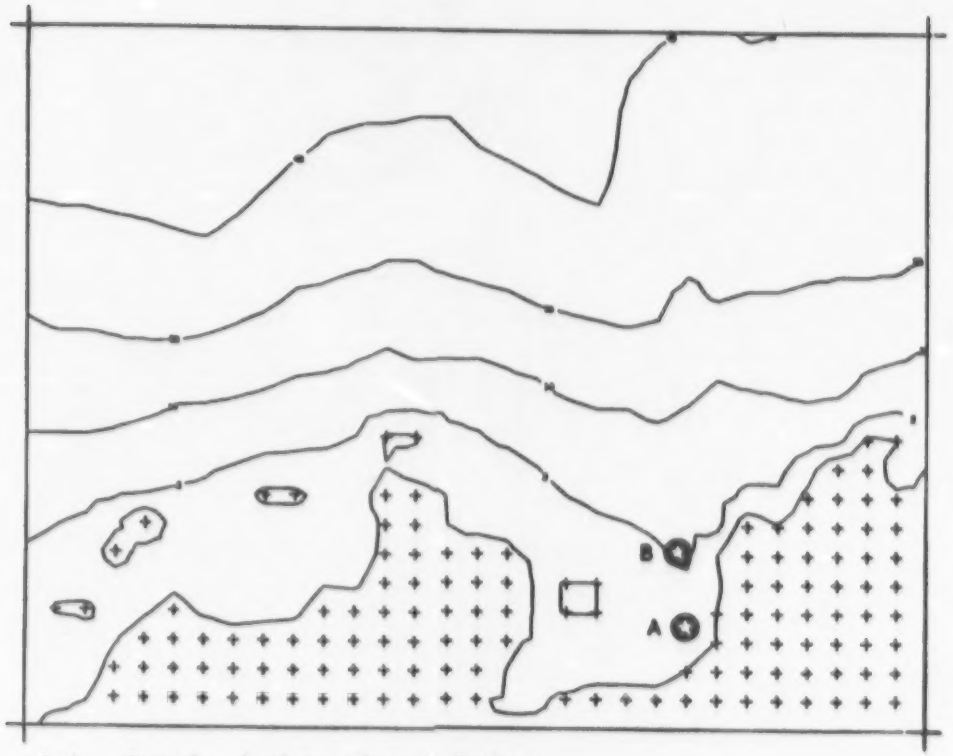

(a) depths below Chart Datum

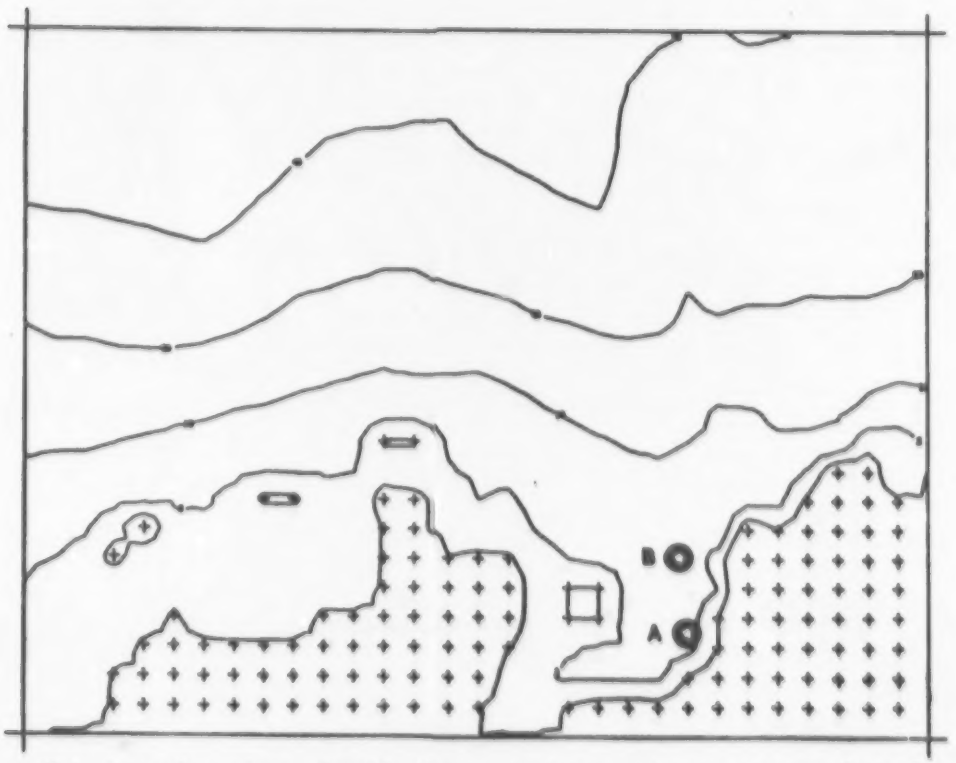

(b) total water depth for maximum storm surge levels

Figure 10 Water depths in meters and shoreline as resolved by 5 km grid spacing.

Seacomsult

Table 3

Directional Wave Energy Spectrum at Site A for $\bar{\theta}_o$=340°T

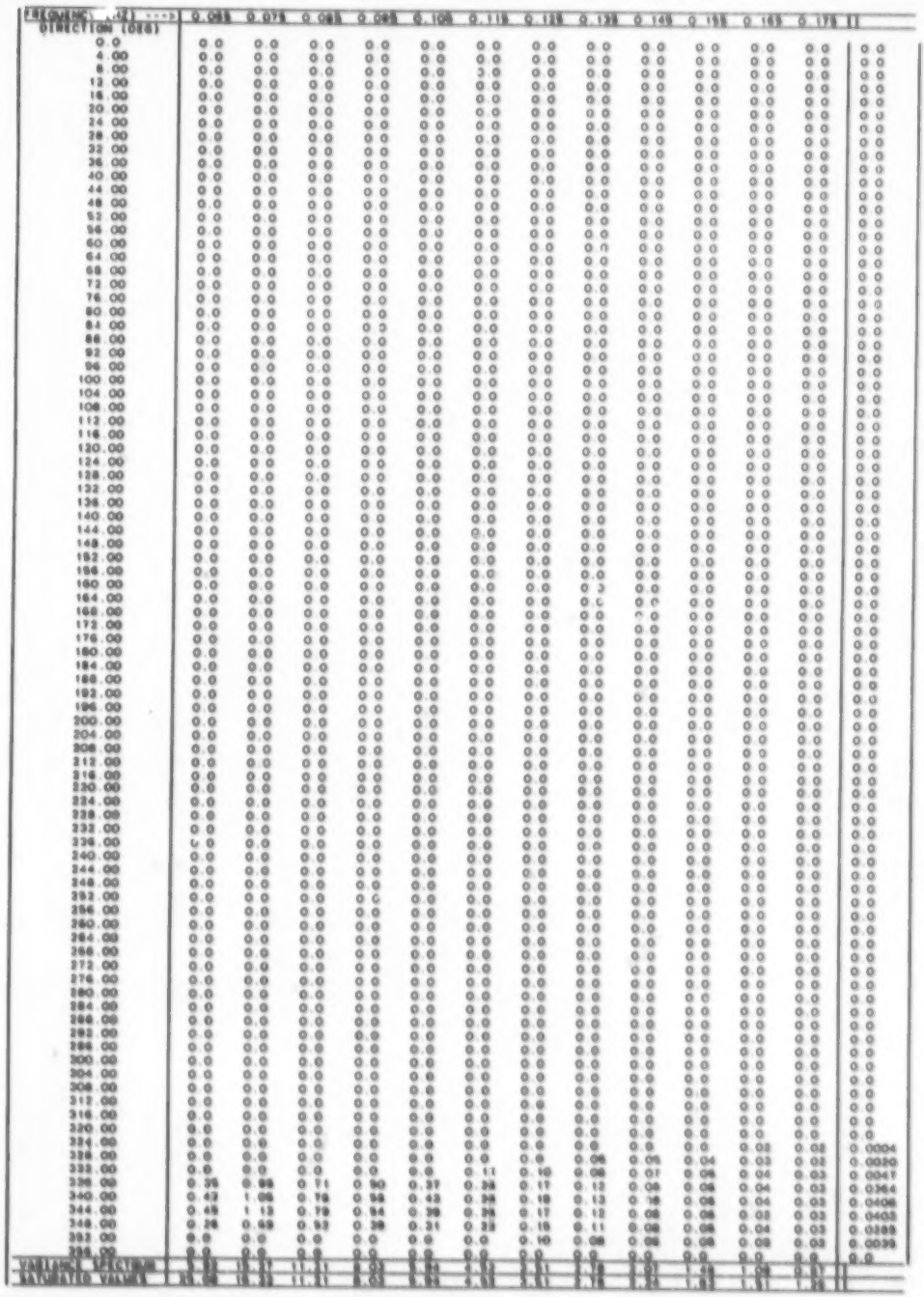

FREQUENCY (HZ) ---> / DIRECTION (DEG)	0.048	0.058	0.068	0.078	0.088	0.098	0.108	0.118	0.128	0.138	0.148	0.158	0.168	0.178	
0.0	0.0	0.0	0.0	0.0	0.0	0.0	0.0	0.0	0.0	0.0	0.0	0.0	0.0	0.0	0.0
4.00	0.0	0.0	0.0	0.0	0.0	0.0	0.0	0.0	0.0	0.0	0.0	0.0	0.0	0.0	0.0
8.00	0.0	0.0	0.0	0.0	0.0	0.0	0.0	0.0	0.0	0.0	0.0	0.0	0.0	0.0	0.0
12.00	0.0	0.0	0.0	0.0	0.0	0.0	3.0	0.0	0.0	0.0	0.0	0.0	0.0	0.0	0.0
16.00	0.0	0.0	0.0	0.0	0.0	0.0	0.0	0.0	0.0	0.0	0.0	0.0	0.0	0.0	0.0
20.00	0.0	0.0	0.0	0.0	0.0	0.0	0.0	0.0	0.0	0.0	0.0	0.0	0.0	0.0	0.0
24.00	0.0	0.0	0.0	0.0	0.0	0.0	0.0	0.0	0.0	0.0	0.0	0.0	0.0	0.0	0.0
28.00	0.0	0.0	0.0	0.0	0.0	0.0	0.0	0.0	0.0	0.0	0.0	0.0	0.0	0.0	0.0
32.00	0.0	0.0	0.0	0.0	0.0	0.0	0.0	0.0	0.0	0.0	0.0	0.0	0.0	0.0	0.0
36.00	0.0	0.0	0.0	0.0	0.0	0.0	0.0	0.0	0.0	0.0	0.0	0.0	0.0	0.0	0.0
40.00	0.0	0.0	0.0	0.0	0.0	0.0	0.0	0.0	0.0	0.0	0.0	0.0	0.0	0.0	0.0
44.00	0.0	0.0	0.0	0.0	0.0	0.0	0.0	0.0	0.0	0.0	0.0	0.0	0.0	0.0	0.0
48.00	0.0	0.0	0.0	0.0	0.0	0.0	0.0	0.0	0.0	0.0	0.0	0.0	0.0	0.0	0.0
52.00	0.0	0.0	0.0	0.0	0.0	0.0	0.0	0.0	0.0	0.0	0.0	0.0	0.0	0.0	0.0
56.00	0.0	0.0	0.0	0.0	0.0	0.0	0.0	0.0	0.0	0.0	0.0	0.0	0.0	0.0	0.0
60.00	0.0	0.0	0.0	0.0	0.0	0.0	0.0	0.0	0.0	0.0	0.0	0.0	0.0	0.0	0.0
64.00	0.0	0.0	0.0	0.0	0.0	0.0	0.0	0.0	0.0	0.0	0.0	0.0	0.0	0.0	0.0
68.00	0.0	0.0	0.0	0.0	0.0	0.0	0.0	0.0	0.0	0.0	0.0	0.0	0.0	0.0	0.0
72.00	0.0	0.0	0.0	0.0	0.0	0.0	0.0	0.0	0.0	0.0	0.0	0.0	0.0	0.0	0.0
76.00	0.0	0.0	0.0	0.0	0.0	0.0	0.0	0.0	0.0	0.0	0.0	0.0	0.0	0.0	0.0
80.00	0.0	0.0	0.0	0.0	0.0	0.0	0.0	0.0	0.0	0.0	0.0	0.0	0.0	0.0	0.0
84.00	0.0	0.0	0.0	0.0	0.0	0.0	0.0	0.0	0.0	0.0	0.0	0.0	0.0	0.0	0.0
88.00	0.0	0.0	0.0	0.0	0.0	0.0	0.0	0.0	0.0	0.0	0.0	0.0	0.0	0.0	0.0
92.00	0.0	0.0	0.0	0.0	0.0	0.0	0.0	0.0	0.0	0.0	0.0	0.0	0.0	0.0	0.0
96.00	0.0	0.0	0.0	0.0	0.0	0.0	0.0	0.0	0.0	0.0	0.0	0.0	0.0	0.0	0.0
100.00	0.0	0.0	0.0	0.0	0.0	0.0	0.0	0.0	0.0	0.0	0.0	0.0	0.0	0.0	0.0
104.00	0.0	0.0	0.0	0.0	0.0	0.0	0.0	0.0	0.0	0.0	0.0	0.0	0.0	0.0	0.0
108.00	0.0	0.0	0.0	0.0	0.0	0.0	0.0	0.0	0.0	0.0	0.0	0.0	0.0	0.0	0.0
112.00	0.0	0.0	0.0	0.0	0.0	0.0	0.0	0.0	0.0	0.0	0.0	0.0	0.0	0.0	0.0
116.00	0.0	0.0	0.0	0.0	0.0	0.0	0.0	0.0	0.0	0.0	0.0	0.0	0.0	0.0	0.0
120.00	0.0	0.0	0.0	0.0	0.0	0.0	0.0	0.0	0.0	0.0	0.0	0.0	0.0	0.0	0.0
124.00	0.0	0.0	0.0	0.0	0.0	0.0	0.0	0.0	0.0	0.0	0.0	0.0	0.0	0.0	0.0
128.00	0.0	0.0	0.0	0.0	0.0	0.0	0.0	0.0	0.0	0.0	0.0	0.0	0.0	0.0	0.0
132.00	0.0	0.0	0.0	0.0	0.0	0.0	0.0	0.0	0.0	0.0	0.0	0.0	0.0	0.0	0.0
136.00	0.0	0.0	0.0	0.0	0.0	0.0	0.0	0.0	0.0	0.0	0.0	0.0	0.0	0.0	0.0
140.00	0.0	0.0	0.0	0.0	0.0	0.0	0.0	0.0	0.0	0.0	0.0	0.0	0.0	0.0	0.0
144.00	0.0	0.0	0.0	0.0	0.0	0.0	0.0	0.0	0.0	0.0	0.0	0.0	0.0	0.0	0.0
148.00	0.0	0.0	0.0	0.0	0.0	0.0	0.0	0.0	0.0	0.0	0.0	0.0	0.0	0.0	0.0
152.00	0.0	0.0	0.0	0.0	0.0	0.0	0.0	0.0	0.0	0.0	0.0	0.0	0.0	0.0	0.0
156.00	0.0	0.0	0.0	0.0	0.0	0.0	0.0	0.0	0.0	0.0	0.0	0.0	0.0	0.0	0.0
160.00	0.0	0.0	0.0	0.0	0.0	0.0	0.0	0.0	0.0	0.0	0.0	0.0	0.0	0.0	0.0
164.00	0.0	0.0	0.0	0.0	0.0	0.0	0.0	0.0	0.0	0.0	0.0	0.0	0.0	0.0	0.0
168.00	0.0	0.0	0.0	0.0	0.0	0.0	0.0	0.0	0.0	0.0	0.0	0.0	0.0	0.0	0.0
172.00	0.0	0.0	0.0	0.0	0.0	0.0	0.0	0.0	0.0	0.0	0.0	0.0	0.0	0.0	0.0
176.00	0.0	0.0	0.0	0.0	0.0	0.0	0.0	0.0	0.0	0.0	0.0	0.0	0.0	0.0	0.0
180.00	0.0	0.0	0.0	0.0	0.0	0.0	0.0	0.0	0.0	0.0	0.0	0.0	0.0	0.0	0.0
184.00	0.0	0.0	0.0	0.0	0.0	0.0	0.0	0.0	0.0	0.0	0.0	0.0	0.0	0.0	0.0
188.00	0.0	0.0	0.0	0.0	0.0	0.0	0.0	0.0	0.0	0.0	0.0	0.0	0.0	0.0	0.0
192.00	0.0	0.0	0.0	0.0	0.0	0.0	0.0	0.0	0.0	0.0	0.0	0.0	0.0	0.0	0.0
196.00	0.0	0.0	0.0	0.0	0.0	0.0	0.0	0.0	0.0	0.0	0.0	0.0	0.0	0.0	0.0
200.00	0.0	0.0	0.0	0.0	0.0	0.0	0.0	0.0	0.0	0.0	0.0	0.0	0.0	0.0	0.0
204.00	0.0	0.0	0.0	0.0	0.0	0.0	0.0	0.0	0.0	0.0	0.0	0.0	0.0	0.0	0.0
208.00	0.0	0.0	0.0	0.0	0.0	0.0	0.0	0.0	0.0	0.0	0.0	0.0	0.0	0.0	0.0
212.00	0.0	0.0	0.0	0.0	0.0	0.0	0.0	0.0	0.0	0.0	0.0	0.0	0.0	0.0	0.0
216.00	0.0	0.0	0.0	0.0	0.0	0.0	0.0	0.0	0.0	0.0	0.0	0.0	0.0	0.0	0.0
220.00	0.0	0.0	0.0	0.0	0.0	0.0	0.0	0.0	0.0	0.0	0.0	0.0	0.0	0.0	0.0
224.00	0.0	0.0	0.0	0.0	0.0	0.0	0.0	0.0	0.0	0.0	0.0	0.0	0.0	0.0	0.0
228.00	0.0	0.0	0.0	0.0	0.0	0.0	0.0	0.0	0.0	0.0	0.0	0.0	0.0	0.0	0.0
232.00	0.0	0.0	0.0	0.0	0.0	0.0	0.0	0.0	0.0	0.0	0.0	0.0	0.0	0.0	0.0
236.00	0.0	0.0	0.0	0.0	0.0	0.0	0.0	0.0	0.0	0.0	0.0	0.0	0.0	0.0	0.0
240.00	0.0	0.0	0.0	0.0	0.0	0.0	0.0	0.0	0.0	0.0	0.0	0.0	0.0	0.0	0.0
244.00	0.0	0.0	0.0	0.0	0.0	0.0	0.0	0.0	0.0	0.0	0.0	0.0	0.0	0.0	0.0
248.00	0.0	0.0	0.0	0.0	0.0	0.0	0.0	0.0	0.0	0.0	0.0	0.0	0.0	0.0	0.0
252.00	0.0	0.0	0.0	0.0	0.0	0.0	0.0	0.0	0.0	0.0	0.0	0.0	0.0	0.0	0.0
256.00	0.0	0.0	0.0	0.0	0.0	0.0	0.0	0.0	0.0	0.0	0.0	0.0	0.0	0.0	0.0
260.00	0.0	0.0	0.0	0.0	0.0	0.0	0.0	0.0	0.0	0.0	0.0	0.0	0.0	0.0	0.0
264.00	0.0	0.0	0.0	0.0	0.0	0.0	0.0	0.0	0.0	0.0	0.0	0.0	0.0	0.0	0.0
268.00	0.0	0.0	0.0	0.0	0.0	0.0	0.0	0.0	0.0	0.0	0.0	0.0	0.0	0.0	0.0
272.00	0.0	0.0	0.0	0.0	0.0	0.0	0.0	0.0	0.0	0.0	0.0	0.0	0.0	0.0	0.0
276.00	0.0	0.0	0.0	0.0	0.0	0.0	0.0	0.0	0.0	0.0	0.0	0.0	0.0	0.0	0.0
280.00	0.0	0.0	0.0	0.0	0.0	0.0	0.0	0.0	0.0	0.0	0.0	0.0	0.0	0.0	0.0
284.00	0.0	0.0	0.0	0.0	0.0	0.0	0.0	0.0	0.0	0.0	0.0	0.0	0.0	0.0	0.0
288.00	0.0	0.0	0.0	0.0	0.0	0.0	0.0	0.0	0.0	0.0	0.0	0.0	0.0	0.0	0.0
292.00	0.0	0.0	0.0	0.0	0.0	0.0	0.0	0.0	0.0	0.0	0.0	0.0	0.0	0.0	0.0
296.00	0.0	0.0	0.0	0.0	0.0	0.0	0.0	0.0	0.0	0.0	0.0	0.0	0.0	0.0	0.0
300.00	0.0	0.0	0.0	0.0	0.0	0.0	0.0	0.0	0.0	0.0	0.0	0.0	0.0	0.0	0.0
304.00	0.0	0.0	0.0	0.0	0.0	0.0	0.0	0.0	0.0	0.0	0.0	0.0	0.0	0.0	0.0
308.00	0.0	0.0	0.0	0.0	0.0	0.0	0.0	0.0	0.0	0.0	0.0	0.0	0.0	0.0	0.0
312.00	0.0	0.0	0.0	0.0	0.0	0.0	0.0	0.0	0.0	0.0	0.0	0.0	0.0	0.0	0.0
316.00	0.0	0.0	0.0	0.0	0.0	0.0	0.0	0.0	0.0	0.0	0.0	0.0	0.0	0.0	0.0
320.00	0.0	0.0	0.0	0.0	0.0	0.0	0.0	0.0	0.0	0.0	0.0	0.0	0.0	0.0	0.0
324.00	0.0	0.0	0.0	0.0	0.0	0.0	0.0	0.0	0.0	0.0	0.0	0.0	0.0	0.0	0.0
328.00	0.0	0.0	0.0	0.0	0.0	0.0	0.0	0.0	0.0	0.06	0.05	0.04	0.03	0.02	0.0004
332.00	0.0	0.0	0.0	0.0	0.0	0.11	0.10	0.08	0.07	0.06	0.04	0.03	0.02	0.0020	
336.00	0.35	0.88	0.71	0.90	0.37	0.26	0.17	0.12	0.08	0.06	0.04	0.03	0.0047		
340.00	0.42	1.06	0.78	0.98	0.43	0.26	0.18	0.13	0.10	0.06	0.04	0.03	0.0364		
344.00	0.45	1.13	0.78	0.94	0.39	0.26	0.17	0.12	0.08	0.06	0.03	0.03	0.0408		
348.00	0.26	0.69	0.52	0.38	0.31	0.22	0.15	0.11	0.08	0.05	0.04	0.03	0.0403		
352.00	0.0	0.0	0.0	0.0	0.0	0.0	0.10	0.08	0.06	0.05	0.03	0.03	0.0389		
356.00	0.0	0.0	0.0	0.0	0.0	0.0	0.0	0.0	0.0	0.0	0.0	0.0	0.0039		
360.00	0.0	0.0	0.0	0.0	0.0	0.0	0.0	0.0	0.0	0.0	0.0	0.0	0.0	0.0	0.0
VARIANCE SPECTRUM	0.01	0.03	0.01	0.03	0.04	0.04	0.01	0.01	0.01	0.01	0.01	0.01	0.01	0.01	
SATURATED VALUES	11.08	10.33	11.11	8.03	5.84	4.18	3.01	2.18	1.58	1.15	0.83	0.60	0.43	0.31	

HMO = 3.17 M TP = 13.33 S PRINCIPAL DIRECTION = 340. DEG

Table 4

Directional Wave Energy Spectrum at Site A for $\bar{\theta}_o$=8°T

FREQUENCY (HZ) ---->	0.068	0.078	0.088	0.098	0.108	0.118	0.128	0.138	0.148	0.158	0.168	0.178	TI
DIRECTION (DEG)													
0.00	0.0	0.0	0.0	0.0	0.0	0.0	0.0	0.0	0.0	0.0	0.0	0.0	0.0
4.00	0.0	0.0	0.0	0.0	0.0	0.0	0.0	0.0	0.0	0.0	0.0	0.0	0.0
8.00	0.0	0.0	0.0	0.0	0.0	0.0	0.0	0.0	0.0	0.0	0.0	0.0	0.0
12.00	0.0	0.0	0.0	0.0	0.0	0.0	0.0	0.0	0.0	0.0	0.0	0.0	0.0
16.00	0.0	0.0	0.0	0.0	0.0	0.0	0.0	0.0	0.0	0.0	0.0	0.0	0.0
20.00	0.0	0.0	0.0	0.0	0.0	0.0	0.0	0.0	0.0	0.0	0.0	0.0	0.0
24.00	0.0	0.0	0.0	0.0	0.0	0.0	0.0	0.0	0.0	0.0	0.0	0.0	0.0
28.00	0.0	0.0	0.0	0.0	0.0	0.0	0.0	0.0	0.0	0.0	0.0	0.0	0.0
32.00	0.0	0.0	0.0	0.0	0.0	0.0	0.0	0.0	0.0	0.0	0.0	0.0	0.0
36.00	0.0	0.0	0.0	0.0	0.0	0.0	0.0	0.0	0.0	0.0	0.0	0.0	0.0
40.00	0.0	0.0	0.0	0.0	0.0	0.0	0.0	0.0	0.0	0.0	0.0	0.0	0.0
44.00	0.0	0.0	0.0	0.0	0.0	0.0	0.0	0.0	0.0	0.0	0.0	0.0	0.0
48.00	0.0	0.0	0.0	0.0	0.0	0.0	0.0	0.0	0.0	0.0	0.0	0.0	0.0
52.00	0.0	0.0	0.0	0.0	0.0	0.0	0.0	0.0	0.0	0.0	0.0	0.0	0.0
56.00	0.0	0.0	0.0	0.0	0.0	0.0	0.0	0.0	0.0	0.0	0.0	0.0	0.0
60.00	0.0	0.0	0.0	0.0	0.0	0.0	0.0	0.0	0.0	0.0	0.0	0.0	0.0
64.00	0.0	0.0	0.0	0.0	0.0	0.0	0.0	0.0	0.0	0.0	0.0	0.0	0.0
68.00	0.0	0.0	0.0	0.0	0.0	0.0	0.0	0.0	0.0	0.0	0.0	0.0	0.0
72.00	0.0	0.0	0.0	0.0	0.0	0.0	0.0	0.0	0.0	0.0	0.0	0.0	0.0
76.00	0.0	0.0	0.0	0.0	0.0	0.0	0.0	0.0	0.0	0.0	0.0	0.0	0.0
80.00	0.0	0.0	0.0	0.0	0.0	0.0	0.0	0.0	0.0	0.0	0.0	0.0	0.0
84.00	0.0	0.0	0.0	0.0	0.0	0.0	0.0	0.0	0.0	0.0	0.0	0.0	0.0
88.00	0.0	0.0	0.0	0.0	0.0	0.0	0.0	0.0	0.0	0.0	0.0	0.0	0.0
92.00	0.0	0.0	0.0	0.0	0.0	0.0	0.0	0.0	0.0	0.0	0.0	0.0	0.0
96.00	0.0	0.0	0.0	0.0	0.0	0.0	0.0	0.0	0.0	0.0	0.0	0.0	0.0
100.00	0.0	0.0	0.0	0.0	0.0	0.0	0.0	0.0	0.0	0.0	0.0	0.0	0.0
104.00	0.0	0.0	0.0	0.0	0.0	0.0	0.0	0.0	0.0	0.0	0.0	0.0	0.0
108.00	0.0	0.0	0.0	0.0	0.0	0.0	0.0	0.0	0.0	0.0	0.0	0.0	0.0
112.00	0.0	0.0	0.0	0.0	0.0	0.0	0.0	0.0	0.0	0.0	0.0	0.0	0.0
116.00	0.0	0.0	0.0	0.0	0.0	0.0	0.0	0.0	0.0	0.0	0.0	0.0	0.0
120.00	0.0	0.0	0.0	0.0	0.0	0.0	0.0	0.0	0.0	0.0	0.0	0.0	0.0
124.00	0.0	0.0	0.0	0.0	0.0	0.0	0.0	0.0	0.0	0.0	0.0	0.0	0.0
128.00	0.0	0.0	0.0	0.0	0.0	0.0	0.0	0.0	0.0	0.0	0.0	0.0	0.0
132.00	0.0	0.0	0.0	0.0	0.0	0.0	0.0	0.0	0.0	0.0	0.0	0.0	0.0
136.00	0.0	0.0	0.0	0.0	0.0	0.0	0.0	0.0	0.0	0.0	0.0	0.0	0.0
140.00	0.0	0.0	0.0	0.0	0.0	0.0	0.0	0.0	0.0	0.0	0.0	0.0	0.0
144.00	0.0	0.0	0.0	0.0	0.0	0.0	0.0	0.0	0.0	0.0	0.0	0.0	0.0
148.00	0.0	0.0	0.0	0.0	0.0	0.0	0.0	0.0	0.0	0.0	0.0	0.0	0.0
152.00	0.0	0.0	0.0	0.0	0.0	0.0	0.0	0.0	0.0	0.0	0.0	0.0	0.0
156.00	0.0	0.0	0.0	0.0	0.0	0.0	0.0	0.0	0.0	0.0	0.0	0.0	0.0
160.00	0.0	0.0	0.0	0.0	0.0	0.0	0.0	0.0	0.0	0.0	0.0	0.0	0.0
164.00	0.0	0.0	0.0	0.0	0.0	0.0	0.0	0.0	0.0	0.0	0.0	0.0	0.0
168.00	0.0	0.0	0.0	0.0	0.0	0.0	0.0	0.0	0.0	0.0	0.0	0.0	0.0
172.00	0.0	0.0	0.0	0.0	0.0	0.0	0.0	0.0	0.0	0.0	0.0	0.0	0.0
176.00	0.0	0.0	0.0	0.0	0.0	0.0	0.0	0.0	0.0	0.0	0.0	0.0	0.0
180.00	0.0	0.0	0.0	0.0	0.0	0.0	0.0	0.0	0.0	0.0	0.0	0.0	0.0
184.00	0.0	0.0	0.0	0.0	0.0	0.0	0.0	0.0	0.0	0.0	0.0	0.0	0.0
188.00	0.0	0.0	0.0	0.0	0.0	0.0	0.0	0.0	0.0	0.0	0.0	0.0	0.0
192.00	0.0	0.0	0.0	0.0	0.0	0.0	0.0	0.0	0.0	0.0	0.0	0.0	0.0
196.00	0.0	0.0	0.0	0.0	0.0	0.0	0.0	0.0	0.0	0.0	0.0	0.0	0.0
200.00	0.0	0.0	0.0	0.0	0.0	0.0	0.0	0.0	0.0	0.0	0.0	0.0	0.0
204.00	0.0	0.0	0.0	0.0	0.0	0.0	0.0	0.0	0.0	0.0	0.0	0.0	0.0
208.00	0.0	0.0	0.0	0.0	0.0	0.0	0.0	0.0	0.0	0.0	0.0	0.0	0.0
212.00	0.0	0.0	0.0	0.0	0.0	0.0	0.0	0.0	0.0	0.0	0.0	0.0	0.0
216.00	0.0	0.0	0.0	0.0	0.0	0.0	0.0	0.0	0.0	0.0	0.0	0.0	0.0
220.00	0.0	0.0	0.0	0.0	0.0	0.0	0.0	0.0	0.0	0.0	0.0	0.0	0.0
224.00	0.0	0.0	0.0	0.0	0.0	0.0	0.0	0.0	0.0	0.0	0.0	0.0	0.0
228.00	0.0	0.0	0.0	0.0	0.0	0.0	0.0	0.0	0.0	0.0	0.0	0.0	0.0
232.00	0.0	0.0	0.0	0.0	0.0	0.0	0.0	0.0	0.0	0.0	0.0	0.0	0.0
236.00	0.0	0.0	0.0	0.0	0.0	0.0	0.0	0.0	0.0	0.0	0.0	0.0	0.0
240.00	0.0	0.0	0.0	0.0	0.0	0.0	0.0	0.0	0.0	0.0	0.0	0.0	0.0
244.00	0.0	0.0	0.0	0.0	0.0	0.0	0.0	0.0	0.0	0.0	0.0	0.0	0.0
248.00	0.0	0.0	0.0	0.0	0.0	0.0	0.0	0.0	0.0	0.0	0.0	0.0	0.0
252.00	0.0	0.0	0.0	0.0	0.0	0.0	0.0	0.0	0.0	0.0	0.0	0.0	0.0
256.00	0.0	0.0	0.0	0.0	0.0	0.0	0.0	0.0	0.0	0.0	0.0	0.0	0.0
260.00	0.0	0.0	0.0	0.0	0.0	0.0	0.0	0.0	0.0	0.0	0.0	0.0	0.0
264.00	0.0	0.0	0.0	0.0	0.0	0.0	0.0	0.0	0.0	0.0	0.0	0.0	0.0
268.00	0.0	0.0	0.0	0.0	0.0	0.0	0.0	0.0	0.0	0.0	0.0	0.0	0.0
272.00	0.0	0.0	0.0	0.0	0.0	0.0	0.0	0.0	0.0	0.0	0.0	0.0	0.0
276.00	0.0	0.0	0.0	0.0	0.0	0.0	0.0	0.0	0.0	0.0	0.0	0.0	0.0
280.00	0.0	0.0	0.0	0.0	0.0	0.0	0.0	0.0	0.0	0.0	0.0	0.0	0.0
284.00	0.0	0.0	0.0	0.0	0.0	0.0	0.0	0.0	0.0	0.0	0.0	0.0	0.0
288.00	0.0	0.0	0.0	0.0	0.0	0.0	0.0	0.0	0.0	0.0	0.0	0.0	0.0
292.00	0.0	0.0	0.0	0.0	0.0	0.0	0.0	0.0	0.0	0.0	0.0	0.0	0.0
296.00	0.0	0.0	0.0	0.0	0.0	0.0	0.0	0.0	0.0	0.0	0.0	0.0	0.0
300.00	0.0	0.0	0.0	0.0	0.0	0.0	0.0	0.0	0.0	0.0	0.0	0.0	0.0
304.00	0.0	0.0	0.0	0.0	0.0	0.0	0.0	0.0	0.0	0.0	0.0	0.0	0.0
308.00	0.0	0.0	0.0	0.0	0.0	0.0	0.0	0.0	0.0	0.0	0.0	0.0	0.0
312.00	0.0	0.0	0.0	0.0	0.0	0.0	0.0	0.0	0.0	0.0	0.0	0.0	0.0
316.00	0.0	0.0	0.0	0.0	0.0	0.0	0.0	0.0	0.0	0.0	0.0	0.0	0.0
320.00	0.0	0.0	0.0	0.0	0.0	0.0	0.0	0.0	0.0	0.0	0.0	0.0	0.0
324.00	0.0	0.0	0.0	0.0	0.0	0.0	0.0	0.0	0.0	0.0	0.01	0.01	0.0002
328.00	0.0	0.0	0.0	0.0	0.0	0.0	0.0	0.02	0.03	0.02	0.02	0.01	0.0009
332.00	0.0	0.0	0.0	0.0	0.0	0.04	0.06	0.05	0.04	0.03	0.02	0.02	0.0024
336.00	0.17	0.46	0.38	0.30	0.23	0.18	0.13	0.09	0.07	0.06	0.03	0.02	0.0213
340.00	0.52	1.38	0.86	0.60	0.41	0.28	0.17	0.13	0.08	0.06	0.04	0.03	0.0446
344.00	0.53	1.29	0.85	0.58	0.43	0.31	0.19	0.14	0.08	0.05	0.03	0.03	0.0450
348.00	0.40	1.03	0.71	0.53	0.41	0.30	0.19	0.14	0.08	0.06	0.04	0.03	0.0383
352.00	0.0	0.0	0.0	0.0	0.0	0.0	0.16	0.13	0.08	0.06	0.04	0.03	0.0069
356.00	0.0	0.0	0.0	0.0	0.0	0.0	0.0	0.0	0.0	0.0	0.0	0.0	0.0
TOTAL SPECTRUM	2.15	5.33	3.91	3.01	2.24	1.71	1.13	0.81	0.56	0.42	0.28	0.20	
SIGNIFICANT VALUES	21.08	10.33	11.71	8.03	5.84	4.18	3.41	2.74	2.38	1.88	1.61	1.38	

HMO = 3.30 M TP = 13.33 S PRINCIPAL DIRECTION = 344. DEG

Seaconsult

13

Table 5

Directional Wave Energy Spectrum at Site B for $\bar{\theta}_o$=340°T

FREQUENCY (HZ) ---->	0.065	0.075	0.085	0.095	0.105	0.115	0.125	0.135	0.145	0.155	0.165	0.175	II
DIRECTION (DEG)													
0.0	0.39	0.54	0.36	0.25	0.17	0.12	0.09	0.06	0.05	0.04	0.03	0.02	0.0211
4.00	0.36	0.50	0.33	0.23	0.16	0.11	0.08	0.06	0.05	0.04	0.03	0.02	0.0191
8.00	0.37	0.40	0.27	0.20	0.14	0.10	0.08	0.06	0.04	0.03	0.03	0.02	0.0164
12.00	0.32	0.32	0.23	0.17	0.12	0.09	0.07	0.05	0.04	0.03	0.03	0.02	0.0139
16.00	0.31	0.30	0.21	0.16	0.11	0.08	0.07	0.05	0.04	0.03	0.03	0.02	0.0130
20.00	0.18	0.26	0.18	0.14	0.10	0.08	0.06	0.05	0.03	0.03	0.02	0.02	0.0116
24.00	0.0	0.0	0.0	0.0	0.0	0.06	0.05	0.04	0.03	0.02	0.02	0.02	0.0075
28.00	0.0	0.0	0.0	0.0	0.0	0.0	0.0	0.0	0.0	0.0	0.0	0.0	0.0
32.00	0.0	0.0	0.0	0.0	0.0	0.0	0.0	0.0	0.0	0.0	0.0	0.0	0.0
36.00	0.0	0.0	0.0	0.0	0.0	0.0	0.0	0.0	0.0	0.0	0.0	0.0	0.0
40.00	0.0	0.0	0.0	0.0	0.0	0.0	0.0	0.0	0.0	0.0	0.0	0.0	0.0
44.00	0.0	0.0	0.0	0.0	0.0	0.0	0.0	0.0	0.0	0.0	0.0	0.0	0.0
48.00	0.0	0.0	0.0	0.0	0.0	0.0	0.0	0.0	0.0	0.0	0.0	0.0	0.0
52.00	0.0	0.0	0.0	0.0	0.0	0.0	0.0	0.0	0.0	0.0	0.0	0.0	0.0
56.00	0.0	0.0	0.0	0.0	0.0	0.0	0.0	0.0	0.0	0.0	0.0	0.0	0.0
60.00	0.0	0.0	0.0	0.0	0.0	0.0	0.0	0.0	0.0	0.0	0.0	0.0	0.0
64.00	0.0	0.0	0.0	0.0	0.0	0.0	0.0	0.0	0.0	0.0	0.0	0.0	0.0
68.00	0.0	0.0	0.0	0.0	0.0	0.0	0.0	0.0	0.0	0.0	0.0	0.0	0.0
72.00	0.0	0.0	0.0	0.0	0.0	0.0	0.0	0.0	0.0	0.0	0.0	0.0	0.0
76.00	0.0	0.0	0.0	0.0	0.0	0.0	0.0	0.0	0.0	0.0	0.0	0.0	0.0
80.00	0.0	0.0	0.0	0.0	0.0	0.0	0.0	0.0	0.0	0.0	0.0	0.0	0.0
84.00	0.0	0.0	0.0	0.0	0.0	0.0	0.0	0.0	0.0	0.0	0.0	0.0	0.0
88.00	0.0	0.0	0.0	0.0	0.0	0.0	0.0	0.0	0.0	0.0	0.0	0.0	0.0
92.00	0.0	0.0	0.0	0.0	0.0	0.0	0.0	0.0	0.0	0.0	0.0	0.0	0.0
96.00	0.0	0.0	0.0	0.0	0.0	0.0	0.0	0.0	0.0	0.0	0.0	0.0	0.0
100.00	0.0	0.0	0.0	0.0	0.0	0.0	0.0	0.0	0.0	0.0	0.0	0.0	0.0
104.00	0.0	0.0	0.0	0.0	0.0	0.0	0.0	0.0	0.0	0.0	0.0	0.0	0.0
108.00	0.0	0.0	0.0	0.0	0.0	0.0	0.0	0.0	0.0	0.0	0.0	0.0	0.0
112.00	0.0	0.0	0.0	0.0	0.0	0.0	0.0	0.0	0.0	0.0	0.0	0.0	0.0
116.00	0.0	0.0	0.0	0.0	0.0	0.0	0.0	0.0	0.0	0.0	0.0	0.0	0.0
120.00	0.0	0.0	0.0	0.0	0.0	0.0	0.0	0.0	0.0	0.0	0.0	0.0	0.0
124.00	0.0	0.0	0.0	0.0	0.0	0.0	0.0	0.0	0.0	0.0	0.0	0.0	0.0
128.00	0.0	0.0	0.0	0.0	0.0	0.0	0.0	0.0	0.0	0.0	0.0	0.0	0.0
132.00	0.0	0.0	0.0	0.0	0.0	0.0	0.0	0.0	0.0	0.0	0.0	0.0	0.0
136.00	0.0	0.0	0.0	0.0	0.0	0.0	0.0	0.0	0.0	0.0	0.0	0.0	0.0
140.00	0.0	0.0	0.0	0.0	0.0	0.0	0.0	0.0	0.0	0.0	0.0	0.0	0.0
144.00	0.0	0.0	0.0	0.0	0.0	0.0	0.0	0.0	0.0	0.0	0.0	0.0	0.0
148.00	0.0	0.0	0.0	0.0	0.0	0.0	0.0	0.0	0.0	0.0	0.0	0.0	0.0
152.00	0.0	0.0	0.0	0.0	0.0	0.0	0.0	0.0	0.0	0.0	0.0	0.0	0.0
156.00	0.0	0.0	0.0	0.0	0.0	0.0	0.0	0.0	0.0	0.0	0.0	0.0	0.0
160.00	0.0	0.0	0.0	0.0	0.0	0.0	0.0	0.0	0.0	0.0	0.0	0.0	0.0
164.00	0.0	0.0	0.0	0.0	0.0	0.0	0.0	0.0	0.0	0.0	0.0	0.0	0.0
168.00	0.0	0.0	0.0	0.0	0.0	0.0	0.0	0.0	0.0	0.0	0.0	0.0	0.0
172.00	0.0	0.0	0.0	0.0	0.0	0.0	0.0	0.0	0.0	0.0	0.0	0.0	0.0
176.00	0.0	0.0	0.0	0.0	0.0	0.0	0.0	0.0	0.0	0.0	0.0	0.0	0.0
180.00	0.0	0.0	0.0	0.0	0.0	0.0	0.0	0.0	0.0	0.0	0.0	0.0	0.0
184.00	0.0	0.0	0.0	0.0	0.0	0.0	0.0	0.0	0.0	0.0	0.0	0.0	0.0
188.00	0.0	0.0	0.0	0.0	0.0	0.0	0.0	0.0	0.0	0.0	0.0	0.0	0.0
192.00	0.0	0.0	0.0	0.0	0.0	0.0	0.0	0.0	0.0	0.0	0.0	0.0	0.0
196.00	0.0	0.0	0.0	0.0	0.0	0.0	0.0	0.0	0.0	0.0	0.0	0.0	0.0
200.00	0.0	0.0	0.0	0.0	0.0	0.0	0.0	0.0	0.0	0.0	0.0	0.0	0.0
204.00	0.0	0.0	0.0	0.0	0.0	0.0	0.0	0.0	0.0	0.0	0.0	0.0	0.0
208.00	0.0	0.0	0.0	0.0	0.0	0.0	0.0	0.0	0.0	0.0	0.0	0.0	0.0
212.00	0.0	0.0	0.0	0.0	0.0	0.0	0.0	0.0	0.0	0.0	0.0	0.0	0.0
216.00	0.0	0.0	0.0	0.0	0.0	0.0	0.0	0.0	0.0	0.0	0.0	0.0	0.0
220.00	0.0	0.0	0.0	0.0	0.0	0.0	0.0	0.0	0.0	0.0	0.0	0.0	0.0
224.00	0.0	0.0	0.0	0.0	0.0	0.0	0.0	0.0	0.0	0.0	0.0	0.0	0.0
228.00	0.0	0.0	0.0	0.0	0.0	0.0	0.0	0.0	0.0	0.0	0.0	0.0	0.0
232.00	0.0	0.0	0.0	0.0	0.0	0.0	0.0	0.0	0.0	0.0	0.0	0.0	0.0
236.00	0.0	0.0	0.0	0.0	0.0	0.0	0.0	0.0	0.0	0.0	0.0	0.0	0.0
240.00	0.0	0.0	0.0	0.0	0.0	0.0	0.0	0.0	0.0	0.0	0.0	0.0	0.0
244.00	0.0	0.0	0.0	0.0	0.0	0.0	0.0	0.0	0.0	0.0	0.0	0.0	0.0
248.00	0.0	0.0	0.0	0.0	0.0	0.0	0.0	0.0	0.0	0.0	0.0	0.0	0.0
252.00	0.0	0.0	0.0	0.0	0.0	0.0	0.0	0.0	0.0	0.0	0.0	0.0	0.0
256.00	0.0	0.0	0.0	0.0	0.0	0.0	0.0	0.0	0.0	0.0	0.0	0.0	0.0
260.00	0.0	0.0	0.0	0.0	0.0	0.0	0.0	0.0	0.0	0.0	0.0	0.0	0.0
264.00	0.0	0.0	0.0	0.0	0.0	0.0	0.0	0.0	0.0	0.0	0.0	0.0	0.0
268.00	0.0	0.0	0.0	0.0	0.0	0.0	0.0	0.0	0.0	0.0	0.0	0.0	0.0
272.00	0.0	0.0	0.0	0.0	0.0	0.0	0.0	0.0	0.0	0.0	0.0	0.0	0.0
276.00	0.0	0.0	0.0	0.0	0.0	0.0	0.0	0.0	0.0	0.0	0.0	0.0	0.0
280.00	0.0	0.0	0.0	0.0	0.0	0.0	0.0	0.0	0.0	0.0	0.0	0.0	0.0
284.00	0.0	0.0	0.0	0.0	0.0	0.0	0.0	0.0	0.0	0.0	0.0	0.0	0.0
288.00	0.0	0.0	0.0	0.0	0.0	0.0	0.0	0.0	0.0	0.0	0.0	0.0	0.0
292.00	0.0	0.0	0.0	0.0	0.0	0.0	0.0	0.0	0.0	0.0	0.0	0.0	0.0
296.00	0.0	0.0	0.0	0.0	0.0	0.0	0.0	0.0	0.0	0.0	0.0	0.0	0.0
300.00	0.0	0.0	0.0	0.0	0.0	0.0	0.0	0.0	0.0	0.0	0.0	0.0	0.0
304.00	0.0	0.0	0.0	0.0	0.0	0.0	0.0	0.0	0.0	0.0	0.0	0.0	0.0
308.00	0.0	0.0	0.0	0.0	0.0	0.0	0.0	0.0	0.0	0.0	0.0	0.0	0.0
312.00	0.0	0.0	0.0	0.0	0.0	0.0	0.0	0.0	0.0	0.0	0.0	0.0	0.0
316.00	0.0	0.0	0.0	0.0	0.0	0.0	0.0	0.0	0.0	0.0	0.0	0.0	0.0
320.00	0.0	0.0	0.0	0.0	0.0	0.0	0.0	0.0	0.0	0.0	0.0	0.02	0.0030
324.00	0.0	0.0	0.0	0.0	0.0	0.0	0.0	0.0	0.0	0.02	0.02	0.02	0.0035
328.00	0.0	0.0	0.0	0.0	0.0	0.0	0.0	0.0	0.03	0.02	0.02	0.02	0.0040
332.00	0.0	0.0	0.0	0.0	0.0	0.0	0.0	0.04	0.04	0.03	0.02	0.02	0.0050
336.00	0.0	0.0	0.0	0.0	0.0	0.07	0.07	0.05	0.04	0.03	0.02	0.02	0.0061
340.00	0.40	0.31	0.20	0.17	0.14	0.10	0.08	0.07	0.05	0.04	0.03	0.03	0.0122
344.00	0.38	0.36	0.28	0.25	0.17	0.12	0.10	0.07	0.05	0.04	0.03	0.03	0.0210
348.00	0.47	0.46	0.40	0.28	0.18	0.13	0.10	0.07	0.05	0.04	0.03	0.03	0.0240
352.00	0.38	0.50	0.34	0.24	0.17	0.12	0.09	0.07	0.05	0.04	0.03	0.03	0.0200
356.00	0.39	0.54	0.36	0.25	0.17	0.12	0.09	0.07	0.05	0.04	0.03	0.02	0.0208
VARIANCE SPECTRUM	13.26	10.01	7.08	5.05	3.61	2.58	1.88	1.38	1.02	0.76	0.57	0.43	II
SATURATED VALUES	28.81	18.01	12.08	8.26	5.81	4.18	3.08	2.28	1.69	1.26	0.94	0.71	II

HMO = 3.03 M TP = 13.33 S PRINCIPAL DIRECTION = 340 DEG

94

Table 6

Directional Wave Energy Spectrum at Site B for $\bar{\theta}_o$=8°T

FREQUENCY (HZ) --->	0.065	0.075	0.085	0.095	0.105	0.115	0.125	0.135	0.145	0.155	0.165	0.175	
DIRECTION (DEG)													
0.0	0.45	0.56	0.37	0.26	0.18	0.12	0.10	0.07	0.06	0.04	0.04	0.03	0.0238
4.00	0.45	0.56	0.37	0.26	0.18	0.12	0.10	0.07	0.06	0.04	0.04	0.03	0.0225
8.00	0.40	0.50	0.34	0.24	0.17	0.12	0.09	0.07	0.06	0.04	0.04	0.03	0.0209
12.00	0.35	0.43	0.31	0.22	0.16	0.11	0.08	0.07	0.05	0.04	0.03	0.03	0.0190
16.00	0.33	0.42	0.29	0.21	0.15	0.11	0.08	0.06	0.05	0.04	0.03	0.03	0.0183
20.00	0.29	0.36	0.27	0.20	0.15	0.11	0.08	0.06	0.05	0.04	0.03	0.03	0.0166
24.00	0.0	0.0	0.0	0.0	0.0	0.08	0.06	0.06	0.05	0.04	0.03	0.02	0.0037
28.00	0.0	0.0	0.0	0.0	0.0	0.0	0.0	0.0	0.0	0.0	0.0	0.0	0.0
32.00	0.0	0.0	0.0	0.0	0.0	0.0	0.0	0.0	0.0	0.0	0.0	0.0	0.0
36.00	0.0	0.0	0.0	0.0	0.0	0.0	0.0	0.0	0.0	0.0	0.0	0.0	0.0
40.00	0.0	0.0	0.0	0.0	0.0	0.0	0.0	0.0	0.0	0.0	0.0	0.0	0.0
44.00	0.0	0.0	0.0	0.0	0.0	0.0	0.0	0.0	0.0	0.0	0.0	0.0	0.0
48.00	0.0	0.0	0.0	0.0	0.0	0.0	0.0	0.0	0.0	0.0	0.0	0.0	0.0
52.00	0.0	0.0	0.0	0.0	0.0	0.0	0.0	0.0	0.0	0.0	0.0	0.0	0.0
56.00	0.0	0.0	0.0	0.0	0.0	0.0	0.0	0.0	0.0	0.0	0.0	0.0	0.0
60.00	0.0	0.0	0.0	0.0	0.0	0.0	0.0	0.0	0.0	0.0	0.0	0.0	0.0
64.00	0.0	0.0	0.0	0.0	0.0	0.0	0.0	0.0	0.0	0.0	0.0	0.0	0.0
68.00	0.0	0.0	0.0	0.0	0.0	0.0	0.0	0.0	0.0	0.0	0.0	0.0	0.0
72.00	0.0	0.0	0.0	0.0	0.0	0.0	0.0	0.0	0.0	0.0	0.0	0.0	0.0
76.00	0.0	0.0	0.0	0.0	0.0	0.0	0.0	0.0	0.0	0.0	0.0	0.0	0.0
80.00	0.0	0.0	0.0	0.0	0.0	0.0	0.0	0.0	0.0	0.0	0.0	0.0	0.0
84.00	0.0	0.0	0.0	0.0	0.0	0.0	0.0	0.0	0.0	0.0	0.0	0.0	0.0
88.00	0.0	0.0	0.0	0.0	0.0	0.0	0.0	0.0	0.0	0.0	0.0	0.0	0.0
92.00	0.0	0.0	0.0	0.0	0.0	0.0	0.0	0.0	0.0	0.0	0.0	0.0	0.0
96.00	0.0	0.0	0.0	0.0	0.0	0.0	0.0	0.0	0.0	0.0	0.0	0.0	0.0
100.00	0.0	0.0	0.0	0.0	0.0	0.0	0.0	0.0	0.0	0.0	0.0	0.0	0.0
104.00	0.0	0.0	0.0	0.0	0.0	0.0	0.0	0.0	0.0	0.0	0.0	0.0	0.0
108.00	0.0	0.0	0.0	0.0	0.0	0.0	0.0	0.0	0.0	0.0	0.0	0.0	0.0
112.00	0.0	0.0	0.0	0.0	0.0	0.0	0.0	0.0	0.0	0.0	0.0	0.0	0.0
116.00	0.0	0.0	0.0	0.0	0.0	0.0	0.0	0.0	0.0	0.0	0.0	0.0	0.0
120.00	0.0	0.0	0.0	0.0	0.0	0.0	0.0	0.0	0.0	0.0	0.0	0.0	0.0
124.00	0.0	0.0	0.0	0.0	0.0	0.0	0.0	0.0	0.0	0.0	0.0	0.0	0.0
128.00	0.0	0.0	0.0	0.0	0.0	0.0	0.0	0.0	0.0	0.0	0.0	0.0	0.0
132.00	0.0	0.0	0.0	0.0	0.0	0.0	0.0	0.0	0.0	0.0	0.0	0.0	0.0
136.00	0.0	0.0	0.0	0.0	0.0	0.0	0.0	0.0	0.0	0.0	0.0	0.0	0.0
140.00	0.0	0.0	0.0	0.0	0.0	0.0	0.0	0.0	0.0	0.0	0.0	0.0	0.0
144.00	0.0	0.0	0.0	0.0	0.0	0.0	0.0	0.0	0.0	0.0	0.0	0.0	0.0
148.00	0.0	0.0	0.0	0.0	0.0	0.0	0.0	0.0	0.0	0.0	0.0	0.0	0.0
152.00	0.0	0.0	0.0	0.0	0.0	0.0	0.0	0.0	0.0	0.0	0.0	0.0	0.0
156.00	0.0	0.0	0.0	0.0	0.0	0.0	0.0	0.0	0.0	0.0	0.0	0.0	0.0
160.00	0.0	0.0	0.0	0.0	0.0	0.0	0.0	0.0	0.0	0.0	0.0	0.0	0.0
164.00	0.0	0.0	0.0	0.0	0.0	0.0	0.0	0.0	0.0	0.0	0.0	0.0	0.0
168.00	0.0	0.0	0.0	0.0	0.0	0.0	0.0	0.0	0.0	0.0	0.0	0.0	0.0
172.00	0.0	0.0	0.0	0.0	0.0	0.0	0.0	0.0	0.0	0.0	0.0	0.0	0.0
176.00	0.0	0.0	0.0	0.0	0.0	0.0	0.0	0.0	0.0	0.0	0.0	0.0	0.0
180.00	0.0	0.0	0.0	0.0	0.0	0.0	0.0	0.0	0.0	0.0	0.0	0.0	0.0
184.00	0.0	0.0	0.0	0.0	0.0	0.0	0.0	0.0	0.0	0.0	0.0	0.0	0.0
188.00	0.0	0.0	0.0	0.0	0.0	0.0	0.0	0.0	0.0	0.0	0.0	0.0	0.0
192.00	0.0	0.0	0.0	0.0	0.0	0.0	0.0	0.0	0.0	0.0	0.0	0.0	0.0
196.00	0.0	0.0	0.0	0.0	0.0	0.0	0.0	0.0	0.0	0.0	0.0	0.0	0.0
200.00	0.0	0.0	0.0	0.0	0.0	0.0	0.0	0.0	0.0	0.0	0.0	0.0	0.0
204.00	0.0	0.0	0.0	0.0	0.0	0.0	0.0	0.0	0.0	0.0	0.0	0.0	0.0
208.00	0.0	0.0	0.0	0.0	0.0	0.0	0.0	0.0	0.0	0.0	0.0	0.0	0.0
212.00	0.0	0.0	0.0	0.0	0.0	0.0	0.0	0.0	0.0	0.0	0.0	0.0	0.0
216.00	0.0	0.0	0.0	0.0	0.0	0.0	0.0	0.0	0.0	0.0	0.0	0.0	0.0
220.00	0.0	0.0	0.0	0.0	0.0	0.0	0.0	0.0	0.0	0.0	0.0	0.0	0.0
224.00	0.0	0.0	0.0	0.0	0.0	0.0	0.0	0.0	0.0	0.0	0.0	0.0	0.0
228.00	0.0	0.0	0.0	0.0	0.0	0.0	0.0	0.0	0.0	0.0	0.0	0.0	0.0
232.00	0.0	0.0	0.0	0.0	0.0	0.0	0.0	0.0	0.0	0.0	0.0	0.0	0.0
236.00	0.0	0.0	0.0	0.0	0.0	0.0	0.0	0.0	0.0	0.0	0.0	0.0	0.0
240.00	0.0	0.0	0.0	0.0	0.0	0.0	0.0	0.0	0.0	0.0	0.0	0.0	0.0
244.00	0.0	0.0	0.0	0.0	0.0	0.0	0.0	0.0	0.0	0.0	0.0	0.0	0.0
248.00	0.0	0.0	0.0	0.0	0.0	0.0	0.0	0.0	0.0	0.0	0.0	0.0	0.0
252.00	0.0	0.0	0.0	0.0	0.0	0.0	0.0	0.0	0.0	0.0	0.0	0.0	0.0
256.00	0.0	0.0	0.0	0.0	0.0	0.0	0.0	0.0	0.0	0.0	0.0	0.0	0.0
260.00	0.0	0.0	0.0	0.0	0.0	0.0	0.0	0.0	0.0	0.0	0.0	0.0	0.0
264.00	0.0	0.0	0.0	0.0	0.0	0.0	0.0	0.0	0.0	0.0	0.0	0.0	0.0
268.00	0.0	0.0	0.0	0.0	0.0	0.0	0.0	0.0	0.0	0.0	0.0	0.0	0.0
272.00	0.0	0.0	0.0	0.0	0.0	0.0	0.0	0.0	0.0	0.0	0.0	0.0	0.0
276.00	0.0	0.0	0.0	0.0	0.0	0.0	0.0	0.0	0.0	0.0	0.0	0.0	0.0
280.00	0.0	0.0	0.0	0.0	0.0	0.0	0.0	0.0	0.0	0.0	0.0	0.0	0.0
284.00	0.0	0.0	0.0	0.0	0.0	0.0	0.0	0.0	0.0	0.0	0.0	0.0	0.0
288.00	0.0	0.0	0.0	0.0	0.0	0.0	0.0	0.0	0.0	0.0	0.0	0.0	0.0
292.00	0.0	0.0	0.0	0.0	0.0	0.0	0.0	0.0	0.0	0.0	0.0	0.0	0.0
296.00	0.0	0.0	0.0	0.0	0.0	0.0	0.0	0.0	0.0	0.0	0.0	0.0	0.0
300.00	0.0	0.0	0.0	0.0	0.0	0.0	0.0	0.0	0.0	0.0	0.0	0.0	0.0
304.00	0.0	0.0	0.0	0.0	0.0	0.0	0.0	0.0	0.0	0.0	0.0	0.0	0.0
308.00	0.0	0.0	0.0	0.0	0.0	0.0	0.0	0.0	0.0	0.0	0.0	0.0	0.0
312.00	0.0	0.0	0.0	0.0	0.0	0.0	0.0	0.0	0.0	0.0	0.0	0.0	0.0
316.00	0.0	0.0	0.0	0.0	0.0	0.0	0.0	0.0	0.0	0.0	0.0	0.0	0.0
320.00	0.0	0.0	0.0	0.0	0.0	0.0	0.0	0.0	0.0	0.0	0.0	0.01	0.0001
324.00	0.0	0.0	0.0	0.0	0.0	0.0	0.0	0.0	0.0	0.01	0.01	0.01	0.0003
328.00	0.0	0.0	0.0	0.0	0.0	0.0	0.0	0.0	0.01	0.01	0.01	0.01	0.0005
332.00	0.0	0.0	0.0	0.0	0.0	0.0	0.01	0.02	0.02	0.02	0.02	0.02	0.0011
336.00	0.0	0.0	0.0	0.0	0.03	0.03	0.03	0.03	0.03	0.03	0.03	0.02	0.0022
340.00	0.02	0.07	0.08	0.08	0.07	0.06	0.06	0.05	0.04	0.03	0.03	0.02	0.0060
344.00	0.32	0.29	0.20	0.15	0.11	0.08	0.07	0.06	0.04	0.03	0.03	0.03	0.0131
348.00	0.34	0.42	0.29	0.20	0.15	0.10	0.08	0.06	0.05	0.04	0.03	0.03	0.0178
352.00	0.45	0.56	0.37	0.26	0.18	0.12	0.04	0.07	0.05	0.04	0.03	0.03	0.0230
356.00	0.46	0.56	0.37	0.26	0.18	0.12	0.10	0.07	0.06	0.04	0.01	0.01	0.0222
VARIANCE SPECTRUM	14.87	19.01	13.05	9.34	6.91	5.28	4.08	3.22	2.60	2.11	1.74	1.45	
SATURATED VALUES	29.21	19.01	13.05	9.34	6.91	5.28	4.08	3.22	2.60	2.11	1.74	1.45	

HMO = 2.66 M TP = 13.33 S PRINCIPAL DIRECTION = 0. DEG

Seaconsult

95

SITE A

SITE B

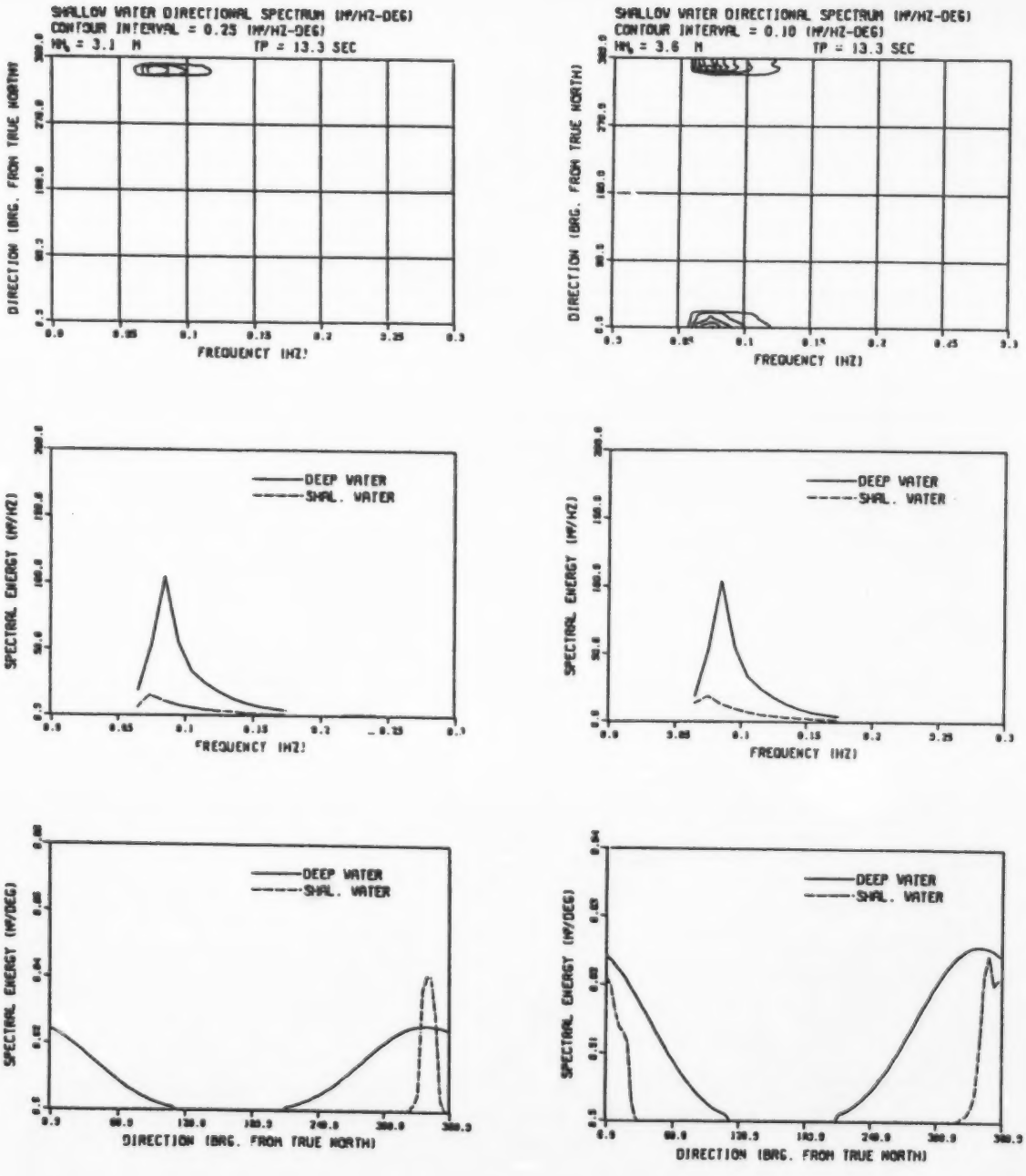

Figure 11 Deep and shallow-water wave energy spectra for $\bar{\theta}_o$=340°T.

SITE A

SITE B

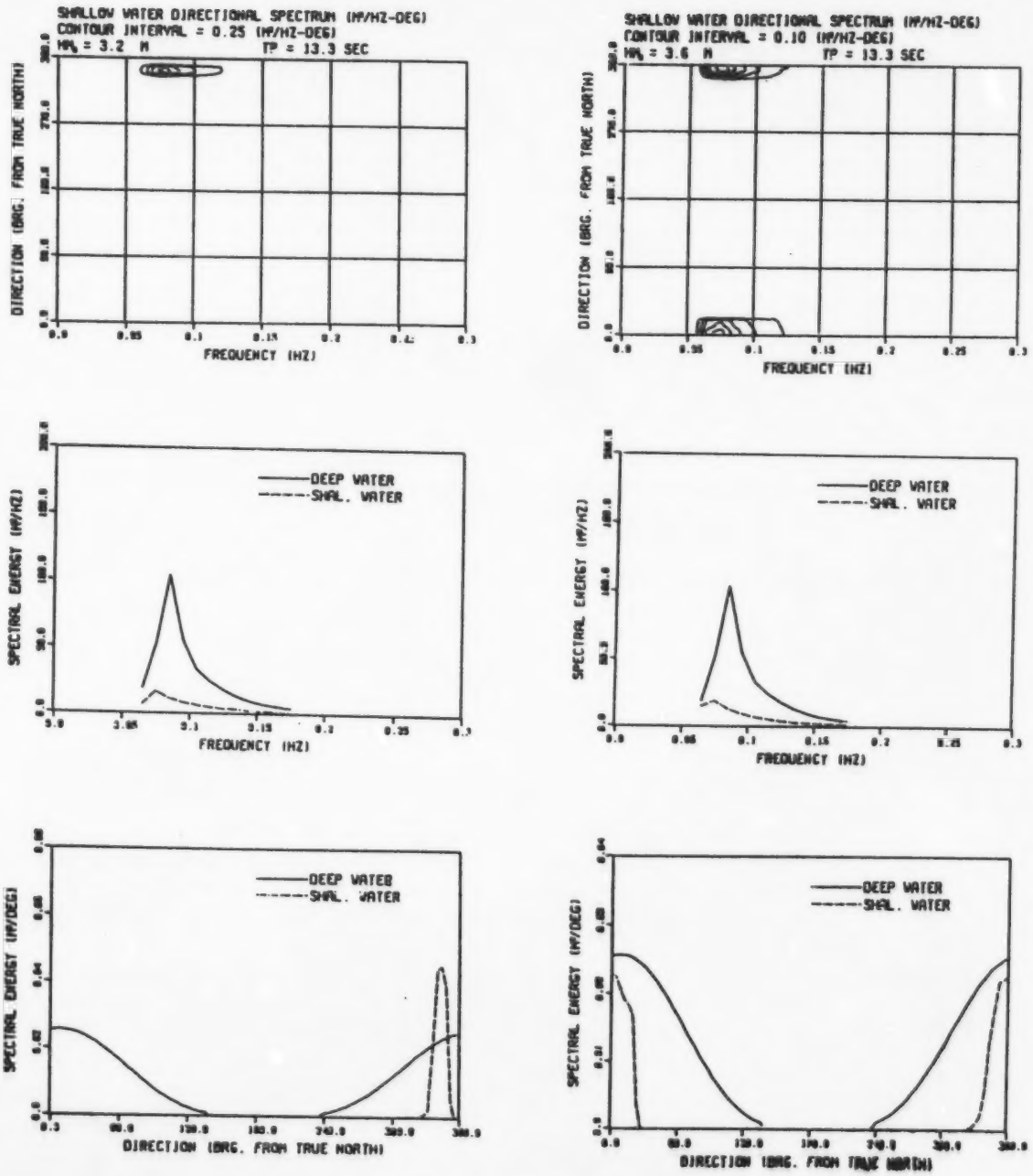

Figure 12 Deep and shallow-water wave energy spectra for $\bar{\theta}_o$=8°T.

Seaconsult

97

Bay occurs at frequencies below 0.08 Hz since the higher frequencies (about 0.14 Hz) contain relatively small, though not negligible, amounts of energy.

The bottom plots in Figure 11 and 12 show that the directional spread of wave energy about the mean is markedly narrower for site A than site B. This is expected when one considers that site A is farther inshore and hence sheltered to a greater degree by the offshore extensions of the headlands to either side of Kugmallit Bay. The reverse ray diagrams presented earlier in Figure 4 illustrate this point: approximately twice the number of rays reach deep water from site B as opposed to site A. The range of direction for which wave energy from the offshore can pass over site A is thus narrower. A practical consequence of this is that the direction of the highest waves can be specified within narrower limits (approximately ±5°) at site A than farther offshore.

A practical high frequency cutoff must be applied to the discretized energy spectra computed by the spectral refraction model: 0.18 Hz ($f_{max}+\Delta f/2$) was used in the present study. Above this frequency, it was assumed that the energy content equalled the saturated condition since the spectra being examined here were close to full development in deep water. Since the parametric deep-water spectra in this analysis contain no energy above the high frequency cutoff, an energy value equivalent to the saturated spectrum, integrated above the high frequency cutoff, was added to the computed shallow-water spectral energy.

The results of the spectral refraction analysis are tabulated in Table 7, which gives the deep and shallow-water values of the significant wave height (H_s), peak period (T_p) and mean incident wave energy direction ($\bar{\theta}$). All H_s values in Table 7 are corrected for the high frequency energy content. Since the estimated shallow-water values for H_s are higher in cases 2 and 4 ($\bar{\theta}_o$=8°),

Seaconsult

98

these values were used to predict the highest wave height expected to occur during the storm.

Table 7

Results of Spectral Refraction Analysis

Case	Site	H_s (m)	T_p (s)	$\bar{\theta}$ (°T)
1	A	3.36 [7.57]	13.3 [11.8]	341 [340]
2	A	3.39 [7.57]	13.3 [11.8]	343 [8]
3	B	3.81 [7.57]	13.3 [11.8]	358 [340]
4	B	3.84 [7.57]	13.3 [11.8]	359 [8]

[ ] figures in brackets are deep-water values.

2.4 Individual and Breaking Wave Heights

Estimates for the maximum wave height (H_m), obtained using the Glukhovskii shallow water distribution as presented in Section 1.2.3, are shown in Table 8. The breaking wave height (H_b) limits derived from the Shore Protection Manual (U.S. Army, 1977) procedure are also given.

Table 8

Maximum Wave Heights

Site	H_s (m)	d (m)	$(H_b)_{min}$ (m)	H_m (m)	$(H_b)_{max}$ (m)
A	3.39	6.85	4.57	4.93	5.35
B	3.84	7.98	5.28	5.63	6.23

For both sites, the maximum wave height predicted by the Glukhovskii

99

distribution is between the empirical breaking wave height limits. As discussed in the previous section, the energy spectrum for the sea state producing these wave heights is saturated over most of the frequency range. Thus, the highest waves at both sites will almost certainly be breaking.

2.5 Periods Associated with Maximum Waves

The period associated with the maximum wave height is needed to establish the steepness of the highest waves. The wave steepness is in turn required to calculate both the wave kinematics and maximum runup along a slope. Savage (1958) determined empirically that the dimensionless wave runup parameter R/H increased with a decrease in the parameter H/T_z^2, where R is runup, H is wave height and T_z is zero-upcrossing wave period. Hence for a given wave height, the runup will increase with increasing period. It is therefore important not to underestimate the wave period for the highest waves in the storm.

At Site A the shallow-water spectra have a peak period of T_p=13.3 s compared to the deep-water value of T_p=11.8 s (see Table 7). The decrease in peak period is explained by the reduction in the wave energy imposed by the energy saturation criterion (1.13) for frequencies greater than or equal to 0.075 Hz. This shift in the frequency of the spectral energy peak is illustrated in Figure 13, which is typical of the four shallow-water spectra predicted by the spectral refraction model (see Tables 3 through 6). Since it is expected that deep-water steepness relations (see Arhan et al. 1980) would not apply in the shallow waters of Kugmallit Bay, due to depth-induced changes in the spectra, and there are no wave data from which to empirically determine limits for H/T_z^2, a maximum wave period of T_m of between 13 and 14 seconds is recommended. This follows from the notion that the highest waves in a sea state will contain the most energy and hence have a period near the hindcast value of T_p=13.3 s.

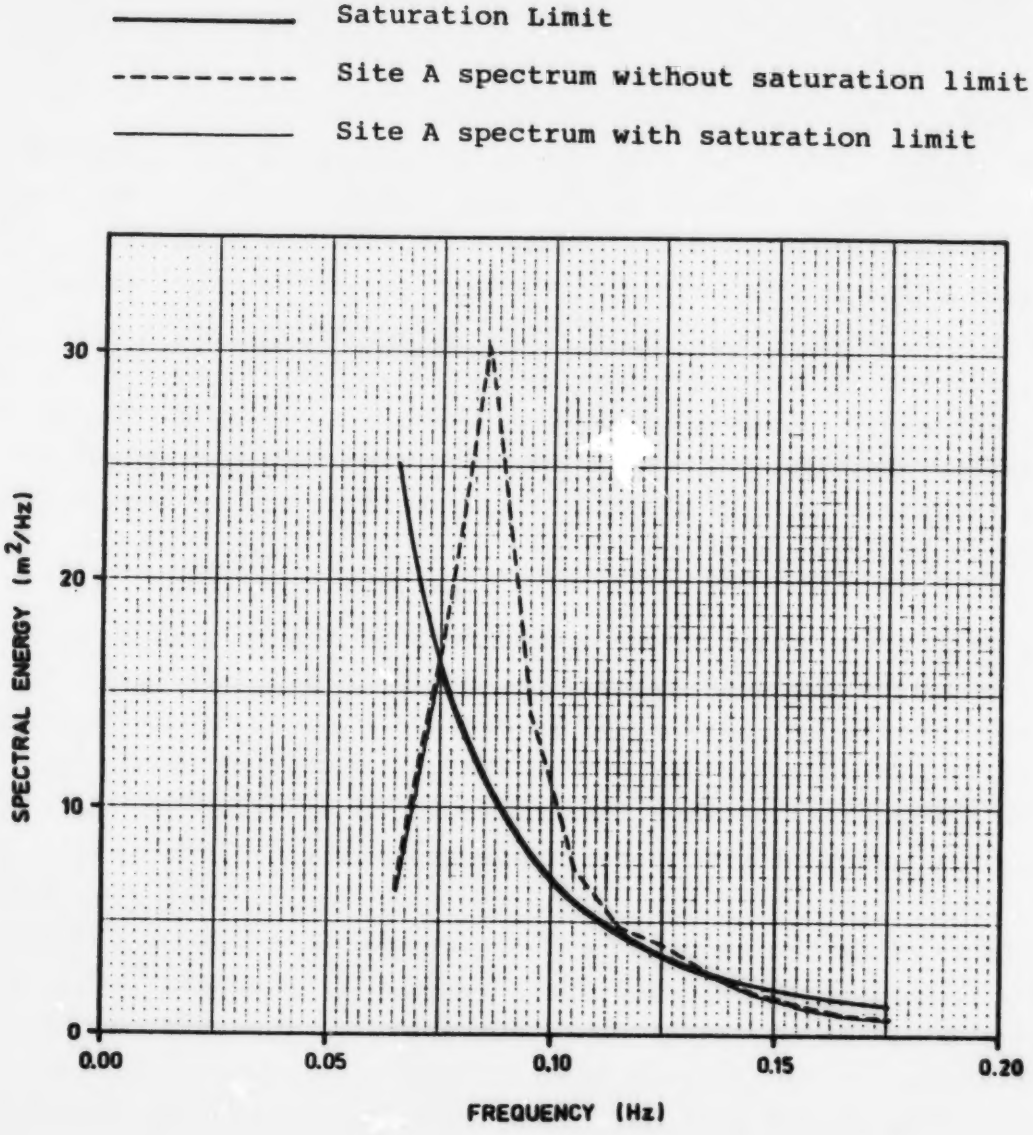

Figure 13 Energy spectrum at Site a for $\bar{\theta}=8°$.

101

3. EXTREME WAVE CONDITIONS

Based on the breaking wave height criteria given in the Shore Protection Manual, and the expected maximum wave height H_m found from the short-term distribution function, extreme waves inshore will be breaking. Wave properties at the two sites are summarized in Table 9.

In general, the manner in which a wave breaks is determined by beach slope and deep-water wave steepness (Figures 14 and 15). The curves separating the different categories of breaking waves are empirical and the transition between breaker types is not as clearly defined as the curves in Figure 15 imply. The very mild slope (<1:1000) at both sites, and in fact throughout the study area, suggests that breaking waves at the entrance to Tuktoyaktuk harbour, and further offshore, will be spilling breakers.

The spectral refraction analysis has also shown that the inshore ocean wave direction at site A averages about 342°T (±1°T), and is not particularly sensitive to the incident direction of deep-water waves $\bar{\theta}_o$. This is because of the influence of the offshore canyon on the wave rays, which tend to be focussed into the site through a comparatively narrow angle (see Figures 4 and 6).

We have also found that wave conditions at the inshore sites are virtually saturated over all but the lowest frequencies which have little energy. Consequently the total energy contained in the inshore spectra are almost independent of the deep water wave conditions. As a result our earlier assumption that refraction effects beyond the 50 m contour are negligible is justified.

There is one additional consequence of this result. Saturated

Table 9

Extreme Wave Parameters

		Site A	Site B
Location		Off entrance to Tuktoyaktuk Harbour	Seaward end of navigation channel
Storm water depth	(m)	6.9	8.0
Significant wave height	(m)	3.4	3.8
Spectral peak period	(s)	13.3	13.3
Mean wave direction	(°T from)	342	355
Maximum wave height (breaking)	(m)	4.9	5.6
Period of maximum wave	(s)	13 to 14	13 to 14

103

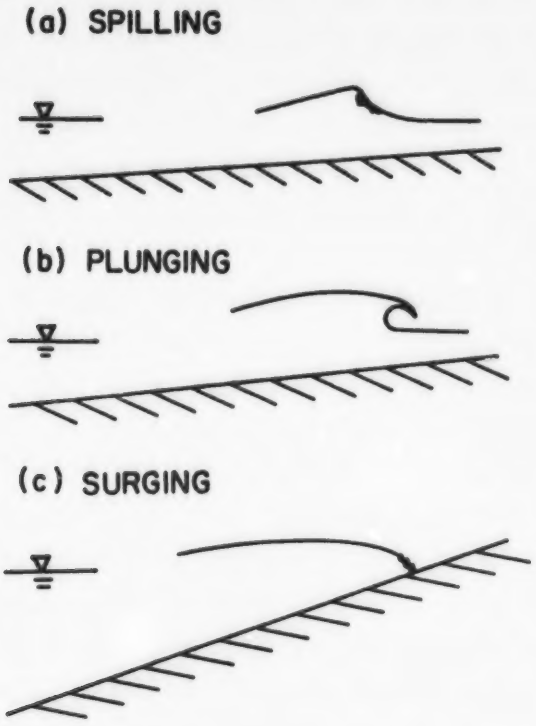

Figure 14 Different breaking wave profiles.
(Source: Sarpkaya and Isaacson, 1981).

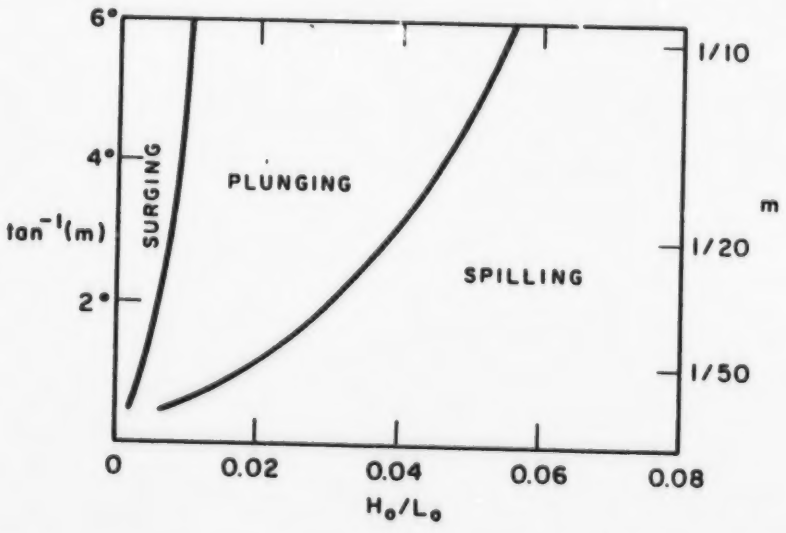

Figure 15 Ranges of deep water wave steepness H_0/L_0 and beach slope m over which different kinds of breakers form.
(Source: Sarpkaya and Isaacson, 1981).

Seaconsult

inshore conditions can be expected for less severe storms, having lower values of H_s in deep water than that hindcasted in this study. Thus the return period of depth-limited waves approaching the values given here may be shorter than the one extreme storm that was modelled. This assumes, however, that the less severe storm will produce a nearly equal surge response along the coast.

The storm wind hindcast has given offshore wave conditions characterized by H_s=7.6 m and T_p=12 s. For waves of this height and greater a zone of spilling breakers may be expected just outside Kugmallit Bay at about the 10 m contour. Further inshore, wave breaking will tend to be more intermittent and depend on local features of the bathymetry. Wave breaking concentrated at shoals such as that off Topkak Point on the east side of the bay may be expected. When offshore waves come from north or just east of north comparatively more wave breaking may be expected along the east side of the bay, in the vicinity of the navigation lights. This is due to the focussing of wave energy by refraction across the extension of the eastern headland of the Bay (see Figure 6(d)). These predictions of breaker patterns are based on the theoretical refraction analysis reported above and empirical criteria; they should, of course, be visually verified on an opportunity basis by vessels in Kugmallit Bay, or by aerial photography.

References

Abernethy, C.L. and G. Gilbert, 1975. "Refraction of Wave Spectra." Hydraulics Research Station, Wallingford, England, Report No. INT 117.

Arhan, M.F., A.G. Cavanié and R.S. Ezraty, 1980. "Determination of the Period Range Associated to the Design Wave," in Sea Climatology. Editions Technip, Paris, 7-26.

Baird, W.F., 1978. "Wave Climate Analysis for Selected Locations in the Gulf of St. Lawrence and Lake Superior." Marine Directorate Report, Public Works, Canada.

Glukhoviskii, B.Kh., 1966. "Investigation of Sea Wind Waves." Leningrad, Gidrometeoizdat. (in Russian).

Hodgins, D.O., 1983. "A Review of Extreme Wave Conditions in the Beaufort Sea." Prepared for Fisheries and Oceans, Canada, by Seaconsult Marine Research Ltd.

Kitaigorodskii, S.A., V.P. Krasitskii and M.M. Zaslavskii, 1975. "Phillips Theory of the Equilibrium Range in the Spectra of Wind-Generated Waves." J. Phys. Oceanogr., 5, 410-420.

LeBlond, P.H., S.M. Calisal and M. Isaacson, 1982. "Wave Spectra in Canadian Waters." Can. Contract Rep. Hydrogr. Ocean Sci. 6.

Markham, W.E., 1981. Ice Atlas, Canadian Arctic Waterways. Minister of Supply and Services, Canada.

Sarpkaya, T. and M. Isaacson, 1981. Mechanics of Wave Forces on Offshore Structures. Van Nostrand and Reinhold Co., New York, 651 pp.

Savage, R.P., 1958. "Wave Runup on Roughened and Permeable Slopes." J. Waterways Harb. Div. (ASCE), 84(WW3).

U.S. Army, 1977. Shore Protection Manual, Vol. I - III. Coastal Engineering Research Centre, Fort Belvoir, Virginia. Third Edition.

Weggel, J.R., 1972. "Maximum Breaker Height." J. Waterways, Harb. and Coastal Eng. Div. (ASCE), 98(WW4).

Wilson, J.R. and W.F. Baird, 1972. "A Discussion of Some Measured Wave Data," Proc. 13th Conf. Coastal Engng., Vancouver, 113-130.

Seaconsult

EXTREME WIND STRESSES OVER BEAUFORT SEA AS DETERMINED FROM TUKTOYAKTUK WINDS

Prepared for

Institute of Ocean Sciences
9860 West Saanich Road
Sidney, B.C. V8L 4B2

Contract Serial No. OSB83-00628

Prepared by

Maurice Danard
and
Mark Gray

Atmospheric Dynamics Corporation
3052 Woodridge Place, R.R. 7
Victoria, B.C. V8X 3X3

March 1984

In the report "Meteorological Conditions for Maximum Storm Surges in the Beaufort Sea", by Atmospheric Dynamics Corporation, July 1983, extreme wind stresses were estimated using geostrophic winds obtained from Arctic Weather Central charts. However, there is an inevitable smoothing in cases of strong winds, particularly when data is sparse. Peak winds are therefore probably underestimated by this method.

The availability of 60-min average winds at Tuktoyaktuk Airport allows one the opportunity to re-examine the problem independently, and to determine whether or not the conclusions reached in the 1983 report are substantiated. Wind data were obtained on magnetic tape for the period 1970-1982 inclusive. Although winds were in principle available for all hours of the day, there were numerous gaps, resulting in an underestimate of maximum speeds.

The data was scanned for the maximum 60-min wind from June to October for each year from a direction of 253° (17° south of west) through north to 073° (17° north of east). Results are shown in Table 1. The highest wind speed of all was 18.9 m/s in the hour ending at 1500 GMT 14 Sep. 1970. This may be compared to the highest geostrophic speed of 19.5 m/s at 0600 GMT 4 Oct. 1981 given in Table 2 of the 1983 report.

Values of Tuktoyaktuk winds for various return periods are shown in Table 2. These are obtained by fitting a Gumbel distribution to the winds in Table 1. The return period speeds are slightly lower for periods of 10 years and more than the geostrophic values given in Table 3 of the 1983 report.

119 Tuktoyaktuk winds for the same times in each year that the extreme geostrophic wind occurred (see Table 2 of the 1983 report) are given in Table 3. By comparing Tables 1 and 3 it is seen that only in 1982, 1980 and 1970 did Tuktoyaktuk's extreme wind occur at or about the same time as the maximum geostrophic wind. In five of the years (1981, 1979, 1978, 1974 and 1972), Tuktoyaktuk's wind was missing at that time. In 1977, 1976 and 1975, the two independent estimates of the time of maximum wind were in different months.

Tables 1-3 refer to Tuktoyaktuk winds, which are usually lighter than those over the Beaufort Sea. Table 4 compares winds at drilling rigs from the Dome data set with those at Tuktoyaktyk. Only those cases with winds at Tuktoyaktyk 20 km/h and higher and from a direction between 253° through north to 073° are considered. The average ratio of Beaufort Sea to Tuktoyaktuk speeds is 1.18. However, there is little directional difference.

Table 5 gives wind stresses (Tx, Ty) and pressure gradients (dPdx, dPdy) over the Beaufort Sea computed as in the paper "A Preliminary Investigation Using a Nova Scotia Storm Surge Prediction Model" by Gray et al, Atmos.-Ocean, 22 (1984). Calculations were made for each of the maximum wind cases in Table 1. The x-axis points east. Computations start 18 h before peak wind and continue for 24 h. The wind speed was multiplied by 1.2 to convert it to an over-water value and then by another factor of 1.2 to convert it to geostrophic. The same Tuktoyaktuk data set was used that was employed in Table 4. Therefore, the message "Data not available" in Table 5 means that Tuktoyaktuk's wind was either offshore, less than 20 km/h, or non-existent.

TABLE 1 Observed extreme onshore surface winds from June to October at Tuktoyaktuk for each year

DATE (GMT/day/mon/yr)	SPEED (m/s)	DIRECTION (deg)
21/27/ 7/82	17.8	320
4/17/ 8/81	16.9	270
12/30/ 8/80	15.3	270
2/17/10/79	12.5	270
6/28/ 8/77	16.9	320
23/21/ 8/76	16.7	320
21/ 5/ 7/75	16.1	320
10/30/ 9/74	14.2	320
6/21/ 7/73	17.8	320
1/10/ 8/72	11.9	270
10/29/ 7/71	16.7	320
15/14/ 9/70	18.9	320

TABLE 2 Extreme wind speeds for various return periods

Year	Speed (m/s)
2	15.7
5	18.1
10	19.7
25	21.8
50	23.3
70	24.1

Sample Size = 12

TABLE 3 Observed onshore surface winds from June to October at Tuktoyaktuk

DATE (GMT/day/mon/yr)	SPEED (m/s)	DIRECTION (deg)
0/28/ 7/82	17.5	320
6/ 4/10/81	*****	*****
12/30/ 8/80	15.3	270
18/14/ 6/79	*****	*****
0/26/ 8/78	*****	*****
18/21/ 9/77	9.4	320
18/18/10/76	11.7	320
12/27/ 8/75	8.9	320
12/11/ 8/74	*****	*****
12/ 2/ 9/72	*****	*****
18/14/ 9/70	14.7	270

***** denotes missing data

TABLE 4 Comparison of offshore and Tuktoyaktuk winds in the summer of 1982.

Station	Lat.	Long.	Speed ratio	Angle diff.(°)	Number of wind pairs
Tarsiut Island	69.8	136.2	1.28	0.1	367
McKinley Bay	69.9	131.2	1.01	0.9	117
Irkaluk B-35			1.16	-0.6	241
Nerlerk M-98	70.5	133.5	1.12	0.4	136
Orvilruk O-3	70.3	136.5	1.18	-0.4	201
Kenalook J-94	70.7	134.0	1.19	-0.3	335
Kiggavik H-32			1.18	-0.5	244
Aiverk I-45			1.05	0.2	96
All stations			1.18	-0.1	1737

TABLE 5 Wind stress and pressure gradient derived from computed offshore winds

Date (GMT/day/mon/yr)	Geostrophic Speed (m/s)	Angle (deg)	Tx (Pa)	Ty (Pa)	dPdx (Pa/m)	dPdy (Pa/m)
3/27/ 7/82	12.4	270	0.2	0.1	0.00E+00	-0.17E-02
4/27/ 7/82	10.8	270	0.2	0.0	0.00E+00	-0.14E-02
5/27/ 7/82			Data not available			
6/27/ 7/82			Data not available			
7/27/ 7/82			Data not available			
8/27/ 7/82			Data not available			
9/27/ 7/82			Data not available			
10/27/ 7/82			Data not available			
11/27/ 7/82			Data not available			
12/27/ 7/82			Data not available			
13/27/ 7/82			Data not available			
14/27/ 7/82			Data not available			
15/27/ 7/82			Data not available			
16/27/ 7/82			Data not available			
17/27/ 7/82			Data not available			
18/27/ 7/82			Data not available			
19/27/ 7/82	20.0	270	0.6	0.2	0.00E+00	-0.27E-02
20/27/ 7/82	21.2	270	0.7	0.2	0.00E+00	-0.28E-02
21/27/ 7/82	25.6	320	0.9	-0.6	-0.26E-02	-0.22E-02
22/27/ 7/82	22.4	320	0.7	-0.4	-0.23E-02	-0.19E-02
23/27/ 7/82	24.4	320	0.8	-0.5	-0.25E-02	-0.21E-02
0/28/ 7/82	25.2	320	0.9	-0.6	-0.26E-02	-0.22E-02
1/28/ 7/82	21.2	320	0.6	-0.4	-0.22E-02	-0.18E-02
2/28/ 7/82	21.2	320	0.6	-0.4	-0.22E-02	-0.18E-02
3/28/ 7/82	20.0	320	0.5	-0.3	-0.20E-02	-0.17E-02

TABLE 5 Wind stress and pressure gradient derived from computed offshore winds

Date (GMT/day/mon/yr)	Geostrophic Speed (m/s)	Geostrophic Angle (deg)	Tx (Pa)	Ty (Pa)	dPdx (Pa/m)	dPdy (Pa/m)
10/16/ 8/81			Data not available			
11/16/ 8/81			Data not available			
12/16/ 8/81			Data not available			
13/16/ 8/81			Data not available			
14/16/ 8/81			Data not available			
15/16/ 8/81			Data not available			
16/16/ 8/81			Data not available			
17/16/ 8/81	18.0	270	0.5	0.1	0.00E+00	-0.24E-02
18/16/ 8/81	19.2	270	0.5	0.2	0.00E+00	-0.26E-02
19/16/ 8/81	18.8	270	0.5	0.2	0.00E+00	-0.25E-02
20/16/ 8/81	17.2	270	0.4	0.1	0.00E+00	-0.23E-02
21/16/ 8/81	18.0	270	0.5	0.1	0.00E+00	-0.24E-02
22/16/ 8/81	16.0	270	0.4	0.1	0.00E+00	-0.21E-02
23/16/ 8/81	18.0	270	0.5	0.1	0.00E+00	-0.24E-02
0/17/ 8/81	20.0	320	0.5	-0.3	-0.20E-02	-0.17E-02
1/17/ 8/81	21.2	320	0.6	-0.4	-0.22E-02	-0.18E-02
2/17/ 8/81	20.0	270	0.6	0.2	0.00E+00	-0.27E-02
3/17/ 8/81	21.2	270	0.7	0.2	0.00E+00	-0.28E-02
4/17/ 8/81	24.4	270	0.9	0.3	0.00E+00	-0.33E-02
5/17/ 8/81	23.2	270	0.8	0.3	0.00E+00	-0.31E-02
6/17/ 8/81	24.0	270	0.9	0.3	0.00E+00	-0.32E-02
7/17/ 8/81	22.4	270	0.8	0.2	0.00E+00	-0.30E-02
8/17/ 8/81	21.2	270	0.7	0.2	0.00E+00	-0.28E-02
9/17/ 8/81	22.4	270	0.8	0.2	0.00E+00	-0.30E-02
10/17/ 8/81	21.2	270	0.7	0.2	0.00E+00	-0.28E-02

TABLE 5 Wind stress and pressure gradient derived from computed offshore winds

Date (GMT/day/mon/yr)	Geostrophic Speed (m/s)	Geostrophic Angle (deg)	Tx (Pa)	Ty (Pa)	dPdx (Pa/m)	dPdy (Pa/m)
18/29/ 8/80			Data not available			
19/29/ 8/80			Data not available			
20/29/ 8/80			Data not available			
21/29/ 8/80			Data not available			
22/29/ 8/80			Data not available			
23/29/ 8/80	10.4	320	0.1	-0.1	-0.11E-02	-0.89E-03
0/30/ 8/80	16.0	320	0.3	-0.2	-0.16E-02	-0.14E-02
1/30/ 8/80	18.8	320	0.5	-0.3	-0.19E-02	-0.16E-02
2/30/ 8/80	17.2	320	0.4	-0.2	-0.18E-02	-0.15E-02
3/30/ 8/80	17.2	320	0.4	-0.2	-0.18E-02	-0.15E-02
4/30/ 8/80	17.2	320	0.4	-0.2	-0.18E-02	-0.15E-02
5/30/ 8/80	15.6	320	0.3	-0.2	-0.16E-02	-0.13E-02
6/30/ 8/80	14.8	320	0.3	-0.2	-0.15E-02	-0.13E-02
7/30/ 8/80	14.8	270	0.3	0.1	0.00E+00	-0.20E-02
8/30/ 8/80	17.2	270	0.4	0.1	0.00E+00	-0.23E-02
9/30/ 8/80	16.8	270	0.4	0.1	0.00E+00	-0.22E-02
10/30/ 8/80	16.8	270	0.4	0.1	0.00E+00	-0.22E-02
11/30/ 8/80	20.0	270	0.6	0.2	0.00E+00	-0.27E-02
12/30/ 8/80	22.0	270	0.7	0.2	0.00E+00	-0.29E-02
13/30/ 8/80	20.4	270	0.6	0.2	0.00E+00	-0.27E-02
14/30/ 8/80	20.0	270	0.6	0.2	0.00E+00	-0.27E-02
15/30/ 8/80	18.8	270	0.5	0.2	0.00E+00	-0.25E-02
16/30/ 8/80	18.0	270	0.5	0.1	0.00E+00	-0.24E-02
17/30/ 8/80			Data not available			
18/30/ 8/80			Data not available			

TABLE 5 Wind stress and pressure gradient derived from computed offshore winds

Date (GMT/day/mon/yr)	Geostrophic Speed (m/s)	Geostrophic Angle (deg)	Tx (Pa)	Ty (Pa)	dPdx (Pa/m)	dPdy (Pa/m)
8/16/10/79	8.4	320	0.1	-0.1	-0.86E-03	-0.72E-03
9/16/10/79	10.4	270	0.1	0.0	0.00E+00	-0.14E-02
10/16/10/79	10.4	320	0.1	-0.1	-0.11E-02	-0.89E-03
11/16/10/79	11.6	320	0.2	-0.1	-0.12E-02	-0.99E-03
12/16/10/79	10.8	320	0.1	-0.1	-0.11E-02	-0.93E-03
13/16/10/79	10.8	270	0.2	0.0	0.00E+00	-0.14E-02
14/16/10/79	12.4	270	0.2	0.1	0.00E+00	-0.17E-02
15/16/10/79	12.8	270	0.2	0.1	0.00E+00	-0.17E-02
16/16/10/79	12.8	320	0.2	-0.1	-0.13E-02	-0.11E-02
17/16/10/79	13.6	320	0.2	-0.1	-0.14E-02	-0.12E-02
18/16/10/79	13.6	270	0.2	0.1	0.00E+00	-0.18E-02
19/16/10/79	16.0	270	0.4	0.1	0.00E+00	-0.21E-02
20/16/10/79	16.0	270	0.4	0.1	0.00E+00	-0.21E-02
21/16/10/79	14.8	270	0.3	0.1	0.00E+00	-0.20E-02
22/16/10/79	17.2	320	0.4	-0.2	-0.18E-02	-0.15E-02
23/16/10/79	15.6	320	0.3	-0.2	-0.16E-02	-0.13E-02
0/17/10/79	14.8	320	0.3	-0.2	-0.15E-02	-0.13E-02
1/17/10/79	14.8	270	0.3	0.1	0.00E+00	-0.20E-02
2/17/10/79	18.0	270	0.5	0.1	0.00E+00	-0.24E-02
3/17/10/79	14.8	320	0.3	-0.2	-0.15E-02	-0.13E-02
4/17/10/79	14.0	320	0.2	-0.2	-0.14E-02	-0.12E-02
5/17/10/79	12.8	320	0.2	-0.1	-0.13E-02	-0.11E-02
6/17/10/79	15.6	320	0.3	-0.2	-0.16E-02	-0.13E-02
7/17/10/79	12.4	320	0.2	-0.1	-0.13E-02	-0.11E-02
8/17/10/79	11.6	320	0.2	-0.1	-0.12E-02	-0.99E-03

TABLE 5 Wind stress and pressure gradient derived from computed offshore winds

Date (GMT/day/mon/yr)	Geostrophic Speed (m/s)	Geostrophic Angle (deg)	Tx (Pa)	Ty (Pa)	dPdx (Pa/m)	dPdy (Pa/m)
12/27/ 8/77			Data not available			
13/27/ 8/77	9.2	320	0.1	-0.1	-0.94E-03	-0.79E-03
14/27/ 8/77			Data not available			
15/27/ 8/77			Data not available			
16/27/ 8/77	10.8	320	0.1	-0.1	-0.11E-02	-0.93E-03
17/27/ 8/77	12.8	320	0.2	-0.1	-0.13E-02	-0.11E-02
18/27/ 8/77	14.8	320	0.3	-0.2	-0.15E-02	-0.13E-02
19/27/ 8/77	13.6	320	0.2	-0.1	-0.14E-02	-0.12E-02
20/27/ 8/77	16.0	320	0.3	-0.2	-0.16E-02	-0.14E-02
21/27/ 8/77	16.0	320	0.3	-0.2	-0.16E-02	-0.14E-02
22/27/ 8/77	10.8	320	0.1	-0.1	-0.11E-02	-0.93E-03
23/27/ 8/77	8.4	320	0.1	-0.1	-0.86E-03	-0.72E-03
0/28/ 8/77	17.2	320	0.4	-0.2	-0.18E-02	-0.15E-02
1/28/ 8/77	16.8	320	0.4	-0.2	-0.17E-02	-0.14E-02
2/28/ 8/77	23.2	320	0.7	-0.5	-0.24E-02	-0.20E-02
3/28/ 8/77	23.2	320	0.7	-0.5	-0.24E-02	-0.20E-02
4/28/ 8/77	22.0	320	0.7	-0.4	-0.22E-02	-0.19E-02
5/28/ 8/77	23.2	320	0.7	-0.5	-0.24E-02	-0.20E-02
6/28/ 8/77	24.4	320	0.8	-0.5	-0.25E-02	-0.21E-02
7/28/ 8/77	23.2	320	0.7	-0.5	-0.24E-02	-0.20E-02
8/28/ 8/77	22.0	320	0.7	-0.4	-0.22E-02	-0.19E-02
9/28/ 8/77	23.2	320	0.7	-0.5	-0.24E-02	-0.20E-02
10/28/ 8/77	22.0	320	0.7	-0.4	-0.22E-02	-0.19E-02
11/28/ 8/77	23.2	320	0.7	-0.5	-0.24E-02	-0.20E-02
12/28/ 8/77	22.0	320	0.7	-0.4	-0.22E-02	-0.19E-02

TABLE 5 Wind stress and pressure gradient derived from computed offshore winds

Date (GMT/day/mon/yr)	Geostrophic Speed (m/s)	Geostrophic Angle (deg)	Tx (Pa)	Ty (Pa)	dPdx (Pa/m)	dPdy (Pa/m)
5/21/ 8/76			Data not available			
6/21/ 8/76			Data not available			
7/21/ 8/76			Data not available			
8/21/ 8/76			Data not available			
9/21/ 8/76			Data not available			
10/21/ 8/76			Data not available			
11/21/ 8/76			Data not available			
12/21/ 8/76			Data not available			
13/21/ 8/76			Data not available			
14/21/ 8/76			Data not available			
15/21/ 8/76			Data not available			
16/21/ 8/76			Data not available			
17/21/ 8/76			Data not available			
18/21/ 8/76			Data not available			
19/21/ 8/76			Data not available			
20/21/ 8/76	14.0	320	0.2	-0.2	-0.14E-02	-0.12E-02
21/21/ 8/76	18.8	320	0.5	-0.3	-0.19E-02	-0.16E-02
22/21/ 8/76	20.4	320	0.6	-0.4	-0.21E-02	-0.17E-02
23/21/ 8/76	24.0	320	0.8	-0.5	-0.24E-02	-0.21E-02
0/22/ 8/76	23.2	320	0.7	-0.5	-0.24E-02	-0.20E-02
1/22/ 8/76	20.4	320	0.6	-0.4	-0.21E-02	-0.17E-02
2/22/ 8/76	20.0	360	0.2	-0.6	-0.27E-02	-0.59E-08
3/22/ 8/76	18.8	320	0.5	-0.3	-0.19E-02	-0.16E-02
4/22/ 8/76	16.8	320	0.4	-0.2	-0.17E-02	-0.14E-02
5/22/ 8/76	14.0	320	0.2	-0.2	-0.14E-02	-0.12E-02

TABLE 5 Wind stress and pressure gradient derived from computed offshore winds

Date (GMT/day/mon/yr)	Geostrophic Speed (m/s)	Geostrophic Angle (deg)	Tx (Pa)	Ty (Pa)	dPdx (Pa/m)	dPdy (Pa/m)
3/ 5/ 7/75	9.6	320	0.1	-0.1	-0.98E-03	-0.82E-03
4/ 5/ 7/75	9.2	320	0.1	-0.1	-0.94E-03	-0.79E-03
5/ 5/ 7/75	8.4	320	0.1	-0.1	-0.86E-03	-0.72E-03
6/ 5/ 7/75	8.4	320	0.1	-0.1	-0.86E-03	-0.72E-03
7/ 5/ 7/75	Data not available					
8/ 5/ 7/75	Data not available					
9/ 5/ 7/75	Data not available					
10/ 5/ 7/75	Data not available					
11/ 5/ 7/75	Data not available					
12/ 5/ 7/75	Data not available					
13/ 5/ 7/75	Data not available					
14/ 5/ 7/75	9.6	270	0.1	0.0	0.00E+00	-0.13E-02
15/ 5/ 7/75	10.4	270	0.1	0.0	0.00E+00	-0.14E-02
16/ 5/ 7/75	10.8	270	0.2	0.0	0.00E+00	-0.14E-02
17/ 5/ 7/75	12.4	270	0.2	0.1	0.00E+00	-0.17E-02
18/ 5/ 7/75	13.6	270	0.2	0.1	0.00E+00	-0.18E-02
19/ 5/ 7/75	16.8	270	0.4	0.1	0.00E+00	-0.22E-02
20/ 5/ 7/75	21.2	320	0.6	-0.4	-0.22E-02	-0.18E-02
21/ 5/ 7/75	23.2	320	0.7	-0.5	-0.24E-02	-0.20E-02
22/ 5/ 7/75	20.4	320	0.6	-0.4	-0.21E-02	-0.17E-02
23/ 5/ 7/75	18.0	320	0.4	-0.3	-0.18E-02	-0.15E-02
0/ 6/ 7/75	17.2	320	0.4	-0.2	-0.18E-02	-0.15E-02
1/ 6/ 7/75	16.8	320	0.4	-0.2	-0.17E-02	-0.14E-02
2/ 6/ 7/75	15.6	320	0.3	-0.2	-0.16E-02	-0.13E-02
3/ 6/ 7/75	13.6	320	0.2	-0.1	-0.14E-02	-0.12E-02

TABLE 5 Wind stress and pressure gradient derived from computed offshore winds

Date (GMT/day/mon/yr)	Geostrophic Speed (m/s)	Geostrophic Angle (deg)	Tx (Pa)	Ty (Pa)	dPdx (Pa/m)	dPdy (Pa/m)
16/29/ 9/74			Data not available			
17/29/ 9/74			Data not available			
18/29/ 9/74			Data not available			
19/29/ 9/74			Data not available			
20/29/ 9/74			Data not available			
21/29/ 9/74			Data not available			
22/29/ 9/74			Data not available			
23/29/ 9/74			Data not available			
0/30/ 9/74			Data not available			
1/30/ 9/74			Data not available			
2/30/ 9/74			Data not available			
3/30/ 9/74			Data not available			
4/30/ 9/74			Data not available			
5/30/ 9/74			Data not available			
6/30/ 9/74	14.8	270	0.3	0.1	0.00E+00	-0.20E-02
7/30/ 9/74	15.6	270	0.3	0.1	0.00E+00	-0.21E-02
8/30/ 9/74	16.8	270	0.4	0.1	0.00E+00	-0.22E-02
9/30/ 9/74	19.2	320	0.5	-0.3	-0.20E-02	-0.16E-02
10/30/ 9/74	20.4	320	0.6	-0.4	-0.21E-02	-0.17E-02
11/30/ 9/74	18.8	320	0.5	-0.3	-0.19E-02	-0.16E-02
12/30/ 9/74	16.8	320	0.4	-0.2	-0.17E-02	-0.14E-02
13/30/ 9/74	14.8	320	0.3	-0.2	-0.15E-02	-0.13E-02
14/30/ 9/74	12.8	320	0.2	-0.1	-0.13E-02	-0.11E-02
15/30/ 9/74	13.6	320	0.2	-0.1	-0.14E-02	-0.12E-02
16/30/ 9/74	9.2	320	0.1	-0.1	-0.94E-03	-0.79E-03

TABLE 5 Wind stress and pressure gradient derived from computed offshore winds

Date (GMT/day/mon/yr)	Geostrophic Speed (m/s)	Geostrophic Angle (deg)	Tx (Pa)	Ty (Pa)	dPdx (Pa/m)	dPdy (Pa/m)
12/20/ 7/73	16.0	320	0.3	-0.2	-0.16E-02	-0.14E-02
13/20/ 7/73	14.8	320	0.3	-0.2	-0.15E-02	-0.13E-02
14/20/ 7/73	12.4	320	0.2	-0.1	-0.13E-02	-0.11E-02
15/20/ 7/73	10.4	320	0.1	-0.1	-0.11E-02	-0.89E-03
16/20/ 7/73	9.6	320	0.1	-0.1	-0.98E-03	-0.82E-03
17/20/ 7/73	Data not available					
18/20/ 7/73	Data not available					
19/20/ 7/73	Data not available					
20/20/ 7/73	Data not available					
21/20/ 7/73	Data not available					
22/20/ 7/73	Data not available					
23/20/ 7/73	Data not available					
0/21/ 7/73	Data not available					
1/21/ 7/73	Data not available					
2/21/ 7/73	Data not available					
3/21/ 7/73	18.0	270	0.5	0.1	0.00E+00	-0.24E-02
4/21/ 7/73	19.2	270	0.5	0.2	0.00E+00	-0.26E-02
5/21/ 7/73	22.0	270	0.7	0.2	0.00E+00	-0.29E-02
6/21/ 7/73	25.6	320	0.9	-0.6	-0.26E-02	-0.22E-02
7/21/ 7/73	24.0	320	0.8	-0.5	-0.24E-02	-0.21E-02
8/21/ 7/73	18.0	320	0.4	-0.3	-0.18E-02	-0.15E-02
9/21/ 7/73	16.8	320	0.4	-0.2	-0.17E-02	-0.14E-02
10/21/ 7/73	18.8	320	0.5	-0.3	-0.19E-02	-0.16E-02
11/21/ 7/73	18.0	320	0.4	-0.3	-0.18E-02	-0.15E-02
12/21/ 7/73	16.0	320	0.3	-0.2	-0.16E-02	-0.14E-02

TABLE 5 Wind stress and pressure gradient derived from computed offshore winds

Date (GMT/day/mon/yr)	Geostrophic Speed (m/s)	Geostrophic Angle (deg)	Tx (Pa)	Ty (Pa)	dPdx (Pa/m)	dPdy (Pa/m)
7/ 9/ 8/72			Data not available			
8/ 9/ 8/72			Data not available			
9/ 9/ 8/72			Data not available			
10/ 9/ 8/72			Data not available			
11/ 9/ 8/72			Data not available			
12/ 9/ 8/72			Data not available			
13/ 9/ 8/72			Data not available			
14/ 9/ 8/72			Data not available			
15/ 9/ 8/72			Data not available			
16/ 9/ 8/72			Data not available			
17/ 9/ 8/72			Data not available			
18/ 9/ 8/72			Data not available			
19/ 9/ 8/72			Data not available			
20/ 9/ 8/72			Data not available			
21/ 9/ 8/72			Data not available			
22/ 9/ 8/72			Data not available			
23/ 9/ 8/72			Data not available			
0/10/ 8/72	10.8	270	0.2	C.0	0.00E+00	-0.14E-02
1/10/ 8/72	17.2	270	0.4	C.1	0.00E+00	-0.23E-02
2/10/ 8/72	17.2	270	0.4	0.1	0.00E+00	-0.23E-02
3/10/ 8/72	16.8	270	0.4	0.1	0.00E+00	-0.22E-02
4/10/ 8/72	14.8	270	0.3	0.1	0.00E+00	-0.20E-02
5/10/ 8/72	15.6	320	0.3	-0.2	-0.16E-02	-0.13E-02
6/10/ 8/72	15.6	320	0.3	-0.2	-0.16E-02	-0.13E-02
7/10/ 8/72	14.8	320	0.3	-C.2	-0.15E-02	-0.13E-02

TABLE 5 Wind stress and pressure gradient derived from computed offshore winds

Date (GMT/day/mon/yr)	Geostrophic Speed (m/s)	Geostrophic Angle (deg)	Tx (Pa)	Ty (Pa)	dPdx (Pa/m)	dPdy (Pa/m)
16/28/ 7/71			Data not available			
17/28/ 7/71			Data not available			
18/28/ 7/71			Data not available			
19/28/ 7/71			Data not available			
20/28/ 7/71			Data not available			
21/28/ 7/71			Data not available			
22/28/ 7/71			Data not available			
23/28/ 7/71	15.6	270	0.3	0.1	0.00E+00	-0.21E-02
0/29/ 7/71	13.6	270	0.2	0.1	0.00E+00	-0.18E-02
1/29/ 7/71	15.6	270	0.3	0.1	0.00E+00	-0.21E-02
2/29/ 7/71	16.0	270	0.4	0.1	0.00E+00	-0.21E-02
3/29/ 7/71	20.4	270	0.6	0.2	0.00E+00	-0.27E-02
4/29/ 7/71	18.8	270	0.5	0.2	0.00E+00	-0.25E-02
5/29/ 7/71	20.0	320	0.5	-0.3	-0.20E-02	-0.17E-02
6/29/ 7/71	20.4	270	0.6	0.2	0.00E+00	-0.27E-02
7/29/ 7/71	22.0	270	0.7	0.2	0.00E+00	-0.29E-02
8/29/ 7/71	23.2	270	0.8	0.3	0.00E+00	-0.31E-02
9/29/ 7/71	21.2	270	0.7	0.2	0.00E+00	-0.28E-02
10/29/ 7/71	24.0	320	0.8	-0.5	-0.24E-02	-0.21E-02
11/29/ 7/71	22.0	320	0.7	-0.4	-0.22E-02	-0.19E-02
12/29/ 7/71	20.0	320	0.5	-0.3	-0.20E-02	-0.17E-02
13/29/ 7/71	20.4	320	0.6	-0.4	-0.21E-02	-0.17E-02
14/29/ 7/71	17.2	320	0.4	-0.2	-0.18E-02	-0.15E-02
15/29/ 7/71	12.8	320	0.2	-0.1	-0.13E-02	-0.11E-02
16/29/ 7/71	14.8	320	0.3	-0.2	-0.15E-02	-0.13E-02

TABLE 5 Wind stress and pressure gradient derived from computed offshore winds

Date (GMT/day/mon/yr)	Geostrophic Speed (m/s)	Geostrophic Angle (deg)	Tx (Pa)	Ty (Pa)	dPdx (Pa/m)	dPdy (Pa/m)
21/13/ 9/70	20.0	320	0.5	-0.3	-0.20E-02	-0.17E-02
22/13/ 9/70	17.2	320	0.4	-0.2	-0.18E-02	-0.15E-02
23/13/ 9/70	15.6	320	0.3	-0.2	-0.16E-02	-0.13E-02
0/14/ 9/70	12.8	320	0.2	-0.1	-0.13E-02	-0.11E-02
1/14/ 9/70	9.6	320	0.1	-0.1	-0.98E-03	-0.82E-03
2/14/ 9/70	8.4	320	0.1	-0.1	-0.86E-03	-0.72E-03
3/14/ 9/70	12.8	320	0.2	-0.1	-0.13E-02	-0.11E-02
4/14/ 9/70	10.8	270	0.2	0.0	0.00E+00	-0.14E-02
5/14/ 9/70	Data not available					
6/14/ 9/70	Data not available					
7/14/ 9/70	Data not available					
8/14/ 9/70	Data not available					
9/14/ 9/70	Data not available					
10/14/ 9/70	Data not available					
11/14/ 9/70	25.6	270	1.0	0.3	0.00E+00	-0.34E-02
12/14/ 9/70	25.6	270	1.0	0.3	0.00E+00	-0.34E-02
13/14/ 9/70	25.2	320	0.9	-0.6	-0.26E-02	-0.22E-02
14/14/ 9/70	25.6	320	0.9	-0.6	-0.26E-02	-0.22E-02
15/14/ 9/70	27.2	320	1.1	-0.7	-0.28E-02	-0.23E-02
16/14/ 9/70	25.6	320	0.9	-0.6	-0.26E-02	-0.22E-02
17/14/ 9/70	23.2	270	0.8	0.3	0.00E+00	-0.31E-02
18/14/ 9/70	21.2	270	0.7	0.2	0.00E+00	-0.28E-02
19/14/ 9/70	27.2	270	1.2	0.4	0.00E+00	-0.36E-02
20/14/ 9/70	26.4	270	1.1	0.4	0.00E+00	-0.35E-02
21/14/ 9/70	14.0	270	0.3	0.1	0.00E+00	-0.19E-02